ISTANBUL TECHNICAL UNIVERSITY ★ GRADUATE SCHOOL

INVESTIGATION OF DIFFUSION OF REDOX SENSITIVE ELEMENTS IN NUCLEAR WASTE IN POLYMER-BASED BARRIER SYSTEMS

PhD THESIS

Ruveyda Kubra ILERI DURMUS

Department of Energy Science and Technology

Energy Science and Technology Programme

SEPTEMBER 2023

ISTANBUL TECHNICAL UNIVERSITY ★ GRADUATE SCHOOL

INVESTIGATION OF DIFFUSION OF REDOX SENSITIVE ELEMENTS IN NUCLEAR WASTE IN POLYMER-BASED BARRIER SYSTEMS

PhD THESIS

Ruveyda Kubra ILERI DURMUS
(301152005)

Department of Energy Science and Technology

Energy Science and Technology Programme

Thesis Advisor: Prof. Dr. Sema ERENTURK

SEPTEMBER 2023

ISTANBUL TEKNİK ÜNİVERSİTESİ ★ LİSANSÜSTÜ EĞİTİM ENSTİTÜSÜ

NÜKLEER ATIKLARDAKİ REDOKS DUYARLI ELEMENTLERİN POLİMER BAZLI BARİYER SİSTEMLERİNDE DİFÜZYONUNUN İNCELENMESİ

DOKTORA TEZİ

Rüveyda Kübra İLERİ DURMUŞ
(301152005)

Enerji Bilim ve Teknoloji Anabilim Dalı

Enerji Bilim ve Teknoloji Programı

Tez Danışmanı: Prof. Dr. Sema ERENTÜRK

EYLÜL 2023

Ruveyda Kubra ILERI DURMUS, a Ph.D. student of ITU Graduate School student ID 301152005, successfully defended the thesis/dissertation entitled "INVESTIGATION OF DIFFUSION OF REDOX SENSITIVE ELEMENTS IN NUCLEAR WASTE IN POLYMER-BASED BARRIER SYSTEMS", which she prepared after fulfilling the requirements specified in the associated legislations, before the jury whose signatures are below.

Thesis Advisor :	**Prof. Dr. Sema ERENTURK** Istanbul Technical University	.....
Jury Members :	**Prof. Dr. Mahmut A.A. ASLANI** Ege University	.....
	Prof. Dr. B. Filiz SENKAL Istanbul Technical University	.....
	Assoc. Prof. Dr. Senem SENTURK LULE Istanbul Technical University	.....
	Assoc Prof. Dr. Umit H. KAYNAR Izmir Bakircay University	.....

Date of Submission : 16 May 2023
Date of Defense : 14 September 2023

To my well-beloved spouse, my sweety son and my valuable parents,

FOREWORD

Here is the point that last touch to my thesis. I thought writing the foreword was the easiest part of the thesis but unfortunately not. Every stage of my PhD flashed before my eyes like a movie because it is a long, sensible and dense story. During this period, I found a job, quit one, participated in varied international conference / seminars / technical site visits, changed residence city, found another job, got married, travelled between Ankara and Istanbul for laboratory studies for PhD, stayed at home due to Covid-19 pandemic for 3 years, had a baby boy and here we are.

I saved many individuals throughout my long PhD history, and I am incredibly grateful to them all. First and foremost, I would like to express my profound thanks and appreciation to Prof. Dr. Sema ERENTURK, who has been my PhD supervisor and supported and helped me throughout my graduate academic adventure as well as in my professional and personal life with her wisdom, expertise, experience, and excellent, guidance and patience. She is the source of my scientific stance. Without her assistance and the inspiration, she gave, it would not have been possible to carry out and finish this study.

I would like to also express my gratitude to Prof. Dr. Bahire Filiz ŞENKAL and Prof. Dr. Mahmut Ali Asker ASLANİ, members of the committee who helped guide this thesis work and gave invaluable guidance and insights. With their wealth of knowledge, they also helped to further improve the study's quality.

I would like to also thank Alpaslan Erentürk, who helped me with all manner of technical support during my experimental investigations.

I acknowledge The Scientific and Technological Research Council of Turkey (TÜBİTAK) for supporting me with the 2211-C National PhD Scholarship Program in the Priority Fields in Science and Technology.

Moreover, I am thankful to the Istanbul Technical University Scientific Research Projects Unit for supporting this study (Project number: TDK-2018-41684).

I also admit to thank for the GoldSim Technology Group for the providing of the GoldSim Radionuclide Transport Module for Students, Teachers, Professors and Academic Researchers.

Moreover, I thank to my collegues Şenol Şen to writing this thesis by supporting in terms of editorial preparation and editorial review. I could asked any Microsoft Word problem to his with no hesitation and answered with his patence and his knowledge and skills.

I would like to thank my valuable parents for their unconditional love and everlasting support. They have always respected my opinions and wishes, given me opportunities and help, and have always been by my side and will always be.

Last but not least, but most important of all, I owe my deepest gratitude, and appreciation to my well-beloved spouse Cihangir DURMUŞ, who walked through the PhD journey together with me for his endless love, continuous and unique support,

great encouragement, critical and inquiry attitude and indispensable assistance in performing this study. He has always been by my side with his laugh, love, foresight, knowledge, motivation and being. Thank you for being. Moreover, I should thank my dear son Süreyya Alp for his patient, his curiosity, tolerance to my endless studies and awaking me at night. I am so delighted and peaceful to explore the world with you and amazed by you.

May 2023

Ruveyda Kubra ILERI DURMUS
(Physicist)

TABLE OF CONTENTS

Page

ABBREVIATIONS

ADD	: Annual Daily Intake
ALARA	: As Low As Reasonably Achievable
ANDRA	: Agence nationale pour la gestion des déchets radioactifs (France National Agency for Radioactive Waste Management)
APC	: Akkuyu Project Company
BWR	: Boiled Water Reactor
CEA	: Commissariat à l'énergie atomique (The French Atomic Energy Commission)
CEC	: Cation Exchange Capacity
CR	: Concentration Value
DMF	: Dimethylformamide
DOE	: US Department of Energy
D-R	: Dubinin–Radushkevich
ELCR	: Excess Lifetime Cancer Risks
EMCL	: Environmental Media Concentration Limits
EPA	: Environmental Protection Agency
EPDK	: Energy Market Regulatory Authority
ERICA	: Environmental Risk from Ionizing Contaminants: Assessment and Management
EU	: Eurepean Union
FWHM	: Full Width At Half Maximum
GBq/te	: Giga-Becquerels per Tonne
GHG	: Greenhouse Gas
GNP	: Gross National Product
GSG	: General Safety Guide
GW	: Giga-watt
GWh	: Giga-watt hour
HAW	: Higher Activity Radioactive Waste
HEPA	: High Efficiency Particulate Air
HI	: Hazard Index
HLW	: High Level Wastes
HQ	: Hazard Ratio
IAEA	: International Atomic Energy Agency
ICP-OES	: Inductively Coupled Plasma Optical Emission Spectroscopy
ICRP	: International Commission on Radiological Protection
IGA	: Intergovermental Aggreement
ILW	: Intermediate Level Wastes
ITU	: Istanbul Technical University
IU	: Istanbul University
JNFL	: Japan Nuclear Fuel Limited
kWh	: Kilo-watt hour
LILW-LL	: Low Intermediate Level Waste Long-Lived
LILW-SL	: Low Intermediate Level Waste Short-Lived
LLW	: Low Level Wastes

LWR : Light Water Reactors
MENR : Minister of Energy and Natural Resources
MoU : Memorandum of Understanding
MOX : Mixed Oxide Fuel
MWe : Mega-watt Electric
NDK : Nuclear Regulatory Authority
NIST : National Institute of Standards and Technology
NPP : Nuclear Power Plant
NUMO : Nuclear Waste Management Organization of Japan
NWMO : Canada's Nuclear Waste Management Organisation
OECD : Organisation for Economic Co-operation and Development
ONR : Office of Nuclear Regulation
P&T : Portioning and Mutation
PAN : Polyacrylonitrile
PRIS : Power Reactor Information System
PV : Photovoltaic
PWR : Pressurized Water Reactor
R&D : Research and Development
RQ : Risk Quotients
SKB : Svensk Kärnbränslehantering Aktiebolag (The Swedish Nuclear Fuel and Waste Management Company)
SMR : Small Modular Reactors
TAEK : Turkish Atomic Energy Agency
TCR : Total Carcinogenic Risk
TEİAŞ : Turkish Electricity Transmission Corporation
TGA : Thermogravimetric Analysis
tHM : Ton Heavy Metal
TRU : Transuranic
TUNAS : Turkish Nuclear Energy Company
UK : United Kingdom
ULPA : Ultra-Low Penetration Air
UNSCEAR : United Nations Scientific Committee on the Effects of Atomic Radiation
USA : United States
VLLW : Very Low Level Wastes
VSLW : Very Short-Lived Wastes
WNA : World Nuclear Association
XPS : X-ray Photoelectron Spectroscopy

SYMBOLS

A : Activity (Bq)
a : Abundance
ABS : Dermal absorption factor
ADD_{dermal} : Average daily intake by absorption of the metal (mg kg^{-1} day^{-1})
ADD_{ing} : Average daily intake by ingestion (mg kg^{-1} day^{-1})
ADD_{inh} : Average daily intake by inhalation (mg kg^{-1} day^{-1})
A_e : Activity concentration of the solution in equilibrium (Bq mL^{-1})
AF : Adhesion factor
A_i : Activity concentration of the initial solution (Bq mL^{-1})
A_S : Surface area of the loaded activated charcoal particles (m^2 m^{-3}-activated charcoal)
AT : Average time in days
b : Desorption constant (g mg^{-1}).
BW : Body weight of the exposed individual
C : Metal concentration in the medium (mg kg^{-1})
C_{ads} : Amount of the adsorbate at equilibrium
C_e : Ion concentration of the solution in equilibration (μg mL^{-1})
C_i : Initial ion concentration of the solution (μg mL^{-1})
C_{in} : Concentration of radioactive aerosol concentration at the filter inlet (Bq m^{-3})
C_{out} : Concentration of radioactive aerosol concentration at the filter outlet (Bq m^{-3})
CR : Concentration value (Bq kg^{-1})
D_E : Annual effective dose
DL : Average duration of life
E : Capture efficiency of HEPA filters
E_a : Activation energy
ED : Duration of exposure
EF : Frequency of exposure to the selected metal
$EMCL_n$: Environmental Media Concentration Limit for radionuclide "n"
IngR : Rate of ingestion
InhR : Rate of inhalation
k_1 : Rate constant of the equation (min^{-1}).
K_a : Association constant
K_C : Gas film mass transfer coefficient (m s^{-1})
K_d : Distribution coefficient (mL mg^{-1})
K_D : Hill constant
L : Thickness of the activated charcoal bed (m)
L_0 : Theoretical combustion air (N_m^3 kg-$waste^{-1}$)
m : Amount of the composite barrier material (g).
M : Molarity of the substance (kg mol^{-1})
N_A : Avogadro's number (mol^{-1})
n_H : Hill cooperation coefficient

PC : Nominal probability coefficient for detriment
PEF : Emission factor
q_e : Adsorption capacity (mg g^{-1})
Q_H : Adsorbate maximum uptake (mg g^{-1})
q_t : Amount of ions adsorbed at time t (mg g^{-1})
R : Gas constant (kJ mol^{-1})
RfD : Standard exposure level
RQ : Total Risk quotient
SA : Surface area of the exposed skin
SF : Slope factor
T : Gas constant (kJ mol^{-1})
$t_{1/2}$: Half-life of the nuclei (s)
U : Filtration rate (m s^{-1})
V : Volume of the solution (mL)
V_w : Amount of wet combustion gas (N_m^3 kg-$waste^{-1}$)
X_m : Maximum adsorption capacity
β : Constant related to energy
ΔG° : Free Gibbs Energy change (kJ mol^{-1})
ΔH° : Enthalpy change (kJ mol^{-1} K^{-1})
ΔS° : Entropy change (J mol^{-1} K^{-1})
ε : Polanyi potential
η : Collection efficiency

LIST OF TABLES

Page

LIST OF FIGURES

Page

INVESTIGATION OF DIFFUSION OF REDOX SENSITIVE ELEMENTS IN NUCLEAR WASTE IN POLYMER-BASED BARRIER SYSTEMS

SUMMARY

Despite the promotion of nuclear power due to its high capacity factor, low volume of wastes, low operation cost, and low greenhouse effect contribution, some issues, such as high radioactive wastes, continue to be a concern. Nonetheless, research into the disposal and storage of radioactive waste in waste repositories has continued. The migration of radioactive waste into the biosphere and the access of water to waste repositories are the main issues with these facilities. There is widespread agreement that waste repositories should have multiple barriers made up of geological formation and engineered barriers. Where the radionuclides first come into contact, the engineered barrier typically consists of buffer material. In this work, the composite barrier material PAN/clinoptilolite composite ion exchanger was used to describe interactions with ^{126}Sn and ^{79}Se adsorption behavior.

This PhD thesis' findings have been presented at two conferences internationally and published in three top-notch peer-reviewed journals.

The first chapter mentions the importance of nuclear, the challenges of nuclear, Turkiye’s position in nuclear and problems that will arise in the future for radioactive waste issues. Being reliable, high capacity factor, solution for the concerns of climate change and environment and providing the high-technology opportunity make the nuclear power attractive. Besides these brilliant advantages, there are some concerns about nuclear power to create hesitation in public such as safety and radioactive wastes. The root reasons of these concerns and the persuasive arguments are presented. Moreover, the motivation, driven force and objectives and aims of this study are explained in this chapter. The comply with the energy strategy of Turkiye, the nucler power plants, that can vary different technologies such as SMRs are planned to serve and the amount of waste generation because of the NPPs need to manage. Therefore, the radioactive waste management should be planned in detail.

The second chapter present the literature review belonging to the key concepts of this study. The position of the radioactive waste in nuclear fuel cycle, the classification and production of the radioactive wastes, applied radioactive waste management and immolization techniques in the world, disposal of the radioactive wastes, the types of the disposal and some applications of the disposal in some countries are taken into account. Furthermore, the adsorption concept tin and selenium, which are the two of the most important but rarely found in literature redox-sensitive radionuclides in the radioactive waste area are taken account. With this motivation, it is aimed to develop and characterize new barrier materials with more effective and safe barrier properties

that will be an alternative to existing barrier systems and to examine the applicability of these barrier materials for the retention of ^{126}Sn and ^{79}Se.

The third chapter is related with the used material and applied method during this study. A new polymer/clay nanocomposite material as a barrier material are synthesized and characteristic of this new barrier material are investigated in terms of thermal stability and surface analysis. Moreover, interaction between tin and selenium radionuclides in the radioactive waste area and developed barrier material are characterized by data collected with examining under different circumstances, such as variable initial concentrations, interaction times, and temperatures and using adsorption isotherms, kinetic calculations, thermodynamic parameters, kinetic models based on diffusion. Furthermore, the risk assessments because of tin and selenium from radioactive waste area are analyzed in terms of radiologicaly dose assessment for freshwater and terrestrial biotas by using the ERICA Assessment Tool, exposure in human because of accidental migration of the these radionuclides by using the GoldSim Monte Carlo Simulation Software and carcinogenic and non-carcinogenic risks and excess lifetime cancer risks.

The forth chapter gives the result and discussion of the experiments and analysis mentioned above. The tin ion adsorption on the barrier material has been seen to fit into the D-R isotherm model. The thermodynamic characteristics were used to determine that the tin's adsorption onto the barrier was endothermic. The tin adsorption process was shown to be consistent with the pseudo second-order model based on the kinetic evaluation. Using GOLDSIM Monte Carlo Simulation Software, the risk of ^{126}Sn migration as a result of an accident in the radioactive waste repository was evaluated. Tin was assessed for its excess lifetime cancer risks and its carcinogenic and non-carcinogenic risks. For selenium, it has been found as a consequence that a crucial part of the composite barrier material's effectiveness in preventing selenium transfer from the waste storage region to the biosphere is played by this. For adults, the total carcinogenic risk (TCR) values for ingestion ranged from 4.93E-17 to 4.03E-16, while for infants, they ranged from 6.30E-22 to 5.16E-21. For adults, TCR values for the dermal way vary from 5.28E-21 to 4.32E-20, whereas for infants, they range from 7.74E-31 to 6.34E- 30. The exposed total dose range of reference biota as such crustaceans, phytoplankton, and vascular plants in freshwater was calculated as 4.02E6-3.87E9 $\mu G\ h^{-1}$ for ^{126}Sn isotope, and 3.35E07-1.92E12 $\mu G\ h^{-1}$ for ^{79}Se isotope using composite barrier material. In terrestrial reference biota such as annelids, grasses and grasses, lichens, and bryophytes, mammals and trees, the exposed total dose range was calculated as 4.51E06-7.41E04 $\mu G\ h^{-1}$ for ^{126}Sn and 2.15E06-5.53E09 $\mu G\ h^{-1}$ for ^{79}Se. Thus, it was determined that the existence of barrier material significantly reduced the total exposure of freshwater and terrestrial biota.

The fifth and last chapter includes the chapter mentioned key findings of all these studies.

NÜKLEER ATIKLARDAKİ REDOKS DUYARLI ELEMENTLERİN POLİMER BAZLI BARİYER SİSTEMLERİNDE DİFÜZYONUNUN İNCELENMESİ

ÖZET

Yüksek kapasite faktörü, düşük atık hacmi, düşük işletme maliyeti ve düşük sera etkisi katkısı nedeniyle nükleer enerji enerji üretiminde yeniden cazibeli olmasına rağmen, yüksek radyoaktif atıklar gibi bazı konular endişe kaynağı olmaya devam etmektedir. Bununla birlikte, radyoaktif atıkların atık havuzlarında depolanması ve bertarafına yönelik araştırmalar devam etmektedir. Bu tesislerin temel amacı radyoaktif atıkların biyosfere göçünü ve suyun atık depolarına erişimini engellemektir. Atık bertaraf tesislerinin jeolojik oluşumlardan ve mühendislik beriyerlerinden oluşan çoklu bariyer sistemine sahip olması gerektiği konusunda yaygın bir fikir birliği vardır. Radyonüklitlerin ilk kez temas ettikleri yerde, mühendislik bariyerleri tipik olarak tampon malzemeden oluşur.

Bu çalışmada, ^{126}Sn ve ^{79}Se adsorpsiyon davranışı ile etkileşimleri tanımlamak için kompozit bariyer malzemesi PAN/klinoptilolit kompozit iyon değiştirici kullanılmıştır. Bu bariyer malzemenin bu çalışmada kullanılan ^{126}Sn ve ^{79}Se malzemeleri ile etkileşimlerinin tanımlanması kritik bir öneme sahiptir. Zira, radyoaktif atık bertaraf alanı içerisinde bariyer malzeme ile sözkonusu radyonüklidlerin davranışları ve insan ve biyotalar üzerinde maruz kalınan olası dozlar, atık bertaraf alanının tasarımını etkilemektedir. Bu sebeple, bu çalışma birbirini tamamlayan ve ikisi Q1 dergide ve tamamı uluslararası dergilerde yayınlanmış ve 2 uluslararası konferansta sunulmuş 3 makaleden oluşmaktadır.

Birinci bölümde nükleerin önemi, nükleerin zorlukları, Türkiye'nin nükleerdeki konumu ve radyoaktif atık konusunda gelecekte ortaya çıkacak sorunlardan bahsedilmektedir. Güvenilir olması, yüksek kapasite faktörü, iklim değişikliği ve çevre endişelerine çözüm olması ve yüksek teknoloji imkanı sağlaması nükleer enerjiyi cazip kılmaktadır. Bu parlak avantajların yanı sıra, güvenlik ve radyoaktif atıklar gibi kamuoyunda tereddüt yaratacak nükleer enerji ile ilgili bazı endişeler bulunmaktadır. Bu bölümde bu endişelerin temel nedenleri ve ikna edici argümanlar sunulmaktadır. Bunun yanısıra Türkiye'nin artan enerji ihtiyacı, ulusal enerji strateji planı ve nükleer konusundaki pozisyonu ele alınmıştır. Buna göre, halihazırda inşaat halinde olan ve önerilen nükleer güç santralleri Akkuyu, Sinop ve Trakya Sahalarıdır. Bununla birlikte küçük modüler reaktörler de Türkiye'nin enerji planlamasında nükleer sınıfta yerini aldığı ifade edilmiştir. Türkiye Ulusal Enerji Planına göre 2035 yılına kadar toplam nükleer enerji santrali kurulu gücü 7.2 GW'a ulaşmaktadır. Bu durum, medikal, endüstri ve araştırma ve geliştirme faaliyetlerinden gelen atıkların yanısıra ciddi bir atık miktarının gelmesi demek olup bunlarla ilgili aksiyon alınması gerektiğinden bahsedilmektedir.

İkinci bölümde, bu çalışmanın anahtar kavramlarına ait literatür taraması sunulmaktadır. Radyoaktif atıkların nükleer yakıt çevrimindeki yeri, radyoaktif atıkların sınıflandırılması ve farklı ülkelerde uygulama farklılıkları, radyoaktif atıkların üretimi, dünyada uygulanan radyoaktif atık yönetimi ve farklılıkları, radyoaktif atıkların immolizasyon teknikleri, radyoaktif atıkların bertarafı, bertaraf türleri ve bazı bölgelerde bertaraf uygulamaları ülkeler dikkate alınır. Ayrıca adsorpsiyon kavramı ile radyoaktif atık alanındaki redoks duyarlı radyonüklidlerin en önemlilerinden olan ancak literatürde nadiren bulunan kalay ve selenyum da dikkate alınmıştır. Bu motivasyonla, mevcut bariyer sistemlerine alternatif olacak daha etkin ve güvenli bariyer özelliklerine sahip yeni bariyer malzemelerinin geliştirilmesi, karakterize edilmesi ve bu bariyer malzemelerinin ^{126}Sn ve ^{79}Se tutulması için uygulanabilirliğinin incelenmesi amaçlanmaktadır.

Üçüncü bölüm, bu çalışmada kullanılan malzeme ve uygulanan yöntemle ilgilidir. Bariyer malzemesi olarak yeni bir polimer/kil nanokompozit malzemesi sentezlenmiş ve bu yeni bariyer malzemesinin karakteristiği termal kararlılık ve yüzey analizi açısından incelenmiştir. Ayrıca, radyoaktif atık alanındaki kalay ve selenyum radyonüklitleri ile geliştirilen yeni bariyer malzemesi arasındaki etkileşim, başlangıç konsantrasyonları, etkileşim süreleri ve sıcaklıklar gibi farklı koşullar altında incelenerek adsorpsiyon izotermleri, kinetik hesaplamalar, termodinamik parametreler, difüzyona dayalı kinetik modeller oluşturulmuş ve toplanan verilerle karakterize edilmiştir. Ayrıca, radyoaktif atık alanından yayılan kalay ve selenyum nedeniyle risk değerlendirmeleri yapılmıştır. Buna göre, ERICA Assessment Tool kullanılarak tatlı su ve karasal biyotalar için radyolojik doz değerlendirmesi, GoldSim Monte Carlo Simülasyon Yazılımı kullanılarak bu radyonüklidlerin herhangi bir kaza sonucu biyosfere göçü sebebiyle insanların maruz kalacağı doz ve kanserojen ve kanserojen olmayan riskler ve yaşam boyu kanser riskleri hesaplanmıştır.

Dördüncü bölümde, yukarıda belirtilen deney ve analizlerin sonuçları ve tartışmaları verilmiştir. Buna göre, kalay iyonlarının bariyer malzemesi üzerine adsorpsiyonunun D-R izoterm modeline uyduğu gözlenmiştir. Termodinamik parametrelerden kalayın bariyer üzerine adsorpsiyonunun endotermik olduğu belirlenmiştir. Kinetik değerlendirmeden, kalay adsorpsiyon işleminin pseude-ikinci dereceden model ile uyumlu olduğu görülmüştür. Radyoaktif atık bertaraf tesisindeki bir kaza sonucunda ^{126}Sn'nin göç etme riski, GOLDSIM Monte Carlo Simülasyon Yazılımı kullanılarak değerlendirilmiştir. Buna göre, 2 milyon yıl sonra radyoaktif atık deposundan kaza nedeniyle sızan ^{126}Sn'nin neden olduğu doz maruziyeti bebekler için 2.85E-19 mSv iken, yetişkinler için 1.49E-20 mSv'dir. ICRP103'te tanımlanan ve UAEA Genel Güvenlik Rehberi No. GSG-8 ile desteklenen izin verilen etkin doz limiti ve UNSCEAR tarafından belirlenen doğal radyoaktivite dikkate alındığında, simülasyondan elde edilen etkin doz limitlerinin izin verilen doz limitlerinden daha düşük olduğu söylenebilir. Kalayın kanserojen ve kanserojen olmayan riskleri ve yaşam boyu kanser riskleri (ELCR) değerlendirilmiştir. Sindirim yoluyla toplam kanserojen risk yetişkinler için 3.00E-25 ve bebekler için 2.41E-23, dermal yol ile yetişkinler için 3.42E-10 ve bebekler için 2.56E-09 bulunmuştur. Buna göre, kanser riski değerleri 10^{-4}'ün altında olduğu için radyoaktif atık deposundan yayılan kalayın yetişkinler ve çocuklar için önemli bir risk oluşturmadığı söylenebilir. Selenyum kompozit bariyer malzeme ile adsorpsiyonunda D-R izoterm modeli ve Temkin izoterm modeli ile uyumlu olduğu görülmüştür. Termodinamik parametrelerden selenyumun bariyer üzerine adsorpsiyonun egzotermik olduğu belirlenmiştir. Kinetik değerlendirmeden, selenyum ve bariyer malzemenin adsorpsiyonun pseude-ikinci

dereceden model ile uyumlu olduğu görülmüştür. Olası bir kaza durumunda ^{79}Se'nin oluşturabileceği çevre ve sağlık riskleri, Monte Carlo tabanlı simülasyon programı kullanılarak olası doz değerleri kapsamında değerlendirilmiştir. Bu simülasyona dayanarak, ^{79}Se nedeniyle yetişkinlerin maruz kaldığı doz 7.07E-26 mSv ve bebeklerin maruz kaldığı doz 2.44E-17 mSv bulunmuştur. Sonuç olarak, kullanılan kompozit bariyer malzemesinin selenyumun atık depolama alanından biyosfere geçişini engellemede önemli rol oynadığı belirlenmiştir. Sindirim yolu için toplam kanserojen risk (TCR) değerleri yetişkinler için 4.93E-17 ile 4.03E-16, bebekler için 6.30E-22 ile 5.16E-21 arasında bulunmuştur. Dermal yol için TCR değerleri yetişkinler için 5.28E-21 ile 4.32E-20 ve bebekler için 7.74E-31 ile 6.34E-30 arasında olduğu tespit edilmiştir. Ayrıca, ERICA Assessment Tool kullanılarak, tatlı su referans biyotalardan olan kabuklular, fitoplankton ve vasküler bitkiler için toplam maruz kalınan doz ^{126}Sn izotop için 4.02E6-3.87E9 μG h^{-1} ve ^{79}Se izotop için 3.35E07-1.92E12 μG h^{-1} olduğu tespit edilmiştir. Karasal referans biyotadan olan annelidler, otlar ve çimenler, likenler ve briyofitler, memeliler ve ağaçlar için toplam maruz kalınan doz ^{126}Sn için 4.51E06-7.41E04 μG h^{-1} ve ^{79}Se için 2.15E06-5.53E09 μG h^{-1} olduğu hesaplanmıştır.

Beşinci bölüm, tüm bu çalışmaların söz konusu temel bulgularını ve önerilerini içermektedir.

1. INTRODUCTION

1.1 Background and Motivation

According to The Power Reactor Information System (PRIS) databases developed by IAEA, the number of nuclear power reactors in operation is 443 whose total power is about 400 GWe in 2021. Today, this electrical capacity covers 11% of the world energy demand. In 2030, by increasing the number of nuclear power reactors, total power will be about 450 GWe in 2030 and 715 GWe in 2050. With these numbers, the electricity capacity of nuclear among the world generated electricity capacity will increase. According to these data, it seems that nuclear energy has been adopted to meet the growing energy demand (PRIS, 2020).

One of the best energy options for fulfilling the anticipated demand for electricity as in the past is nuclear power. 20 years after the speech of Eisenhower, US President, on the "Atoms ford Peace" in 1953, the usage of nuclear was stated for the international development phase and so did electricity generation from 1970-1985. While the number of nuclear reactors was 80 in the 1970s, this number increased to 360 at the end of 1985. This growth in the number of reactors covers 65% of atomic energy when taken into account the period 1955-2015 (Prăvălie and Bandoc, 2019). According to PRIS data, North America has the largest nuclear reactor fleet in regard to both the number of reactors and net electrical capacity. Far East Asia and Western Europe follow North America. When shifting the perspective from the region to the country's scale, the USA has the leader in the both number of reactors and net electrical capacity. The second is France in operational reactors (Figure 1.1) (WNA Performance Report, 2020).

However, the appetite for nuclear energy has decreased from time to time. The first dramatic decrease in demand for nuclear energy occurred in 1986 in Chernobyl accident that affected the global scale. From this date, some countries such as Italy, Kazakhstan, and Lithuania declared that the nuclear energy programme has been shut down and adopted non-nuclear energy. Although some countries have decided to the

opponent of nuclear energy, Eastern Europe and Asia such as Japan, South Korea, India, and China has been continued their nuclear energy programme after the 1990s and developed their capacities.

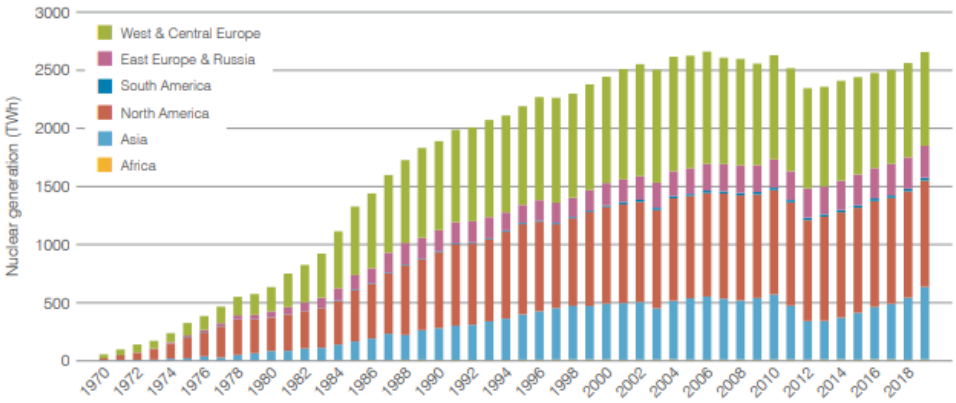

Figure 1.1 : Nuclear Energy Production.

According to PRIS data, when taking into consideration under-construction reactors Far East Asia is the leader in terms of both the number of reactors and net electrical capacity. The Middle East and South Asia follow it. However, in regard to the under-construction reactors, China is the leader county, and South Korea and India follow it (PRIS, 2020).

1.1.1 Why nuclear?

There are several reasons behind the increase in nuclear power plants in some countries.

The first reason is the reliability factor. The reliability of the energy sources is measured by their availability. The capacity of a product or system to be in a state to carry out a required function under certain circumstances at a specific time or over a specific period of time, provided that the necessary external supplies are available is described as availability in the IAEA glossary. There is another term that is related with the availability is capacity factor. The PRIS Glossary defines capacity factor as the difference between the real energy output of an electricity generator and the amount of energy that would be produced if it ran at its maximum power output. In other words, the capacity factor is the ratio of the running period in the specific time of the maximum possible output. It is reported the relationship between the availability and capacity factor is explained by Morales Pedraza, 2019 as the yearly capacity factor of a power plant is a measurement of availability (the manner in which many hours it

is able to produce electricity) and an indirect estimation of the minimal cost of generation (for non-variable sources), as well as other features like adjustability and starting times (Morales Pedraza, 2019).This shows the reliability and continuity of the energy sources. This is important for both the investor to return their investment and the end user to manufacture because even a momentary loss of energy causes a large amount of material loss, as well as a reduction in the workforce.

The capacity factor is one of the most important arguments for nuclear energy. As it is shown in Figure 1.2 (US Department of Energy, 2022), nuclear energy has the most capacity factor among the other energy sources that meet the availability criterion well such as fossil fuel power plants based on oil, coal, hydroelectric and natural gas with proper regime and flow (US Department of Energy, 2022).

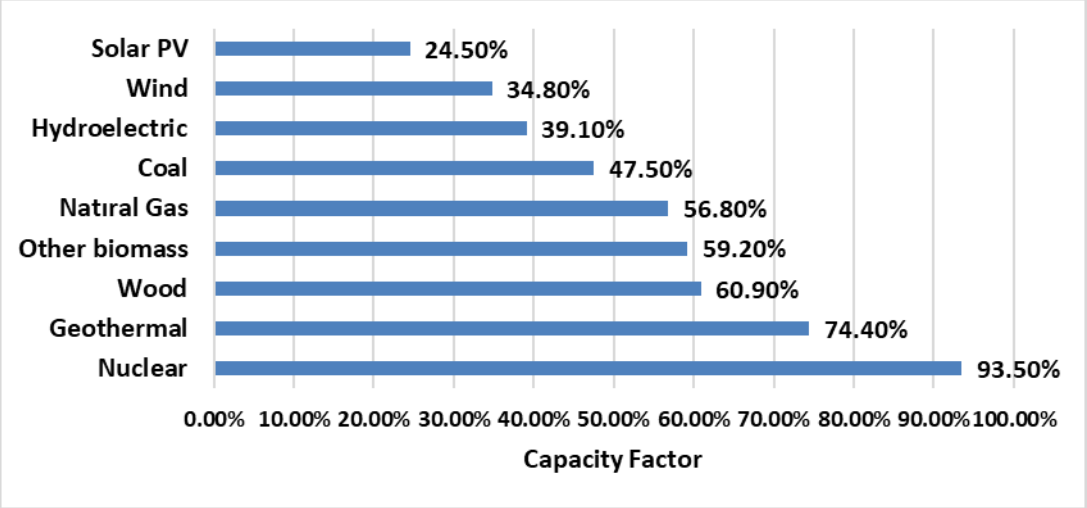

Figure 1.2 : Average capacity factor by selected energy sources.

The other reason nuclear power plants are attractive is environmental concerns related to climate change. Climate change and the greenhouse effect are becoming an issue that has to gain dramatic emergency. Many governments and authorities are agreed that financial and technical developments should be investigated and related actions should be adopted to stop greenhouse gas (GHG) and climate change. Based on scientific consensus, in order to to stop an increase in temperature of more than 2°C by the end of the century, the annual GHG emission should be reduced by at least 50%. The GHG emission is mostly based on the energy sector. Although other sectors such as agriculture and industry contribute the GHG emission, the energy sector produces 70% of all GHG emissions. Gases produced in the energy sector and contributing the GHG emission are methane (CH_4), nitrous oxide (N_2O), and carbon dioxide (CO_2). In

this regard, CO_2 has special importance because CO_2 is responsible for 90% of the total GHG emission. CO_2 is produced by fossil fuel combustion such as coal, gas, and oil. Therefore, passing towards the carbon sources such as nuclear, hydro, and renewables are necessary for avoiding of consequences of global warming, cutting climate change, and stopping GHG emission (NEA, 2015).

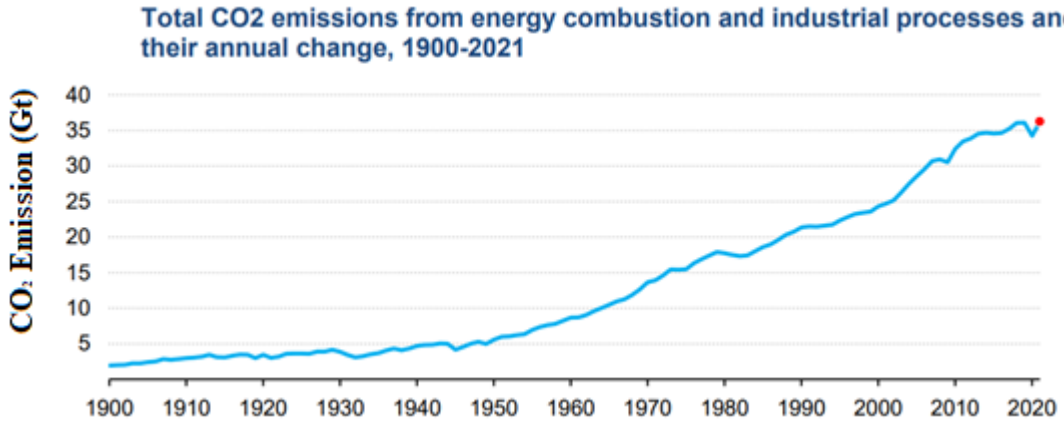

Figure 1.3 : Carbon emission related with energy.

In Figure 1.3 (IEA, 2022), the carbon emission related to energy is shown in the regard of the years. According to Figure 1.3, the emission in 2008 and 2020 is a coincidence with the regional or global crises. However, the time-dropping emission in 2014 is a coincidence with the passing of carbon-free sources such as renewables, hydropower, and nuclear power despite the absence of a major economic crisis. While, the usage of coal, oil, and gas are 44%, 35%, and 20%, respectively in 2013, the usage of coal, oil, and gas are 29%, 31%, and 21%, respectively in 2014. The remaining energy in 2014, 18%, is produced by carbon-free sources such as hydropower, renewables, and nuclear power (NEA, 2015).

In Figure 1.4 (OECD, 2012), the GHG emission is shown in regard to the different electricity generation technologies. According to Figure 1.4 conducted by WNA (2011) Report based on the 20 studies published by international organizations, authorities, governments, and research centers, lignite is the most contributor to GHG emission with a value of 1054 in tonnes CO_2 eq/GWh. Coal, oil, and gas follow the lignite approximately at the same level. After the fossil fuel, the GHG emission is dramatically decreased by up to 85 tonnes CO_2eq/GWh in solar PV. The electricity generation technology that has GHG emissions least is nuclear, wind, and hydroelectric (OECD, 2012).

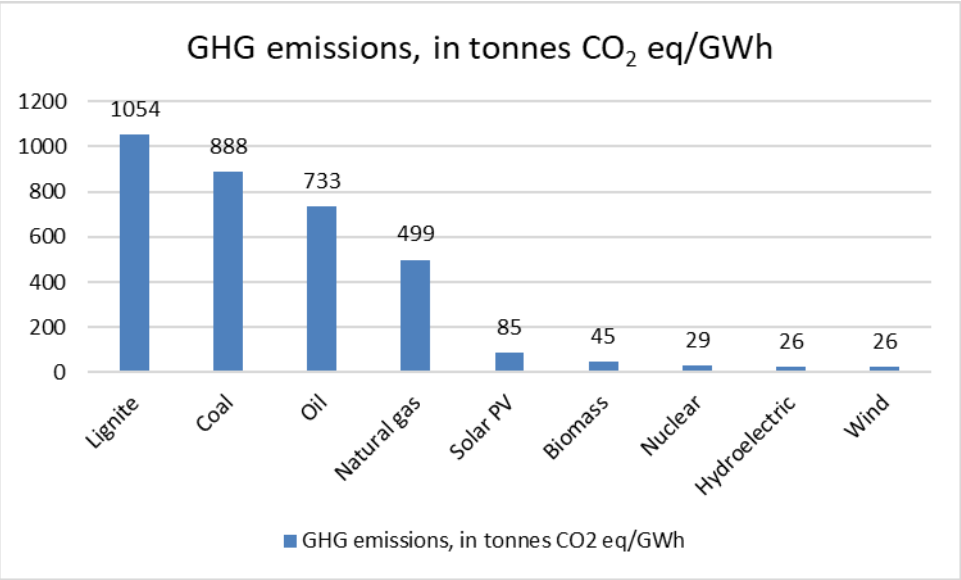

Figure 1.4 : Greenhouse emission based on different electricity source.

In spite of raising concerns about nuclear power after the Fukushima accident, incentives for wind, and solar energies, and some challenges of large-scale nuclear such as the high capital cost and long length construction periods, nuclear energy still remains its baseload position and so important in many countries (NEA, 2015).

Two key findings emerged from the OECD research on climate change:

- Nuclear power will be the greatest source of energy that is low in carbon emissions up to 2050, relative to other technologies;
- Nuclear power would enable the maximum CO_2 emission reductions.

Therefore, nuclear power meets the objectives of the Paris Conference of the Parties (COP 21) to the United Nations Framework Convention on Climate Change, which is the most recent international climate change-related agreement (Prăvălie and Bandoc, 2019).

Another factor that makes nuclear power plants attractive is that they are key to advanced technology such as space technology, hydrogen technology, and nanotechnology. As a result, nuclear power plants are employed for more than just the generation of electricity; they also facilitate the advancement of science and technology. In a nuclear power plant, there are ten thousands of different equipments and components in systems used. Production and manufacturing by technological transfers, then developing of these components, that are qualified and advanced

technology materials are made by knowledge and experience obtained in nuclear power plant (Kok, 2009).

1.1.2 Why not nuclear?

Although nuclear power has many advantages that are explained in the previous section, there are also a few concerns such as safety concerns and radioactive release and wastes.

For safety concerns, nuclear projects are projects that carried out the principle of "Safety First" like the aviation sector. The costs and time of these projects are constructed on safety principles. From the planning to decommissioning phase, each phase has to comply with national and international codes and standards. Moreover, these projects are under independent audit by national and international authorities (Enerji Proje Uygulama Dairesi, 2016).

Defense-in-depth principles are used in the nuclear power facilities design, similar to the Swiss-cheese model. According to Defence-in-Depth, in a hierarchical deployment, many tiers of equipment and processes are established to maintain physical barriers that protect workers, people, and environment from radioactive materials during normal operations anticipated operational occurrences, and accident conditions (IAEA INSAG-10, 1996). According to defense-in-depth explained in INSAG-10, the levels used in defense-in-depth are visualized in Figure 1.5 (IAEA INSAG-10, 1996) as follows. Therefore, nuclear power plants are designed with safety prioritized at every stage.

Another concern about nuclear power plants the public is their sensitivity to radioactive release. When appropriate security measures are taken and the construction of the power plant is carried out based on these safety criteria, there will be no polluting radiation released to the environment.

One of the concerns about nuclear power plants is nuclear waste. Nuclear wastes are including spent fuel and radioactive wastes that have high radioactivity and low volumes. Nuclear fuel is useful for 3-7 years in the reactor core. After removing the fuel from the reactor core, the spent fuel is highly radioactive, especially gamma radiation and neutrons emissions, and generates heat. This spent fuel is handled and stored in order to decay their excess heat and radioactive in a shielding environment (IAEA NW-T-1.24, 2013).

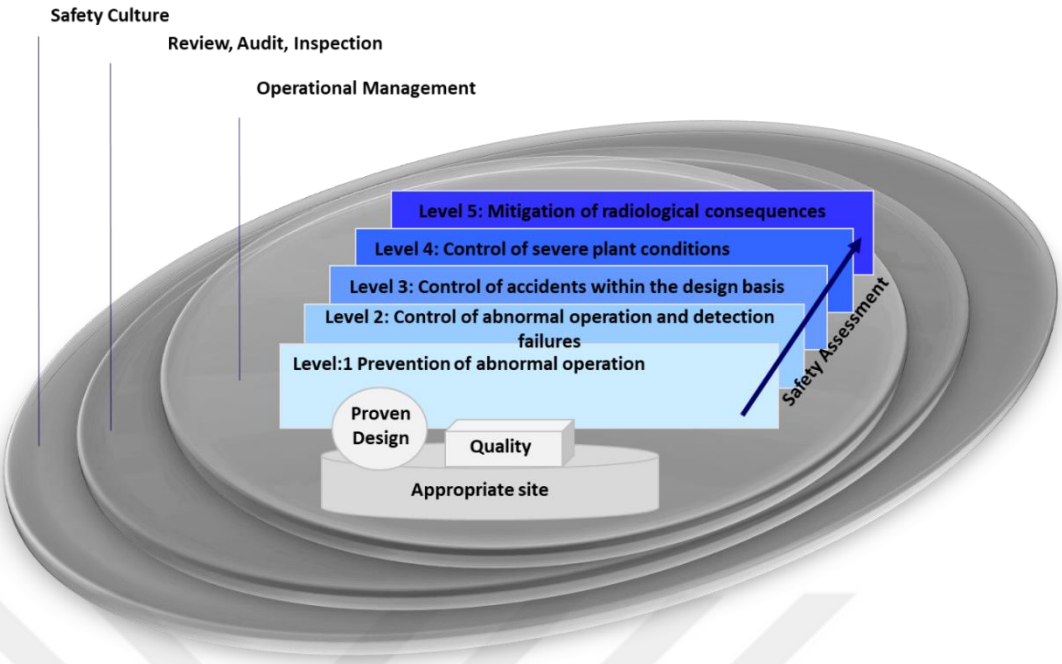

Figure 1.5 : Defense-In-Depth Concept.

Along with spent fuel, radioactive waste can also include concrete, metal, ion exchange filter, and TRU wastes. These are categorized with respect to their radioactivity levels, their forms, and their origins (IAEA NW-T-1.24, 2013).

According to data from IAEA, 2018, radioactive wastes and the overall amount of spent nuclear fuel released by nuclear power reactors are displayed by region in Table 1.1 (IAEA NW-T-1.14, 2018).

There are many waste management methodologies applied in the world. Technical options are important for safe management. Even though there are several waste management options, there are key paths for managing nuclear waste safely.

1.2 Justification

1.2.1 Turkey's view on nuclear

Turkiye's strategic plan stated that "Nuclear energy will be involve in our supply resources and attempts will be continued to expand its ratio in energy supply" (ETKB, 2019). Moreover, according to Turkish National Energy Plan declared in 2022, the installed capacity of nuclear power plants reaches 2.4 GW in 2025, 4.8 GW in 2030, and 7.2 GW in 2035 in total in the system. The portion of nuclear energy in primary energy consuming is 2.3% in 2025, 4.1% in 2023, 5.9% in 2035, and 29.3% in 2053.

Portion of nuclear energy resources in electricity production is 4.9% in 2025, 8.2% in 2030, and 11.1% in 2035 (ETKB, 2022).

The motivation behind the establishment of nuclear power plants in Turkiye is explained in MENR's strategic objectives as follows. “It is predicted that Turkiye's energy demand will reach 450-500 billion kWh in 2023. However, Turkiye's existing hydrocarbon reserves are insufficient to meet the increasing energy demand. It plans to invest in new, domestic, and renewable energy resources. The main course of this plan is nuclear power plants." (Enerji Proje Uygulama Dairesi, 2016).

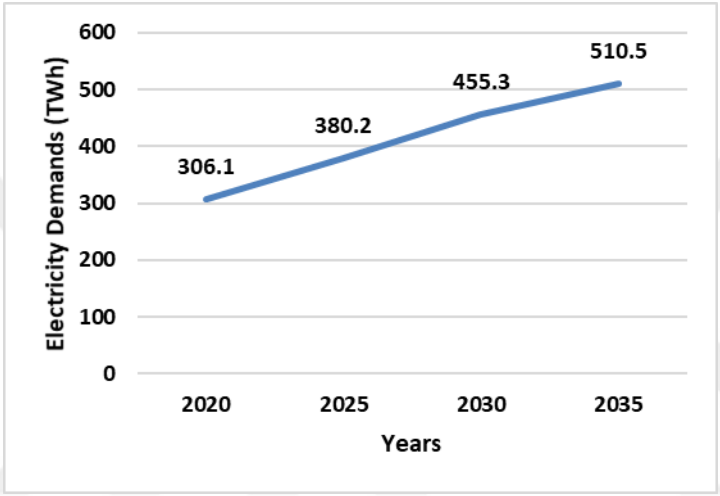

Figure 1.6 : Electricity demand in 2020-2035 according to Turkish National Energy Plan.

According to Turkish National Energy Plan declared in 2022, the electricity demand from 2020 to 2035 is increasing gradually to 300 TWh and it is expected to reach this value 500 GWh by 2035 (Figure 1.6) (ETKB, 2022).

The other motivation behind to establishment of the nuclear power plant is explained in MENR’s strategic objectives as follows:

There is more to nuclear power plants than just being a means of generating electricity. It should be highlighted that the nuclear power plant project, with its estimated 550000 components, would significantly boost the industry in our country by bringing dynamism and opportunities for employment to other sectors (Enerji Proje Uygulama Dairesi, 2016).

South Korea, is an example of the technological transfer from nuclear power that achieved to increase in the GNP from 280 dollars per capita in the 1970s to 30000 dollars per capita in 2017 (World Bank, 2021).

Table 1.1 : Total spent fuel and radioactive waste discharged from nuclear power plants or research reactors.

Region	Spent Fuel discharged from NPP (tHM)	Solid RAW in storage (thousand m^3)				Solid RAW in disposal (thousand m^3)			
		VLLW	LLW	ILW	HLW	VLLW	LLW	ILW	HLW
Africa	900	7	20	1	0	0	14	0	0
Eastern EU	40000	15	2479	101	7	1	911	7	0
Western EU	154100	224	355	269	6	277	1990	8	0
Far East	46400	5	311	4	0	0.8	63.9	0	0
Middle East and South Africa	NA	0	3	0	0	0	0	0	0
South East and Pacific	NA	0	5	1	0	452	4	0	0
North America	121200	2105	248	84	8	7147	17464	91	0
Latin America	5000	0	37	0	0	15	4.5	0	0
Total	367600	2356	3479	460	22	7906	20451	107	0

NPP: Nuclear Power Plant
tHM: ton Heavy Metal
VLLW: Very Low-Level Wastes
LLW: Low-Level Wastes
ILW: Intermediate-Level Wastes
HLW: High-Level Wastes

With the 12 nuclear power plants in 3 NPP sites planned to be established in Turkiye, the generated spent fuel and radioactive wastes in 60-year operation life are estimated based on generic data on the 1000 MWe as shown in Table 1.2 (Cacuci, 2010).

Table 1.2 : Generated spent fuels and radioactive wastes expected in Turkiye.

Nuclear Waste	Spent Fuel	ILW-LL	ILW-SL	VLLW
Amount	14900tHM	1200 m^3	78000 m^3	90000 m^3

ILW-LL: Intermediate Level Wastes- Long-Lived
ILW-SL: Intermediate Level Wastes- Short-Lived
VLLW: Very Low Level Wastes

1.2.2 History and future of nuclear for Turkey

With the world's decision to use nuclear power plants for peaceful purposes in the 1950s, Turkiye became one of the first countries to undertake nuclear initiatives. Turkiye was the first country to sign the "Atom for Peace" agreement with the United States in 1955. In this framework, a reactor committee was established at Istanbul Technical University (ITU) and Istanbul University (IU), and in 1958 it was handed over to the Atomic Energy Commission, and 1982 the Turkish Atomic Energy Agency (TAEK) was established (Ergün et al., 2012).

The idea of establishing a nuclear power plant in Turkiye is an idea that has existed since the establishment of the Atomic Energy Commission. For this purpose, various technologies were discussed with various countries. In 1976, the Mersin Akkuyu site license was obtained as a result of seismic survey results, soil mechanics research and, meteorological, and oceanographic evaluations. In 2010, IGA was signed between Turkiye and Russia for the Akkuyu site. In 2014, the Ministry of Environment and Urbanization approved Environmental Impact Assessment. In 2015, Akkuyu Nükleer AŞ, that is Akkuyu Project Company (APC), has been taken electricity generation license from Energy Market Regulatory Authority (EPDK). In 2017, APC applied for a construction license for the first unit and in the same year, a limited work permit for non-nuclear safety related are taken. In 2018, the construction license is granted and the construction for the first unit has been commenced. In 2019, the core catcher was installed. It is planned that the first unit will start operation in 2023. The construction of the second, third, and fourth units commenced in 2020, 2021, and 2022 respectively. (WNA, 2022).

Turkiye's second nuclear power station, Sinop Nuclear Power station, is anticipated to be established in Sinop. In 2013, an IGA was signed between Turkiye and Japan for the Sinop site. In 2020, after the evaluation of the feasibility report, it has been declared that the partner was reviewed because of falling short of expectations in terms of the construction budget and schedule. However, studies (site studies) for the establishment of an NPP in the Sinop area are currently ongoing. The Ministry of Environment and Urbanisation authorized the Sinop's final Environmental Impact Assessment report in 2020. For the project's support of more detailed feasibility studies, Fugro completed a six-month offshore site characterization project in August 2021 (WNA, 2022).

Thrace Region was confirmed as a third nuclear site in Turkiye by Minister for Energy and Natural Resources in 2018 (WNA, 2022).

Proposed and projected nuclear power plants in Turkiye are shown in Figure 1.7.

Since nuclear power plants are long-lasting and multi-phase projects such as licensing, operation, and decommissioning, Turkiye has been seeking alternative reactor projects such as small modular reactors. Turkish Nuclear Energy Company (TÜNAŞ, previous EUAS International ICC) signed a Memorandum of Understanding (MoU) with UK Rolls-Royce to evaluate the technical, economical, and legal applicability of UK SMR (WNN, 2020). Minister of Energy and Natural Resources stated, “In addition to conventional nuclear power plants, we will add SMRs to our energy portfolio as well as our nuclear power plants that are under construction and that we are planning." (Hurriyet Gazetesi, 2023).

1.3 Problem Statement

Besides the 60-year nuclear studies in research and development, industry, and medicine fields, with the 12 nuclear power plants in 3 sites planned to be established in Turkiye as shown in Figure 1.7 (WNA, 2022), it is necessary to make and accelerate the detailed and planned nuclear studies for the future. In this regard, the issue of nuclear waste, which is currently limited in Turkiye and thus has limited development, will gain importance in the next 50 years.

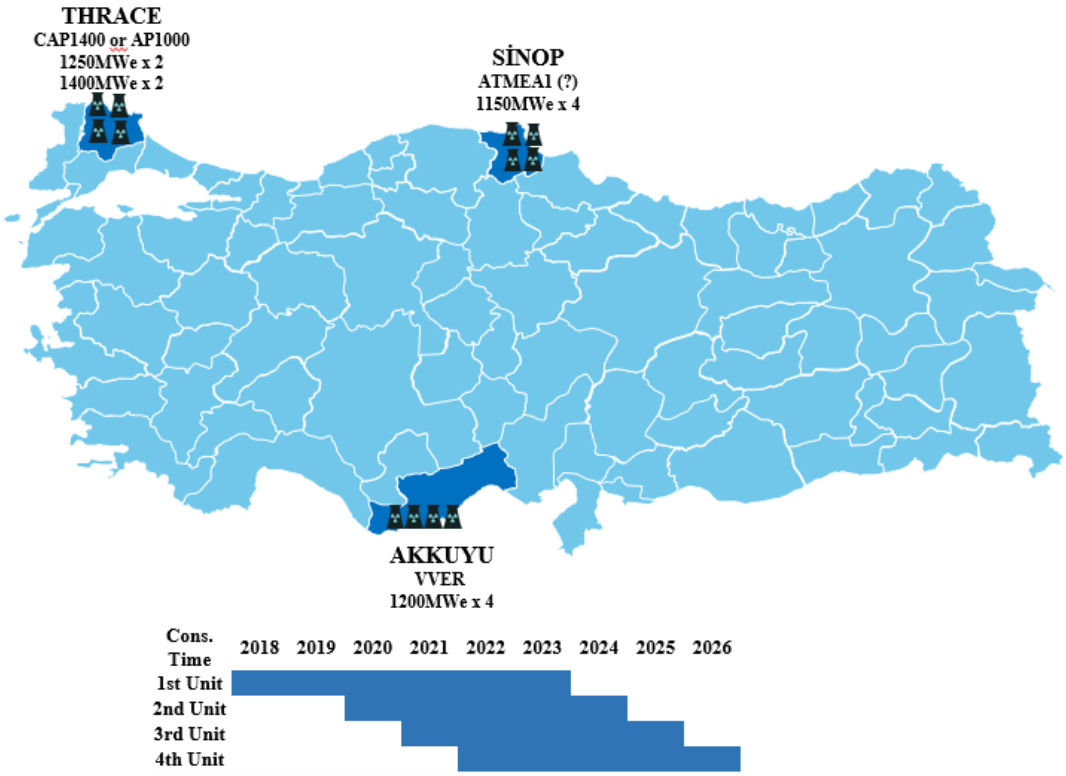

Figure 1.7 : Under construction, and proposed nuclear power plants in Turkiye.

Although many studies have been carried out on intermediate-level long-lived (ILW-LL) and high-level (HLW) nuclear wastes in the world, no agreement has been reached on final disposal and studies are continuing. There are two options for dealing with long-term management. The first is storage in geological formations. The second option is the recycling of fission products (Veliscek-Carolan, 2016). In both two options, there are HLW and ILW-LL radioactive wastes that should be disposed of. After the wastes are stored in geological formations, the most frightening scenario is the spread of radionuclides from the waste repositories to the geological formation and reaching aquatic environments and humans. To avoid this scenario, the use of multiple barrier systems, which is a combination of geological barrier and engineering barriers, is adopted. In order to prevent reaching radionuclides in the aquatic environments and humans, safety assessments such as interaction and redox phenomena between the radionuclide and barrier systems should be known. At this point, knowing the properties of the redox-sensitive radionuclides gain importance (OECD/NEA, 2003).

The most important of the redox-sensitive radionuclides found in nuclear waste is; uranium ($^{238+235}$U), neptunium (^{237}Np), plutonium (^{239}Pu), americium (^{240}Am), technetium (^{99}Tc), iodine (^{129}I), tritium (^{3}H), carbon (^{14}C), chlorine (^{36}Cl), cesium

(^{137}Cs), strontium (^{90}Sr), selenium (^{79}Se), and tin (^{129}Sn). Many studies examining the interactions of redox-sensitive radionuclides with barrier materials have been carried out for many years, especially uranium, iodine, chlorine, technetium, cesium, tritium and strontium are mostly carrying out redox-sensitive radionuclide; however, there are rare studies about selenium and tin (Akyil et al., 2003; Bodur, 2000; Gil-García et al., 2009; Hatipoglu1 et al., 1994; Iijima et al., 2010; Kaygun and Akyil, 2007; Kilincarslan and Akyil, 2005; Olmez et al., 2004; Ejeckam, 2003; Vilks and Baik, 2001; Wang et al., 2009; Yusan et al., 2012; Yusan and Erenturk, 2011).

1.4 Objectives and Aims of the Thesis

This study, it is aimed to develop and characterize new barrier materials with more effective and safe barrier properties that will be an alternative to existing barrier systems and to examine the applicability of these barrier materials for the retention of ^{126}Sn and ^{79}Se.

In this thesis project, it is planned to synthesize a polymer/clay nanocomposite material as a barrier material and to investigate the diffusion of redox-sensitive elements, whose interaction with this barrier material will be examined.

Although many studies in redox-sensitive radionuclide and barrier material interaction have been conducted, studies examining the interaction of long-lived ^{129}Sn and ^{79}Se with barrier materials are not common in the literature. For this reason, while the French National Agency for Radioactive Waste Management (Andra, France) requests the behavior of Se-containing waste packages before they enter the waste repositories (Aguerre and Frechou, 2006), some legal bodies in the world request the behavior of the Sn-containing waste packages before they enter the waste repositories (Silliková and Dulanská, 2017). In order to make a real risk analysis, it is necessary to know the behavior of Sn and Se in storage near and far fields.

The main objectives for attain the aim of this thesis can be given as follows:

- Development and characterization of polymeric nanoclay composites, which have more effective and safer barrier properties that have lower permeability, and higher selectivity against ions to be removed than traditional clay types used in geological waste areas,

- Determining the physicochemical behavior of ^{126}Sn and ^{79}Se in these developed barrier materials and examining the diffusion rates using surface-based reaction kinetic models,
- Establishment of adsorption isotherm models in order to examine the behavior of adsorption belonging to ^{126}Sn and ^{79}Se in barrier material,
- Examining the suitability of the developed barrier systems radiologically, radiological dose risk assessments of ^{79}Se and ^{126}Sn, which are long half-life fission products, can be created by the concentrations that diffuse into the barrier system, using the ERICA program,
- Evaluation of ^{126}Sn and ^{79}Se risk of accidental migration in radioactive waste storage using GOLDSIM Monte Carlo Simulation Software,
- Evaluation of carcinogenic and non-carcinogenic risks and excess lifetime cancer risks of ^{126}Sn and ^{79}Se.

Adsorption and diffusion behavior of ^{79}Se and ^{126}Sn in the barrier material to be synthesized, radiological risk assessment of the diffused part will be the original value of this study.

As a result of this study, it will contribute to the studies on the future of nuclear wastes generated from nuclear power reactors in operation and under construction and stored temporary wastes in the world. Thus, in case of an accident, the behavior of these radionuclides in the synthesized polymer/clay barriers, and the release of these radionuclides to the biosphere will be modeled and it will contribute to the studies carried out in the world for final storage.

2. LITERATURE REVIEW

2.1 Nuclear Fuel Cycle

The nuclear fuel cycle should be researched in order to comprehend the development of nuclear waste (Figure 2.1) (Peluzo & Kraka, 2022). Uranium exploration, which involved analyzing uranium ore using chemical and radiological methods, was the beginning of the nuclear fuel cycle. The uranium ore is mined by surface or open-pit mining technologies and underground methods. While surface or open-pit techniques are used for the shallow and soft deposits, underground techniques are used for the deeper and hard rock strata deposits (CEA, 2005; WNA, 2010).

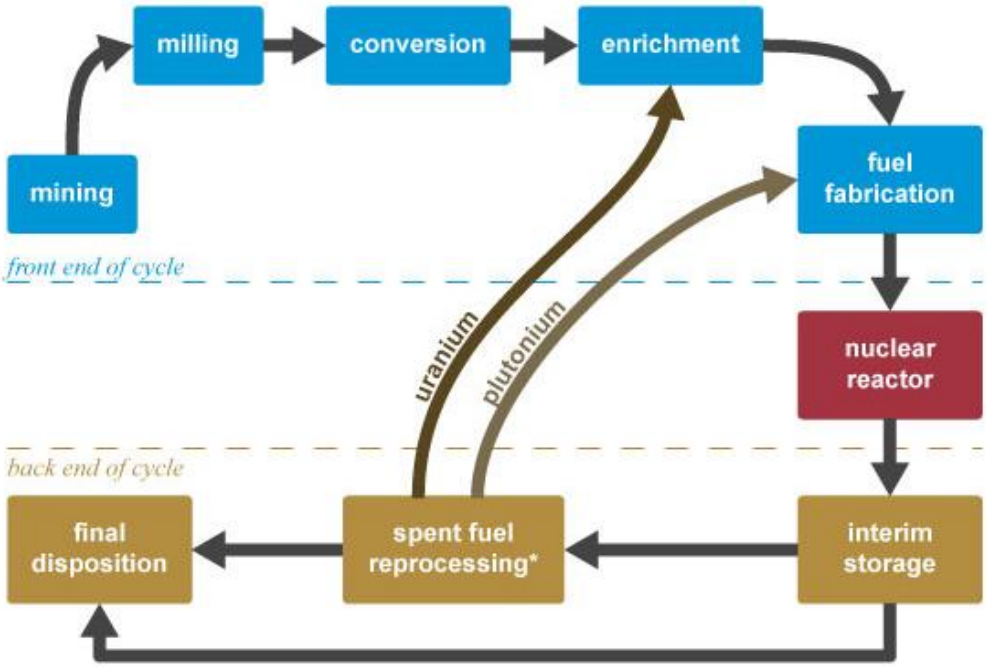

Figure 2.1 : Nuclear Fuel Cycle.

In order to obtain efficient nuclear fuel in a reactor, very high purity uranium is required to collision with the neutrons; therefore, the impurities should be removed not to absorb the neutrons. The first step of purification occurs in the milling step. After the mining of uranium ore, the milling or refining process is applied in close areas to the mining deposits to reduce the amount of uranium ore transportation

necessary. The separation of uranium ore from the bulky ore contains mechanical such as crushing and grinding, and chemical techniques such as leaching in acids, ion exchange, and solvent extraction operations. At the end of these procedures, ammonium diuranate known as the yellow cake is obtained. The remains from the ore such as residues or tailing should be sent to the disposed of (CEA, 2005; WNA, 2010).

After obtaining the yellow cake, chemical conversion is applied for being appropriate to enrichment operations for light water reactors. In the conversion step, the yellow cake is converted into uranium hexafluoride (UF_6) which is the only suitable uranium compound that gas at a low temperature. Two common techniques for conversion from yellow cake into UF_6. Dry fluoride volatility is the first process. In this process, the evenly proportioned yellowcake was reduced to uranium dioxide by reacting with hydrogen at a high temperature. Uranium tetrafluoride (UF_4) is created when hydrofluoric acid reacts with the newly formed UO_2. To create UF_6, UF_4 reacts with gaseous fluoride. In the distillation phase, the light fraction gases and contaminants are eliminated to create pure liquid UF_6 (CEA, 2005; WNA, 2010).

The other technique is the wet process. In the wet process, the yellow cake is treated with nitric acid, extracted by selective solvent, evaporated, denitrated, reduced, hydrofluorinated and fluorinated (CEA, 2005; WNA, 2010).

Some steps such as reduction, hydro fluorination, and fluorination in wet and dry processes are similar; however, in distillation step in the dry process is not required for the wet process because of the involving front-end treatment (CEA, 2005; WNA, 2010).

At the end of the conversion step, the highly purified UF_6 at ^{56}F is obtained for the enrichment steps.

The next phase is the enrichment process, which is the essential step in the preparation of the nuclear fuel for the light water reactors. Natural uranium has two isotopes; however, the most abundant isotope is uranium-238 whose abundance is 99.3% and the other is uranium-235 whose abundance is 0.711%. In light water reactors, the ^{235}U is required for the efficient fission reaction to produce heat. Therefore, in the production of nuclear fuel for light water reactors, a fraction of the ^{235}U is required to enrich to the 2-5% abundance. For enrichment, isotope separation is applied not

chemically but physically. There are two common methods for enrichment (CEA, 2005; WNA, 2010).

- Gaseous diffusion is based on molecular diffusion (NMT, 2020). The thin and semi-porous barriers hold the heavier uranium atoms (^{238}U). Therefore, after accumulating, the ^{235}U concentration is increased (Figure 2.2) (NMT, 2020).

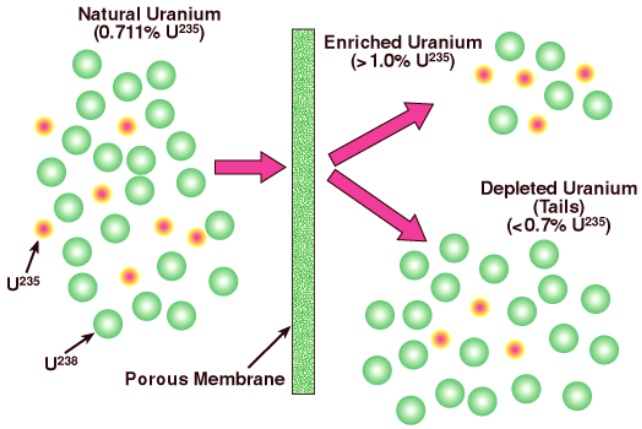

Figure 2.2 : Gaseous Diffusion Uranium Enrichment Process.

- Centrifuge based on the molecular weight. (NMT, 2020). The mixed uranium concentration is subjected to a high-speed centrifuge. The lighter uranium atom (^{235}U) are accumulating in the center and heavier uranium atoms (^{238}U) are driven to the outside (Figure 2.3) (NMT, 2020).

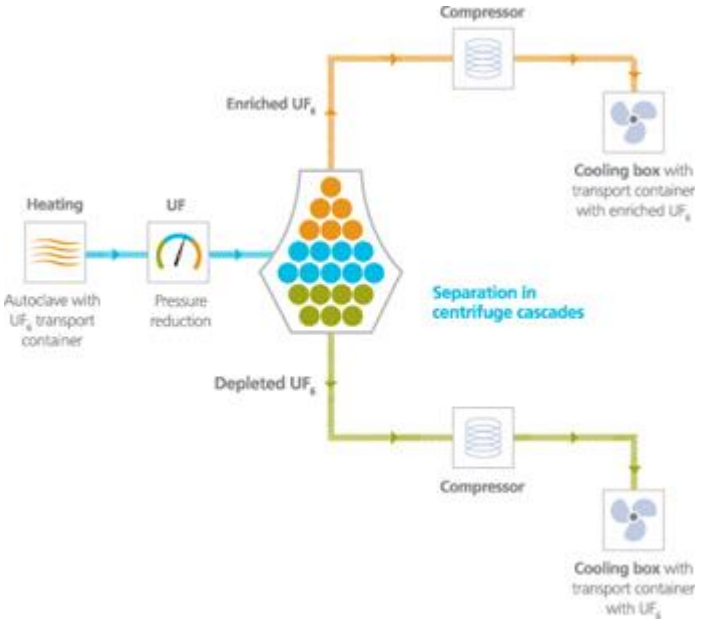

Figure 2.3 : Centrifuge Uranium Enrichment Process.

Fuel fabrication is the final step to producing uranium fuel. In the fuel fabrication step, the enriched UF_6 is converted to the UO_2 by chemical treatment. Long piles of cylindrical pellets made from produced enriched UO_2 powders are placed into zirconium-alloy cladding tubes. These fuel rods are bundled in a technology array. Generally, square arrays are used in light water reactors; however, the Russian designs are used in the hexagonal form (Figure 2.4) (Aksenov, 2004; CEA, 2005; WNA, 2010).

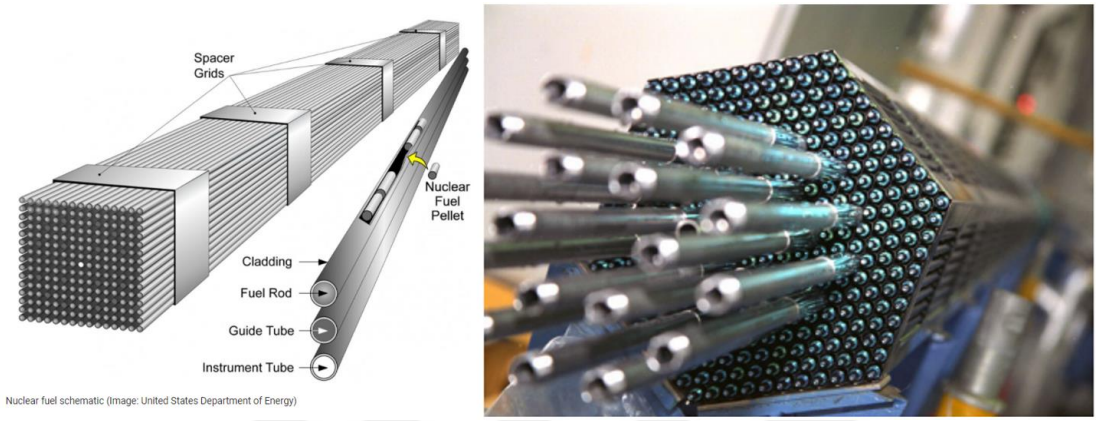

Figure 2.4 : Fuel Assemblies used in LWR and Russion design reactors.

After preparation of the fuel assemblies and loading to the reactor, reactor, ^{235}U is bombarded by the neutrons and splits and releases the energy and fission products. By the way, the neutrons are absorbed by the ^{238}U and ^{239}Pu are produced. After years, the fuel assemblies become depleted by the neutron-absorbing fission products and cannot release energy efficiently. At this point, the fuels are considered spent fuel. They have been taken out of the reactor and placed in the spent fuel pool to cool and decay radioactivity (Figure 2.5) (CEA, 2005; WNA, 2010).

After the cool-down heat and radioactivity, there are two options for the journey of fuel according to the national policy. The first option, which is called an open nuclear fuel cycle, is to send the spent fuel to the disposal in a deep geological repository directly. The second, which is the closed nuclear fuel cycle, is to reprocess the spent fuel. In reprocessing, the U and Pu in spent fuel are extracted from the spent fuel and are sent to the fuel fabrication steps for the produce MOX fuel. The remains from the separated spent fuel are considered high-level waste and it is also sent to the deep geological repository. Therefore, in both options, the final station is the geological repository (CEA, 2005; WNA, 2010).

Figure 2.5 : Spent Fuel Pool in Central Interim Storage Facility (CLAB), Sweden.

According to their national policy, some countries such as Finland, Sweden, and USA adopted the open nuclear fuel cycle while Japan, Russia, India, France, China, Russia, and the UK adopted the closed fuel cycle. Because the deep geological formation is the final step of the nuclear fuel cycle, the countries that are adopted either closed or opened nuclear fuel cycle have much research for the final repository. The accepted technique suggested by the researchers and adopted by the countries is the multiple barrier system. Multi-barrier system is a concept of consisting the both an engineered barrier and a natural barrier. In the engineered part, organic and inorganic components are used while in the natural part, the crystalline bedrock, salt, and clay mining sites are used (CEA, 2005; WNA, 2010). For details the “Chapter 2.2.3 Disposal ".

2.2 Radioactive Wastes

2.2.1 Classification and production of radioactive waste

Radioactive waste can be defined in regard to its physical properties at the generation stage, its source, and its radioactivity levels. This is important because the wastes are treated considering their classification (Nagasaki and Nakayama, 2015).

The first method is classifying in terms of their physical properties at the generation stage. According to this classification method, radioactive wastes can be classified as gaseous, liquid, or solid forms (Nagasaki and Nakayama, 2015).

Gaseous wastes are the wastes that gaseous particles with stuck radioactive materials. These gaseous wastes are comprised of exhaust gas for BWR, purge gas for PWR, and vent gas from different parts. These gaseous include radionuclides such as ^{88}Kr, ^{131}I, and ^{133}Xe. After radiation decay, these gaseous wastes are filtered generally, HEPA filter for removing particulate matter, and this removed particulate matter are subjected to solidification by solidification agent for storage in a durable structure (Nagasaki and Nakayama, 2015).

Liquid wastes are generated during both reactor operations as a coolant, drain, and laundry wastewater and the spent fuel reprocessing and acid recovery process. In terms of their contents, either may be subjected to volume reduction, filtration, evaporation, ion exchange, and solidification or denitrification and solidification (Nagasaki and Nakayama, 2015).

After the treatment processes, the radionuclides in gaseous and liquid wastes are to be solidified and the residue from the radionuclides in gaseous and liquid wastes is discharged after confirming their radioactivity concentration below the regulatory limits (Nagasaki and Nakayama, 2015).

Solid wastes are varied their generation and radioactivity level. Besides the solid radionuclide in gaseous and liquid wastes, paper, fabric, wood chemical matters, and plastics can be defined as compacted and flammable while earth sand, glass, metal, and concrete can be defined as compacted and incombustible. After volume reduction by compacted and combustion, solid wastes are subjected to solidification in metal drums or predetermined containers (Nagasaki and Nakayama, 2015).

The second method of classifying radioactive waste is the classification by source. In the nuclear fuel cycle, varied radioactive levels and different physical forms of radioactive waste are generated. This waste is generated during the process of uranium mining and melting activities, fuel fabrication process, nuclear power plants, reprocessing process, medical and research institutions. Wastes generated in the uranium mining and milling activities are generally low-level (Nagasaki and Nakayama, 2015).

Radioactive wastes comprise the refining effluent, gangue, tailing of ore after uranium mining, and wastes from facility maintenance. Waste can be generated in the uranium fuel fabrication or MOX fuel fabrication. The MOX fuel fabrication is similar to the reprocessing wastes. Its content is generally TRU waste while the fuel fabrication waste includes uranium waste. In the nuclear power plant, wastes are generated in liquid, gaseous, and solid in high-level, low intermediate and very low radioactive wastes. High-level wastes generated in the NPP can be characterized as reactor core internals, spent control rods, and channel boxes. The low-intermediate level waste generated in the NPP can be tagged as filters and spent ion exchange resin. Very low level generated in the NPP is characterized as concrete metals. Wastes generated in the reprocessing facilities are generally high-level wastes and include a greater content of TRU nuclides. Wastes generated in medical and research institutions can be radioisotope wastes such as components, ventilation filters, medical equipment, and used test specimens (Nagasaki and Nakayama, 2015).

The last and most commonly used authorities' classification method is the classification according to the radioactivity level. According to the classification method, radioactive wastes can be classified as very low level, low level, intermediate level, or high level. There are no strict thresholds among these levels. Although there is the high-level consensus on this classification, there are a few differences in application. In IAEA classification, radioactive wastes can be classified are high-level wastes, intermediate-level wastes, low-level wastes, very low-level wastes very short-lived wastes and exempt waste. (Figure 2.6) (IAEA GSG-1, 2009).

According to IAEA GSG No-1 (IAEA GSG-1, 2009), the classification of radioactive wastes is defined as follows:

- Exempt wastes are defined as that wastes cannot exceed the clearance or exempt level of the original regulatory body for radiation protection. They do not have to be subject to extra protection for radiation precautions.
- Very short-lived waste (VSLW) is described as that waste consisting of the short-lived half-life radionuclides and their activities are above the clearance level.

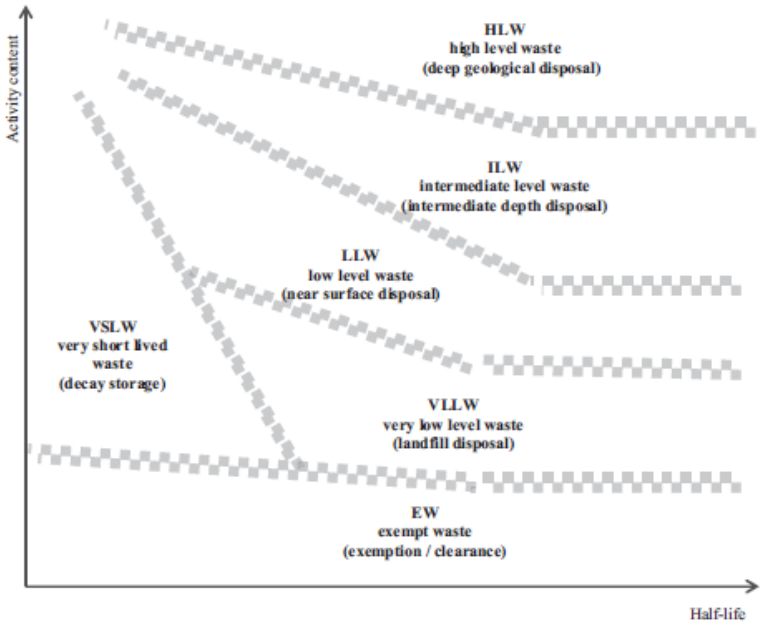

Figure 2.6 : Classification of Radioactive Waste in IAEA.

- Very low-level wastes (VLLW) are defined as wastes above the clearance level but not required for high-level isolation and containment. These are appropriate for near-surface landfill disposal with the control of related authorities. This type of waste contains generally generated soil and rubble during mining activities.
- Low-level waste (LLW) is explained that wastes above the clearance level containing a large variety of the radionuclides such as short-lived but higher activity level, but long-lived but lower activity level.
- Intermediate-level waste (ILW) is defined as wastes are required higher containment and isolation than LLW waste disposal because of its content. ILW generally contains long-lived radionuclides especially alpha emitted and needs to be decayed for activity and heat.
- High-level waste (HLW) is characterized as wastes containing high-concentration activities and heat radionuclides.

While the IAEA classification is defined as above, radioactive waste classification is varied from to country-to-country. For example, In France, the matrix structure is formed for the radioactive waste classification based on the activity level and activity

period, and their treatments are done based on these classifications (Table 2.1) (OECD/NEA, 2015).

In Sweden, the radioactive waste classification is different from the IAEA and France classification methods. In Sweden, the radioactive wastes are classified as Very Low-Level Waste (VLLW), Low Intermediate-Level Waste Short-Lived (LILW-SL), Low Intermediate Level Waste Long Lived (LILW-LL), and Spent Fuel (SF). VLLW originated from the operational waste, decommissioning waste, and waste produced in the fabrication of fuel. LILW-SL are consisting of waste during operational and decommissioning phases, disused sealed sources, and institutional waste. Transuranic waste (TRU-waste), internal components, and high-activity sealed sources constitute LILW-LL. Spent fuel is spent nuclear fuel (OECD/NEA, 2020)

Table 2.1 : Classification of Radioactive Wastes in France.

Activity/period	Very short lived	Short lived	Long lived
Very low level	Management by radioactive decay.	Morvilliers in the Aube disposal facility.	Morvilliers in the Aube disposal facility.
Low level	Management by radioactive decay.	Surface Disposal in Aube.	Dedicated subsurface disposal facility designed for the radium bearing.
Intermediate level	Management by radioactive decay.	Surface Disposal in Aube.	Waste management solution under solution.
High level	Management by radioactive decay.	Waste management solution under solution.	Waste management solution under solution.

Japanese radioactive waste classification is relying on the activity, origin, their activity period as follows (OECD/NEA, 2011):

- High-Level Radioactive Waste (HLW) is composed of both the highly active liquid that results from the reprocessing of spent nuclear fuels and the solid waste that is created when the liquid is vitrified.
- Low-Level Radioactive Waste (LLW*)* is composed of various facilities other than HLW.
- Waste Generated by Nuclear Reactors is major form of LLW.
- Very Low-Level Radioactive Waste (VLLW) is an element of the LLW without the requirement for engineered structures or encapsulation.

- Long Half-Lived Low-Heat Radioactive Waste emerge from the manufacturing of mixed oxide fuel, which includes the TRU waste, and the reprocessing of spent fuel
- Waste from Uranium Fuel Fabrication Facilities is produced during fuel fabrication activites such as fuel fabrication, enrichment actitivies or other similar works. It includes very long-lived uranium and its daughter. This form of waste is primarily VLLW.
- Radioactive Waste from Radioisotopes Use, Nuclear Research and Other Related Facilities are produced generally from medical and industrial facilities.

In England, according to the Office of Nuclear Regulation (ONR), radioactive waste is considered into different categories. High-Level Radioactive Waste (HLW) includes residue from spent nuclear fuel reprocessing. Although intermediate-level radioactive waste (ILW) has a higher radioactivity than low-level radioactive waste (LLW), it does not create sufficient heat to require special concern when establishing storage or disposal facilities. ILW can comprise metal objects like fuel cladding, graphite located in reactor cores, reactor components, and residue from the treatment of liquid effluents. It mostly results from the spent fuel reprocessing acitivies as well as from regular operations and maintenance at nuclear installations. The radioactive concentration of LLW is less than 4 GBq/te of alpha activity or 12 GBq/te of beta-gamma activity. LLW emerges materials during operation, maintenance, and monitoring like plastic, paper, and metal as well as materials during decommissioning like metal parts of reactor and metal equipment, building materials and soil. A subcategory of low-level radioactive waste (LLW), very low-level radioactive waste (VLLW), has been declared obsolete by 2011 legislative changes. Exempt waste is waste for which environmental authorities do not need to provide a radioactive substances permit or license. Exempt waste could be governed by additional environmental regulations due to its non-radiological properties. Higher Activity Radioactive Waste (HAW) is a broad term that covers all HLW, ILW, and certain wastes that are classified as LLW but are presently unsuitable for disposal in LLW facilities (ONR, 2015)

Turkiye has adopted the IAEA radioactive waste classification according to Turkish Regulation on Radioactive Waste Management published in the Official Gazette dated March 09, 2013, and numbered 28582 (NDK 28582, 2013).

Nuclear Regualtory Authority (NDK, formerly known as TAEK) Regulation on Radioactive Waste Management (Official Gazette Number: 28582, Date of Issue: 09.03.2013) (NDK 28582, 2013) defines radioactive waste similarly to in IAEA definition except for the approach the low and intermediate level waste together. According to related regulations;

- Exempt waste that has activity levels below the allowed limits specified in the "Radiation Safety Regulation" is exempt from regulatory control. The "Regulation on Clearance in Nuclear Facilities and Removal of Site from Regulatory Control" describes the clearance levels, processes, and guidelines for radioactive materials and wastes that are products of nuclear installation-related operations.
- Very short-lived radioactive wastes (VSLW) are wastes that are over the exemption level but are eligible for releasing after a storage duration of at most a few years.
- Very low-level wastes (VLLW) are wastes whose activities are higher than exemption levels, and they are not categorized as very short-lived wastes when their activity concentrations are less than about one hundred times the clearance limits.
- Low and Intermediate level radioactive wastes (LILW) are wastes whose activity concentrations exceed those of VLLW and they are not characterized as high-level radioactive wastes.
- High-level radioactive wastes (HLW) are described as spent fuels and byproducts of reprocessing that authority has accepted and may contain fission products and actinides and other radioactive wastes with activity levels that are comparable to those stated aforementioned.

2.2.2 Radioactive waste management and immobilization

Because nuclear power is vulnerable due to its waste, safe and economic radioactive waste management gains more importance. Developing current and new technologies on radioactive waste management have some targets such as reducing the secondary radioactive waste generation, reducing in activity and volume of radioactive waste management, stabilizing waste so that safe handling, transportation, and disposal of

radioactive waste, and reducing released radiation to environment and people (Nuclear Energy Agency, 2003).

Toward these goals, radioactive wastes are treated so that separated and removed from radionuclides. To add to these treatment processes, the barrier system is used to radionuclides cannot attain the groundwater and groundwater cannot attain the radioactive waste area (Nuclear Energy Agency, 2003).

Produced radioactive wastes in nuclear facilities are subjected to three main processes: treatment, transport to the disposal sites, and disposal (Nagasaki and Nakayama, 2015).

Radioactive waste management is applied in order to the radioactive wastes should be disposed of in a safe manner no matter their volume and characteristics. However, the huge volumes and many varied characteristics jeopardize the safe manner of disposing of radioactive waste because the variation of characteristics and huge volumes need varied techniques and more attention. In the framework of this goal, the radioactive wastes are subjected to some treatment technologies that reduced volume and classified the radioactive wastes (Nagasaki and Nakayama, 2015).

Treatment includes three main stages: pre-treatment, treatment, and conditioning (Nagasaki and Nakayama, 2015).

In the pre-treatment stage, wastes are collected, separated, conditioned as chemical components, and decontaminated. Especially liquid and gaseous wastes are decontaminated and reduced in radioactivity concentration to the below clearance limit. Non-radioactive wastes are separated in this stage. The remaining wastes that are above a certain level in radioactivity concentration are passed to the next stage (Nagasaki and Nakayama, 2015) .

The treatment process includes filtration, ion exchange, coagulation, and sedimentation in order to increase safety by changing the properties of radioactive wastes. At the end of the treatment process, some wastes are considered non-radioactive wastes because of the removal of radionuclides (Nagasaki and Nakayama, 2015).

In the conditioning process, radioactive wastes are converted to solid form in sealed containers and packaged in order to safely handle, transport, and the store even disposed of (Nagasaki and Nakayama, 2015).

2.2.2.1 Gaseous waste treatment

In the treatment of radioactive gaseous waste, standard treatment methods are adsorption, filtration, dilution, and attenuation. Radioactive waste in gaseous forms should be thought as

- Radioactive noble gases, i.e. Kr and Xe
- Radioactive iodine
- Particulate matter.

The generated radioactive noble gases in the nuclear power plant are Kr and Xe isotopes as shown in Table 2.2 (Nagasaki and Nakayama, 2015).

Table 2.2 : Half-lives of the Noble Gases in Nucleat Power Plant.

Radioactive Noble Gases	**^{85m}Kr**	**^{87}Kr**	**^{88}Kr**	**^{133}Xe**	**^{133m}Xe**	**^{135}Xe**	**^{138}Xe**
Half life	4.4h	78 min	2.77 h	5.27 d	2.3 d	9.13 h	17 min

The short-lived noble radioactive gaseous waste is subjected to attenuation effect and dilution. However, long-lived noble radioactive gaseous waste is passed through charcoal for a set duration of time to decrease radioactivity. After reaching below the regulatory clearance limits, they are released into the atmosphere.

Radioactive iodine is produced in different chemical forms from nuclear power plants such as I_2, HOI, HOI_3, HIO_4, or organic iodine compounds (CH_3I, C_2H_4I).

Elemental I_2 (8.02 day) removal in charcoal is easy. The adsorption of elemental iodine in charcoal can be shown in Equation 2.1 (Nagasaki and Nakayama, 2015).

$$\eta = \frac{C_{in} - C_{out}}{C_{in}} = 1 - \exp\left(-K_c . A_s . \frac{L}{U}\right) \quad (2.1)$$

C_{in}, radioactive iodine concentration at the inlet filter (Bq m^{-3})

C_{out}: radioactive iodine concentration at the outlet filter (Bq m^{-3})

η: accumulaton efficiency

K_C: gas film mass transfer coefficient (m s^{-1})

A_S: surface area belonging to the activated charcoal particles (m^2 m^3-activated $charcoal^{-1}$)

L: the activated charcoal bed thickness (m)

U: rate of filtration (m s^{-1})

Isotope exchange process employs the iodine filtration technique as organic iodine molecules are less stable than elemental iodine. In iodine, filters contain activated charcoal with potassium iodine, and iodine and radioactive iodine are interchanged for the iodine without radioactivity in the filter is shown as Equation 2.2 (Nagasaki and Nakayama, 2015):

$$\text{KI (activated charcoal)} + CH_3 * I \rightarrow K * I(activated\ charcoal) + CH_3I \quad (2.2)$$

Particulate matters in submicron to a few microns in size are generated in nuclear facilities. These particulates are accumulated by pre-filters and high-efficiency particulate air (HEPA) filters.

Pre-filters are used for rough particles whose size is up to 50 μm in diameter while HEPA filters are used for fine particles whose diameter is up to 0.3 μm at an efficiency of 99.98%. To increase the efficiency, the filtration surface area is increased by folded of the HEPA filters. Fibrous filters in HEPA filters capture the coarse particles by inertial collisions and fine particles by collision with the diffusion sourced by Brownian motion. The efficiency of the HEPA filters is calculated as Equation 2.3 (Nagasaki and Nakayama, 2015).

$$\mathrm{E} = \frac{C_{in} - C_{out}}{C_{in}} \quad (2.3)$$

E: capture efficiency of HEPA filters,

C_{in}: aerosol concentration measured value at the filter inlet,

C_{out}: aerosol concentration measured value at the filter outlet

Besides the HEPA filters, ultra-low penetration air (ULPA) filters whose efficiency is 99.9995% are used in clean rooms. For a comparison of the HEPA filter and ULPA filters, an example can be given. While HEPA filters capture pollen, mold spores, and some cigarette smoke particle whose sizes are 30 μm, 5-10 μm, and 0.01–10 μm, respectively; ULPA filters can only capture the flu viruses whose diameter is 1 μm (Nagasaki and Nakayama, 2015).

2.2.2.2 Liquid waste treatment

Liquid radioactive wastes are treated by concentration and separation of radionuclides. At the end of these processes, the wastes without radioactivity and below the regulatory clearance limit are released into the environment. These are applied to reduce in volume and solidify for easy to handling, transport, and disposal (Nagasaki and Nakayama, 2015).

Treatment methods for liquid wastes can be coagulation-sedimentation, adsorption, evaporation, filtration, and ion exchange. Among treatment methods, the one which is appropriate is determined by the liquid waste properties such as radioactivity level, ion content, and the amount and solid materials (Nagasaki and Nakayama, 2015).

Coagulation-sedimentation, adsorption, method is a procedure that added chemicals into a liquid with insoluble and forms precipitation by removing selected ions and chemicals. In this method, the precipitates are produced by chemical reaction and this method is not appropriate for the liquid containing dissolved constituents (Nagasaki and Nakayama, 2015).

Coagulation-sedimentation method is composed of four main process

- Addition chemicals and pH adjuster to form a precipitate
- Coagulation
- Sedimentation
- Liquid-solid separation (Nagasaki and Nakayama, 2015)

Filtration is the method based on solid-liquid separation in the liquid with insoluble constituents by the filtering medium. These filters in the medium can be produced by using precoat filters, membrane filters, or mechanical filters. Besides these, the solid contents can be removed from liquid waste by using microfiltration, nanofiltration, ultrafiltration and reverse osmosis. These are used for fine particles. While microfiltration uses a symmetric membrane and so effect uniformly entirely, nanofiltration, ultrafiltration, and reverse osmosis use the asymmetric membrane and these use the sieving effect or molecular diffusion for different particle sizes (Nagasaki and Nakayama, 2015).

The evaporation process is the method removing of volatile liquid waste by evaporation by heaters and non-volatile radionuclides are condensed in the remaining liquid waste. Although this method is appropriate for both dissolved and insoluble

constituents especially liquid waste with coarse solid particles and remaining waste from the ion exchange process, the high cost and the small facilities for evaporation are disadvantages (Nagasaki and Nakayama, 2015).

The ion exchange process is the method that removes ions from liquid waste by ion exchanges. This process is more suitable for liquid wastes with small amounts of dissolved ions than liquid waste with high concentrations. Moreover, despite the need for high skill, resin, and resin generation procedures are expensive. Ion exchangers can be synthetic organic ion exchange resin or inorganic ion exchange resins. Synthetic ion exchange resins are produced as functional groups such as positively or negatively ion exchange resin such as H^+ or OH^-. The inorganic ion exchange resin is generally produced from clay materials such as vermiculite and montmorillonite.

The ion exchange method is appropriate for the dissolved constituents, and ions because of the aim the removing ion. However, ion exchange capacity is a constraint for removing the ion (Nagasaki and Nakayama, 2015).

2.2.2.3 Solid waste treatment

Solid wastes are treated by incineration, compaction, and melting based on the radioactive waste type and solidified using an agent.

Some solid waste produced from the operation and maintenance of facilities can be flammable such as rubbers and these wastes can be treated by incineration to reduce volume and produce chemically stable residue that is incineration ash. Theoretically, with the assumption of the 21% of O_2 content of the air, the equation should be defined as Equation 2.4 (Nagasaki and Nakayama, 2015).

$$L_0 = \left(\frac{c}{12} + \frac{h}{2} + \frac{s}{32} - \frac{o}{32}\right).\frac{22.4}{0.21} \qquad (2.4)$$

L_0: the hypothetical flammable air (Nm^3 kg-$waste^{-1}$),

c, h, s, o: carbon, hydrogen, sulphur, and oxygen mass respectively per unit mass of waste (kg kg-$waste^{-1}$).

Unburned gas and ash are created because the flammable air is inadequate for an entire combustion. Therefore, the surfeit air combustion should be taken into account; this is varied based on the waste quality. The used equation is shown below Eq. 2.5 and Eq 2.6 (Nagasaki and Nakayama, 2015). The first part of the equation shows the CO_2

generated, the second one shows H_2O generated, the third one shows SO_2 generated, the fourth one shows excess O_2, and the fifth and sixth parts show N_2 from the air and N_2 generated.

$$V_w = 22.4\left(\frac{c}{12}\right) + 22.4\left(\frac{h}{2} + \frac{W}{18}\right) + 22.4\left(\frac{s}{32}\right) + 0.21(\lambda_a - 1)L_0 \quad (2.5)$$
$$+ 0.79\lambda_a . L_0 + 22.4\left(\frac{n}{28}\right)$$

$$= 1.867c + 11.2h + 1.244W + 0.7s + 0.8n + (\lambda_a - 0.21). L_0 \quad (2.6)$$

V_w : wet flammable gas amount ($N_m^3\ kg^{-1}$-waste),
N : respective nitrogen mass (kg kg^{-1}-waste),
W : the water per unit mass of waste (kg kg^{-1}-waste).

Incineration systems are composed of a tank including waste, incinerator, and ash recovery area off-gas treatment equipment especially for ^{3}H, ^{14}C, ^{129}I, and other components (Nagasaki and Nakayama, 2015).

Compaction is a method that is used for waste volume reduction. For compaction generally, the used force is 50 kN to 3 M. Therefore, the waste can be reduced to 1/10. There are two methods for compaction. The first is the compaction of the drum that contains the waste and the compaction of waste in pressing chambers (Nagasaki and Nakayama, 2015).

Another treatment method for solid wastes is melting which provides significant volume reduction and distributes the radionuclide homogeneously and stabilizes the waste. In the melting method, wastes are given high temperatures up to their melting point, about 1500°C by the plasma heating method, the high-frequency induction heating method, the Joule heating method and the microwave heating method. This method is applicable to wastes that are neither conductive nor flammable such as concrete, glass, and insulation materials. As a result of the melting method, nitrogen oxides are generated and an off-gas treatment system should exist to protect the environment (Nagasaki and Nakayama, 2015).

Besides the solid wastes, after the treatment remaining the liquid and gaseous wastes are solidified and packaged in the drums. Solidification varies depending on the disposal area properties (Nagasaki and Nakayama, 2015).

For low-level radioactive waste, cementation is a widely used treatment methodology for a long time because of the low cost and maintenance required; however, the poor chemical compatibility is poor because of the varying water/cement ratio (Nagasaki and Nakayama, 2015).

Bituminization is the methodology that mixing of low-level liquid or slurry waste with the melting asphalt by heating. This method is beneficial because the asphalt is water-insoluble and shows a high resistance to water diffusion, which means the radioactive wastes, are in safe. Moreover, its cost is low. However, the waste solidified with the bitumen is flammable because the bituminized waste can react with the oxidants such as sodium nitrate. There is fire accident in several countries such as Japan because of bituminization. Moreover, the waste solidified with bitumen has less resistance to radiation than cementation. In other words, radiation generated from waste deteriorates waste solidification. Therefore, the bitumen is limited to use with low-level radioactive waste (Nagasaki and Nakayama, 2015).

For high-level radioactive wastes, vitrification is a commonly used treatment solidification methodology because of the leaching resistance, thermal stability, and radiation resistance. Among the glass adjents, borosilicate glass that is composed of Silicon (Si) and boron (B) is commonly preferred. Some radionuclides in the high-level wastes such as Cs, Sr, and agents such as Na, Li, and Ca are fitted into the glass network as a network creator ion. In vitrification solidification, the liquid wastes and glass material are melted at about 1200°C and this molten glass is poured at the bottom of the stainless steel canister. These are kept for approximately 30-50 years and short-life time radionuclides decayed at this period. After storage, the vitrified canisters are sent to the disposal area (Nagasaki and Nakayama, 2015).

2.2.3 Disposal

Packaged waste forms are transported to the disposal site. There are many controversial disposal sites such as underground; disposed of in overseas, disposed of in sub-seabed, disposed of in ice sheets, and extra-terrestrial disposal. However, among all potential disposal sites, the most applicable site is disposed underground, which is geological disposal (Nagasaki and Nakayama, 2015).

The first concept of geological disposal for radioactive wastes was mentioned in the US National Academy of Sciences. This report is relying on the assumption the liquid

wastes are directly injected into the salt-based geological disposal area and that the convenient time span for the disposition of the radioactive waste was 600 years. Then in Polvanni's report in 1970 and Swedish KBS concepts in the 1980s were established and these are pointed the todays geological disposal systems. According to these systems, the underground tunnel should be excavated and the radioactive wastes packed in corrosion-resistance containers should be placed. However, the challenge is that such type systems are thought to disposition for such radioactive waste the more than 10000 years. Therefore, over the 30 years, the safety and verification of such type systems are developed in R&D projects (Nagasaki and Nakayama, 2015).

Although the disposal of radioactive waste may vary with regard to its content, the type of radioactive waste, and the half-lives of the radioactive waste, the main point should be that the exposure dose for the public should be within the specified limits of ALARA. Taking into this consideration, the radioactive waste repository is constructed based on the multi-barrier systems that consist of an engineered barrier or technical barrier and geological or natural barriers (Nagasaki and Nakayama, 2015).

Geological barriers protect the engineered barriers from external events such as the groundwater, the chemical condition (dissolved oxygen amount in groundwater), and mechanical condition (stresses on tunnels, backfilling material, and canister) and maintain the integrity and function of the engineered barriers. Engineered barriers have the main function of deceleration of the radionuclides release from radioactive wastes to nature. Engineered barriers are expected to design based on the geological barriers; therefore, the engineered barrier and geological barriers are complementary. Conducted studies show that the engineered barriers decayed because of the radionuclides over time. Also, the interphase of the engineered- geological barrier is affected and damaged because of radionuclides decay, rock cracks caused by excavation, groundwater flow changing, and chemical conditions. With the uncertainty of the boundaries in the region, this region the engineered barrier and excavation, damaged zone is called "near field" and the unaffected zone in the natural barrier is called "far-field" (Nagasaki and Nakayama, 2015).

In order to do more research on geological disposal and multi-barrier systems in R&D projects conducted by many countries, a risk-based approach is adopted. According to a risk-based approach, the constraints of the radioactive waste contents, the assumptions such as disposal time, the known variable such as climate, technical

specifications on the engineered barriers, and geological barriers and unknowns are determined and the baseline scenario, the best scenario and the worst scenario are established. Based on these approaches, the probability of the risks and their impacts are evaluated (Nagasaki and Nakayama, 2015).

Among these scenarios, the scariest scenario is groundwater leakage into the radioactive waste repository. According to this scenario, the groundwater attains the radioactive waste repository because of earthquake, volcanic activities or earth processes such as upheaval and erosion and radionuclides release with the groundwater attain the biosphere. Such scenarios end up with the human activity scenarios such as mineral and energy sources or a residential area with the assumption of the current standard human activities despite the uncertainty of human activities in the future (Nagasaki and Nakayama, 2015).

2.2.3.1 Disposal options

Based on the countries' radioactive waste classification and their regulatory limits, the disposal options may vary.

As reported in IAEA GSG No-1, according to the classification of radioactive wastes, their disposal methods are defined as follows (IAEA GSG-1, 2009):

- Liquid and gaseous exempt wastes are controlled by the regulatory body for discharge to the environment. This type of waste is suggested to dispose of in conventional landfills or recycled.
- Very short-lived waste (VSLW) is stored until its activities are decreased below the clearance level. After their activities fall down the clearance level, they are treated as conventional waste. Although there is no limit for specific limit depending on the initial activity and their half-lives, in practice, storage is applied for the radionuclides whose half-lives are less than 100 days.
- Very Low-level Wastes (VLLW) are appropriate to be disposed in near-surface landfill with the regulatory body control. This type of waste contains generally generated soil and rubble during mining activities.
- Low-level waste (LLW) require limited containment and isolation for because of the long-lived radionuclides. Disposal options must vary from the near-surface facilities to the deeper facilities. Therefore, the disposal facilities are

preferred as more complex engineered facilities than the VLLW disposal area and surface disposal down 30 meters. Depending on the origin regulatory body, limits should be established to dispose the long-lived low-level waste. For example, in some areas, the limit is established as 400 Bq g^{-1} on average (400 Bq g^{-1} for one package) for long-lived alpha-emitted particles and higher (up to kBq g^{-1}) for long-lived beta and gamma-emitted particles such as ^{14}C, ^{36}Cl, ^{63}Ni, ^{93}Zr, ^{94}Nb, ^{99}Tc and ^{129}I.

- Intermediate-level waste (ILW) is disposed of ten to a few hundred meters from the surface because of the content, especially alpha-emitted radionuclides.
- High-level waste (HLW) need to be disposed in inaccessible place such as in deep geological formation containing engineered barriers. Heat is also another considerable factor in the design of disposal facility. Activity concentrations of HLW are generally in the range of 10^4 - 10^6 TBq m^{-3}. HLW contains the reprocessing of the spent fuels and for countries that do not adopt the reprocessing, spent fuels are also treated as HLW.

In NDK Regulation on Radioactive Waste Management (Official Gazette Number: 28582, Date of Issue: 09.03.2013) (NDK 28582, 2013) defines the disposal option according to radioactive waste classification. According to this regulation,

- Disposal of VLLW might be carried out in a surface disposal facility.
- Once conditioned with alpha-emitting radionuclide concentrations under 400 Bq g^{-1} for the mean entire package and under 4000 Bq g^{-1} for an individual waste package, LILW may be disposed at near-surface disposal facilities. LILW shall only be disposed at intermediate-depth or deep disposal sites after conditioning it with alpha-emitting radionuclide concentrations that are above the aforementioned limits.
- Only deep disposal facilities shall be used to dispose of high-level radioactive waste.

2.2.3.2 Near-surface disposal

According to the IAEA(IAEA GSG-1, 2009), near-surface disposal is the disposal of radioactive waste at a facility that is located close to the surface and covered by an engineered cover, absence or existence additional engineered barriers.

Near-surface disposal has adopted such safety systems:

- Dispersal prevention has a function to prevent the dispersion of the radioactive waste repository with waste concrete
- Shielding has a function to prevent not release the radiation and heat to the surrounding area.
- Closure has a function to prevent not leaks from artificial structures from radiation waste repositories.
- Suppression of migration has a function to reduce the exposure of local residents to radiation waste repositories in the living environment.
- Isolation has a function to prevent or reduce the impact after exposure.

Landfill near surface disposal

A landfill near-surface disposal is generally used for low-level radioactive wastes. Although this type of radioactive waste comprised 2% of the radioactivity of the total generated radioactivity from the radioactive waste, their volumes are highly huge. It is reported that a typical commercial PWR reactor whose power is 1000 MWe generated 18000 m^3 in operation and 12000 m^3 in decommissioning. These chemically and physically steady wastes are put in unlined near-surface trench. There are two important management stages; the entombment phase and the maintenance phase. While the entombment phase is called the process of the positining of the waste to the disposal area and capping with the soil, the maintenance phase is called the process of the finalization of the capping it with soil of the disposal area and management activities. Concluding management term, the disposal area with the capping with the soil is convenient for the uses (Nagasaki and Nakayama, 2015). Morvilliers disposal facility in France can be given as a commercial example of this type of disposal (Figures 2.7 and Figures 2.8) (Muller, 2015).

Vault disposal

In vault disposal, the low-level solidified radioactive wastes with cement in drums including incineration ash and spent ion exchange resin using the treatment of liquid wastes are put into a pit in shallow depth constructed with concrete (Nagasaki and Nakayama, 2015).

Figure 2.7 : Landfill near surface disposal facility for very low-level waste in Cires, France.

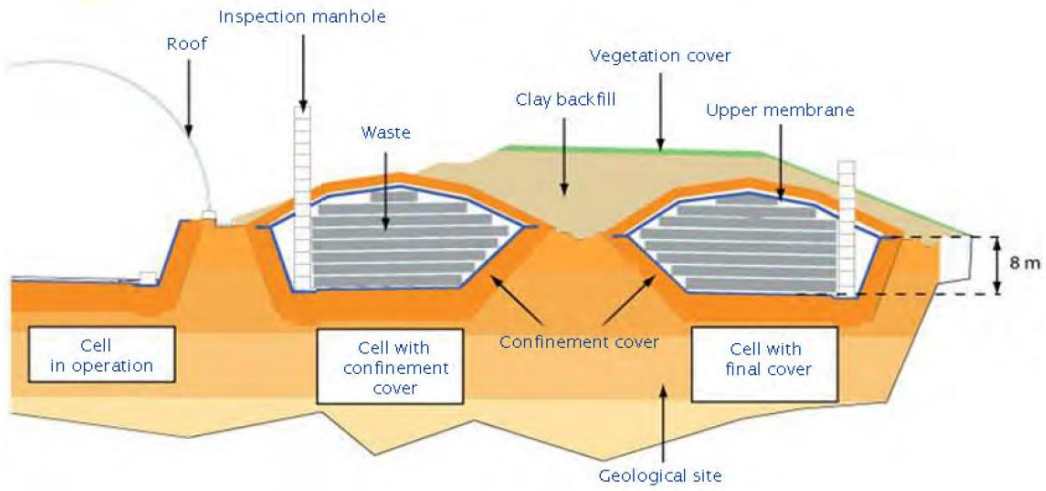

Figure 2.8 : Structure in Cires, France.

This type of disposal is thought of as constructed for 300-400 years. LLW Repository at Drigg in Cumbria in the UK, El Cabril LLW and ILW disposal facility in Spain, Centre de l'Aube, and five LLW Disposal facilities in the USA can be given as examples for vault disposal. Rokkasho Facility for low-Level Radioactive Waste Disposal Center in Japan, Centre de l'Aube in France and El Cabril disposal facility in Spain are shown in Figure 2.9 (Nagasaki and Nakayama, 2015), Figure 2.10 (ANDRA, 2010), and Figure 2.11 (Zuloaga, 2002). In the Low-Level Radioactive Waste Disposal Center of Japan Nuclear Fuel LTD (JNFL) in Rokkasho Village, the waste form is established in cemented drum and entombed in a cement vault. The cement vault and waste drum are filled with mixed soil that can be included in bentonite and soil in order to decrease the permeability of bedrock. Then the vault is closed with soil and capped

by covering material. In the Aube disposal facility, the monitoring tunnels are used for rainwater infiltration instead of using the mixing soil including soil and bentonite (Nagasaki and Nakayama, 2015).

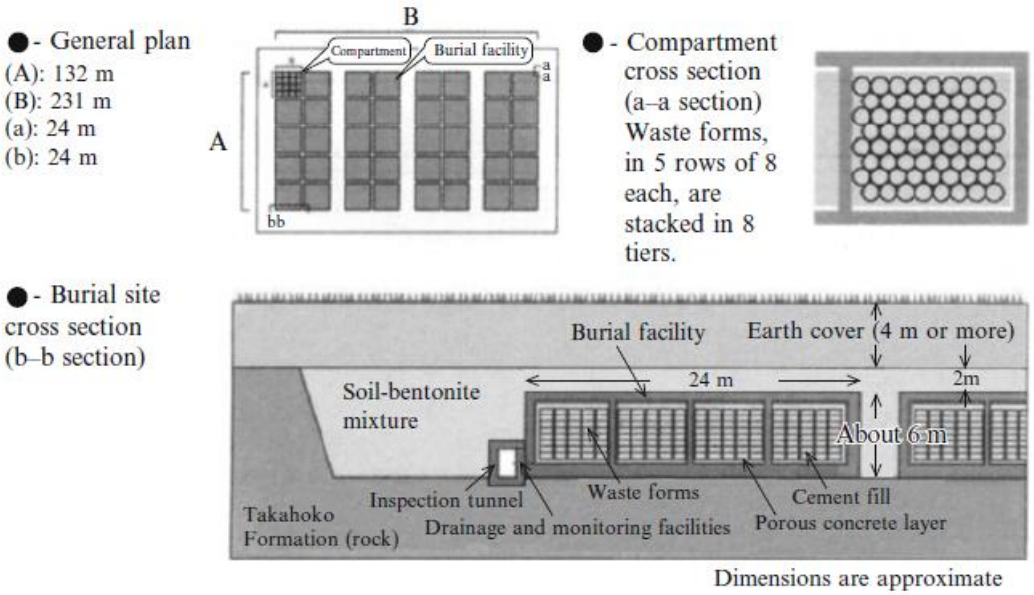

Figure 2.9 : Concept of vault disposal at Japan Nuclear Fuel Limited (JNFL).

Figure 2.10 : Centre de L'Aube disposal facilitiy for LILW-SL in France.

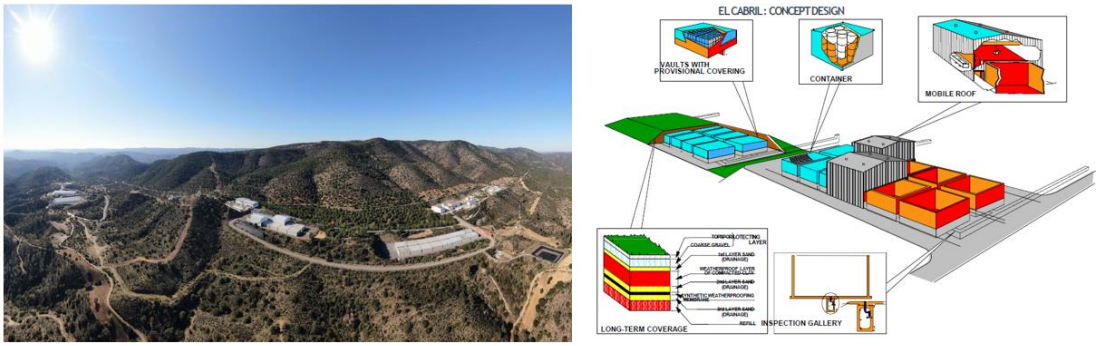

Figure 2.11 : Prefecture and concept design of El Cabril disposal facility for LILW-SL in Spain.

Subsurface disposal

Radioactive wastes varying from reactor internals such as spent fuel rods to short-lived radioactive waste are disposed of in subsurface disposal in engineered drums, called silo in Figure 2.12 (Nagasaki and Nakayama, 2015), in constructed depth 50-100 m. (Nagasaki and Nakayama, 2015). Low-Level Radioactive Waste Disposal Center of Japan Nuclear Fuel LTD (JNFL) in Rokkasho Village in Japan, the SFR final repository for short-lived radioactive waste in Forsmark in Sweden, and the underground repository in Olkiluoto for LLW and ILW in Finland can be given as examples of these types of facilities. This type of disposal facility is similar to vault disposal, however, the disposal facility is constructed in deeper, and 10000-year or greater time frame is used for safety assessment.

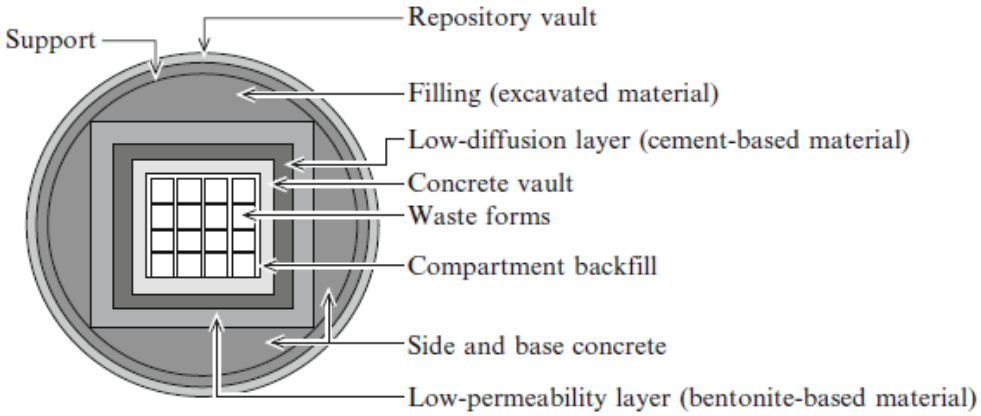

Figure 2.12 : Engineered barriers for subsurface disposal.

2.2.3.3 Geological disposal

Most countries in nuclear such as The USA, Argentina, Canada, the UK, France, Switzerland, Finland, Sweden, Spain, Australia, Belgium, Czechia, The Netherlands

Russia, Japan, and the Republic of Korea have adopted the radioactive wastes especially, high-level wastes, and spent fuels are disposed of in geological disposal facility. Multi-barrier approach gains more importance because of the requirement of protection from higher radioactivity for millions of years. Radioactive wastes disposed of in geological disposal facilities are stored in interim storage to allow the residual power to decay for the heat load to get low enough for geological disposal for 30-50 years. Then wastes are encapsulated by engineered barriers and disposed of in great-depth stable geological bedrock shown in Figure 2.13 (Patrakka, 2010). Olkiluoto in Finland, Forsmark in Sweden, and Bure in France have adopted this type of disposal. While Germany prefers that the waste is disposed of in the salt dome in Gorleben, the USA prefers the Yucca Mountain in Nevada.

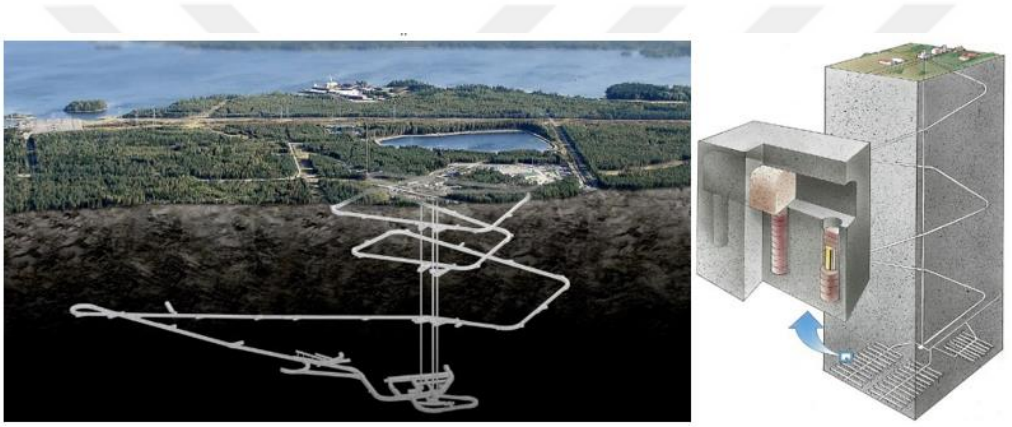

Figure 2.13 : Finland Nuclear Waste Disposal Concept in Bedrock.

2.2.3.4 Some countries application to spent fuel disposal

The US Department of Energy's (DOE) Office of Civilian Radioactive Waste Management is prepared to dispose of spent fuel removing from NPP and high-level waste from weapons at Yucca Mountain in Nevada. The scientific research began in 1978, and the President and Congress authorized it in 2002. The license application had been prepared by the US Nuclear Regulatory Commission. The application was planned in 2004; however, it was delayed because the reason of the standard of Environmental Protection Agency (EPA) are less strict than the court ruling. The disposal concept is based on disposing of the encapsulated waste packages horizontally 300 meters underground. In order to prevent to attain water from nuclear waste repository, the stainless steel barriers and volcanic rock are considered as the barrier.

In Sweden and Finland, the spent fuel disposal concepts are similar in regards to the technology and time schedules and they are in cooperation by the Posiva and SKB

companies. According to the concept, the copper canister with an iron whose length is 4.8 m, diameter 1 m, and weight 25 tons encapsulates the spent fuel and disposed of in the nuclear waste repository that structured in 400-700 m crystalline bedrock in both countries without reprocessing. The void between the bedrock and the canister is filled with bentonite clay. SKB, which is the responsible company in Sweden, is planning to build the nuclear waste repository at the site between the Oskarshamn and Östhammar which have nuclear power plants. Posiva, which is the responsible company in Finland is planning to build the nuclear waste repository at the ONKALO which has nuclear power plants Olkilouto1, Olkilouto2, and Olkilouto3.

In France, radioactive waste management is based on the Tier approaches, whose names are Axis 1, Axis 2, and Axis 3. Axis 1 is defined as partitioning and transmutation. Axis 2 contains the retrievable and non-retrievable geological disposal. Axis 3 is composed of conditioning and long-period of storage. While the ANDRA, which is a national radioactive waste management agency, is in charge of Axis 2, the national research body on nuclear energy, Commissariat à l'énergie atomique (CEA) is responsible for Axis 1 and 3. For Axis 1, the studies on portioning and mutation (P&T) was planned 2005-2020 and the commercialization of P&T were planning for 2040. For Axis 2, a clay depth of 445 m is investigated by ANDRA, and a construction license for the Ciego project for HLW has been applied in 2023. For Axis 3, France has experienced the conditioning and long-term storage in storing vitrified HLW. Research has been conducted for increasing the storage time from 50 years to 100-300 years.

In Canada, the adaptive phased approach is recommended by Canada's Nuclear Waste Management Organization (NWMO). According to this approach, the spent fuel is kept at the reactor area until the selected appropriate site for a deep geological repository and decided whether the building of the centralized underground storage facility for 30 years.

In Switzerland, the Swiss Expert Group on Disposal Concepts for Radioactive Waste proposed the "monitored geological disposal" concept that is adopted in the revised Nuclear Energy Law. According to this approach, the facility should be monitored after emplacing the spent fuel and closing the facility. This approach is based on passive safety in deep disposal in a stable geological formation.

In Japan, because of the adaptation of the reprocessing of the spent fuel, nuclear waste management focuses the HLW disposal. Geological HLW disposal is described in the Specified Radioactive Waste Final Disposal Act and the responsible authority defines as the Nuclear Waste Management Organization of Japan (NUMO). NUMO's purpose is to identify a location for the HLW repository, construct, operate, maintain, close, and maintain post-closure control of it.

2.3 Adsorption

Sorption term is description of capturing substance the external surface of liquid, solid or mesomorphs by or internal porous solids or liquids. This capturing is varied based on the bonding type (Vassilis and Stavros, 2006).

Physical sorption (physisorption) is one of the sorption types. In physical sorption, there is no electron exchange, instead intermolecular attraction between the favorable energy sites. The adsorbate is captured by adsorbent with the Van der Waals force and there may be several layers created. (Vassilis and Stavros, 2006).

Chemical sorption (chemisorption) is other sorption type. Apart from the physical sorption, in chemical sorption, electron exchange between the certain solute and surface molecules occur and chemical bond is formed. The characterization and strength of the bonds of the interaction is determined by the energy between the surface and adsorbate. Generally, single molecule layer is formed (Vassilis and Stavros, 2006)

Electrostatic sorption (ion exchange) is another sorption type. In this type of sorption, the Coulomb attraction between ions and charged functional groups occur.

Adsorption term is used for the capturing of the gaseous or liquid parts of solutions by the exterior and/or interior surface of porous solids. In other words, adsorption is defined as the detachment process of certain components in fluid to the surface of a solid adsorbent (Vassilis and Stavros, 2006).

The principle of the adsorption laid on the competitive forces between the repulsion between the electrons in atoms and van der Waals nuclear attraction force. Impact of nuclear attraction force is shorter because of the radius of the atom. These competitions on capturing occur in the well in the potential energy curve at close to the atoms (Figure 2.14) (Vassilis and Stavros, 2006).

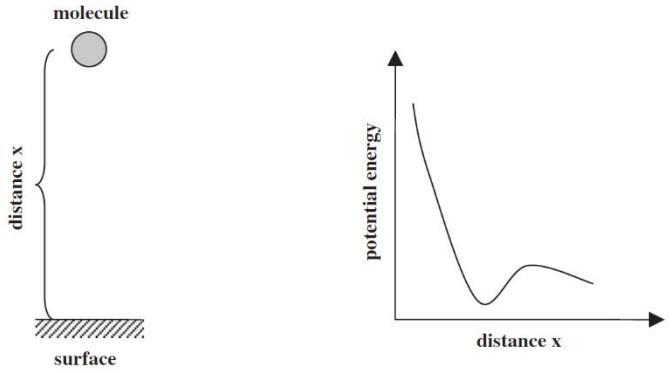

Figure 2.14 : The potential energy vs distance.

All surface is not perfectly smooth; therefore, there are bulges and cavities in microscopic level. Adsorption occur in these areas between the atoms of solids and fluids by attraction. In these surface areas, the pore structure is extremely important for characterize the adsorbent materials. The pore structure varies in terms of number, shape and size; therefore, these affect the adsorption capacity. According to IUPAC, the pores generally can be classified into macro, meso and micro pores (Table 2.3) (Vassilis and Stavros, 2006).

Table 2.3 : Pore Classification in IUPAC.

Type	Macropores	Mesopores	Micropores	Ultramicropores	Supermicropores
Pore Diameter d (nm)	d>50	2≤d≤50	d<2	d<0.7	0.7<[a]d_0<2

[a]d_0 is the pore width for slit-type or the pore diameter for cylindrical pores.

The relation between the pores structure and adsorption capacity can be explained that adsorptive molecules go from the macropores to the mesopores and the micropores. The micropores have the largest volume of the internal surface. Attractive forces are higher here and therefore the pore volumes and size of pore decide the capacity of adsorption (Vassilis and Stavros, 2006).

It can be confused the adsorption processes and ion exchange processes. Since mass transfer from a fluid to a solid phase occurs often in both processes—basically, they are diffusion processes—ion exchange is comparable to adsorption. In contrast to adsorption, which involves the sorption of electrically neutral species, ion exchange is also a sorption process, but ions are the sorbed species.In practical application, they

are accepted as both are sorption processes and most mathematical theories are developed for the sorption processes (Vassilis and Stavros, 2006).

Because the adsorption process have and advantageous for the high removal efficiency, the capacity for systems to be entirely automated, the ability to remove harmful organic compounds, the possibility of compound rehabilitation, easy installation and maintenance, and a wide range of adsorbent, there many application areas. Some examples are removal of water from organic solvents, removal of radon and sulfur compound from the gas stream, wastewater treatment and heavy metal removal in clay barriers. Besides these, there are some disadvantages such as adsorbent deterioration, problems results in particulates in feed, high content of macromolecular compounds, regeneration of spent adsorbent and high capital cost (Vassilis and Stavros, 2006).

For better surface texture, polymers can be supplemented with various fillers. Commonly, nanoscale fillers are used. Because nanoparticles have significant surface area, their involved in the polymer matrix develop various features of the material. Generally, the microstructures of clay/polymer nanocomposites are characterized based on the polymer chain level filling and compaction between the clay layers (Azzam, 2014; Terzopoulou et al., 2016; Zare, 2017). In fact, the amount of filler used in conventional microcomposites with improved properties is higher than nanocomposites using less than 5% by weight filler. As a result, nanofillers facilitate workability with easily extruded and meltable polymers. Moreover, they are more lightweight than conventional polymers, which is considerable with regard to their environmental effect (Rallini and Kenny, 2017; B. Xu et al., 2006; Zare and Garmabi, 2015). Polymeric nanocomposites, due to their advantages such as thermal, mechanical, and physical stability, resistance to fire and chemicals, well-properties in optics and electrics, show better properties than conventional microcomposites with low adsorption capacity and represent a new generation of composite materials (Rallini and Kenny, 2017; B. Xu et al., 2006; Zare and Garmabi, 2015).

2.4 Selenium and Tin

Important isotopes that have long half-life and redox sensitive in high-level radioactive wastes are selenium, technetium, palladium and tin and neptunium from the actinides. Since the solubility and sorption properties of redox sensitive elements are different at

each oxidation level, there are very few studies on estimating their migration in landfills and the doses they can give to the environment (Suter, 1991). Table 2.4 shows the redox sensitivity and oxidation steps of radionuclides in radioactive wastes (Suter, 1991).

Table 2.4 : Redox sensitivity and oxidation steps of radioactive isotopes in waste.

Element	Redox sensitivity	Oxidation level	Element	Redox sensitivity	Oxidation level
H	X	0, +1	**I**	X	+5, 0, -2
Be		+2	**Cs**		+1
C	X	-4 - +4	**Ba**		+2
Si		+4	**Sm**		+3
Cl		-1	**Eu**		+3
Ar		0	**Ho**		+3
K		+1	**Re**	(X)*	+7, (+4, +3, 0)
Ca		+1	**Pb**	X	(+4)*, +2, 0
Ti	(X)*	+4 (+3)*	**Bi**	X	+3, 0
Ni	(X)*	+2, (0, +3)*	**Po**	X	+4, (+2)*, 0
Se	X	-2, 0, +4, +6	**Ra**		+2
Kr		0	**Ac**		+3
Sr		+II	**Th**		+4
Zr		+4	**Pa**		+5
Nb		+5	**U**	X	+6, +5
Mo	X	+6, +4,(+3)*	**Np**	X	+3, +4, +5
Tc	X	+7, +4, (+3, +2, +1)* 0	**Pu**	X	+6, +5, +4, +3
Pd	X	+2, 0	**Am**	X	+3, +4
Ag	X	+1, 0	**Cm**	(X)	+3, (+4)*
Cd		+2	**Cf**		+3
Sn	(X)*	+4, (+2)*			

*Values in parentheses indicate oxidation levels where the pH is at its lowest 2 or 12 highest, or where water predominates under conditions at the margins of its stable environment.

The activity changes of radionuclides in nuclear waste in 1 million years are given in Figure 2.15 (Osmanlioglu, 2018) .

Therefore, redox conditions show what can happen in the real system (Suter, 1991). The reason why selenium and tin emits as fission products in a spent nuclear fuel are radiologically hazardous is the presence of ^{79}Se and ^{126}Sn radioisotopes with a half-life of 3.27×10^5 and 2.35×10^5 years, respectively (Jörg et al., 2010; Nichols et al., 2007). The fission efficiency for ^{79}Se, one of the fission products released from the fission of ^{235}U with thermal neutrons, is 0.0508%, and for ^{126}Sn it is 0.0236% (Nichols et al., 2007). The chemistry of selenium is similar to the chemistry of sulphur among the same periodic group elements. Selenium exists in -II, 0, IV and VI oxidations. The selenide anion (Se^{2-}) is very similar to the sulphide anion (S^{2-}). Selenite mineral is in insoluble form. The oxidation of selenium (Se^{2-}) to the selenide anion (SeO_3^{2-}) is very

rapid under oxidized conditions. The oxidation of the Se^{2-} anion to the selenite anion (SeO_4^{2-}) is slow. In contrast to the sulphur analog sulphide, selenite is stable to oxidation by oxygen in aqueous solution over a wide pH range (Suter, 1991).

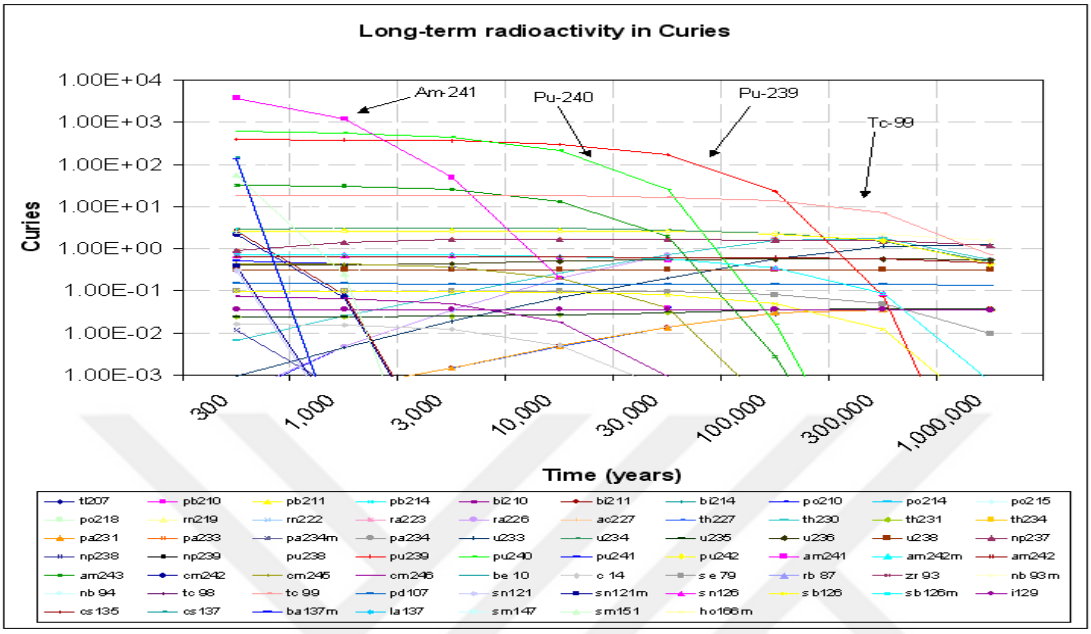

Figure 2.15 : Activity changes of radionuclides in nuclear waste in 1 million years

Tin-126, on the other hand, has a comparatively low yield (around 0.056%). Tin whose half-life 2.35×10^5 years by thermal neturons also has possibly hazardous beta emitter which maximum energy 252 keV and gamma emitter whose energies are 87.6, 86.94 or 64.3 keV. It is a fission product (Silliková, V. and Dulanská, S., 2017). One of the redox sensitive elements, tin, has oxidation states ranging from -4 to +4, yet in aqueous solution it possesses +2 and +4 valences. Sn(II) and Sn(IV) ions exist as dimeric inaction complexes in hydrochloric acid solution. In high acid or basic environments, SnO_2 can become only clearly soluble. SnO has a higher solubility. With the hydrolysis of tin, $SnOH^+$, $Sn_2(OH)_2^{2+}$ and dominant $Sn_3(OH)_4^{2+}$ can be created. The hydrolysis constants (pK) of these complexes are 3.4, 4.77 and 6.88. In alkaline solutions, although the main species is the $[Sn(OH)_3]^-$ complex, it is obvious that the dinuclear ion $[Sn_2(OH)_4O]^{2-}$ is also exist. The main species present in alkaline tin solutions is $[Sn(OH)_6]^{2-}$ (Suter, 1991). Eh-pH diagram for Sn-H_20 system is shown in Figure 2.16. In all ranges where pH is higher than 2 and water stability is redox dominant, only Sn (IV) is significant (Ochs et al., 2016).

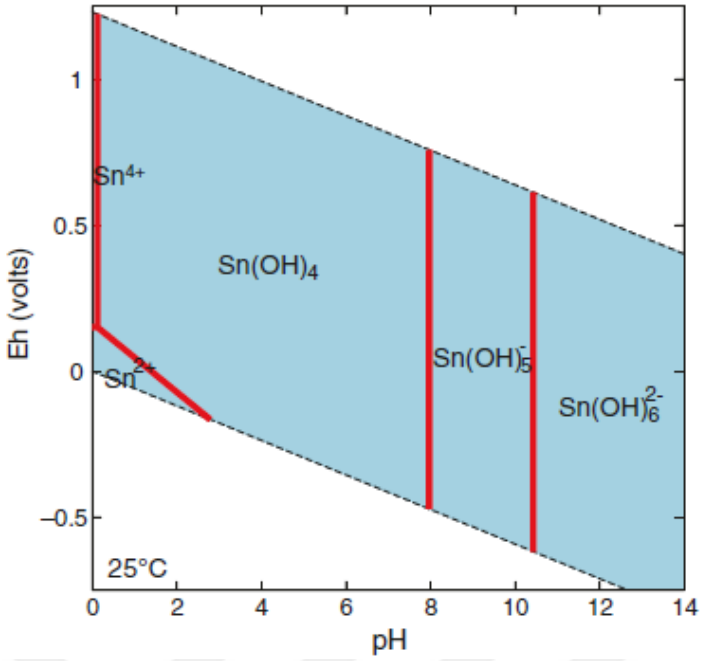

Figure 2.16 : Eh-pH diagram for Sn-H_20 system.

Since the pH is greater than 8 in systems where nuclear wastes are solidified with cement, tin is formed as Sn $(OH)^{5-}$ and Sn $(OH)_6^{2-}$ hydrolysis types (Ochs et al., 2016).

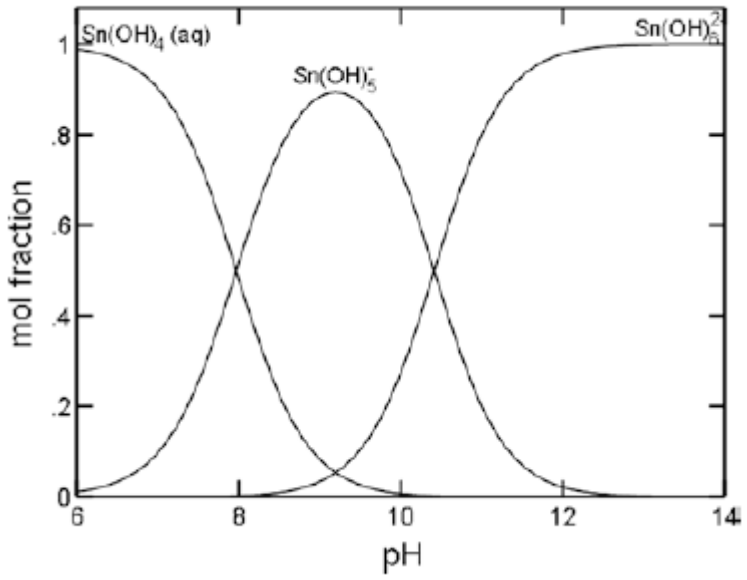

Figure 2.17 : Graph of dissolved pH-Sn species as mole fraction (Sn concentration is 10^{-8} mol/L).

In mixtures where the concentration of tin is smaller than 10^{-7} M, Sn(II) ions can be dissolved under suitable pH and Eh conditions, while Sn(0) and Sn(IV) ions precipitate (Figure 2.17). Under hydrogeological circumstances, Sn (IV) is anticipated to be the

dominating feature at pH 7.3 and Eh -185 mV. Precipitation is not determined in solutions where the concentration of tin is smaller than 10^{-8} M. K_d values are high because the tin solubility raises in the anions existence such as chlorine(Kedziorek et al., 2007).

Measuring of ^{79}Se is challenging due to its low activity and trace quantity of ^{79}Se in nuclear waste. A radiochemical process should be performed to extract the selenium from the medium and concentrate it by mass spectrometry or a nuclear technique prior to measurement (Aguerre and Frechou, 2006).

3. MATERIAL AND METHOD

3.1 Preparation of Barrier Material

Zeolite was used as an inorganic component while polyacrylonitrile (PAN) fibers served as organic binding agent for creation of polymer/zeolite composites. A reflux in a three-necked flask was used to dissolve 5 g of polyacrylonitrile in 11.86 g of dimethylformamide (DMF). Then, 5 g of zeolite was added up in a 1:1 ratio of organic to inorganic materials (Erenturk and Kaygun, 2017). This mixture was stirred for one hour at 70 degrees Celsius before being poured into petri dishes as a thin film layer. Pure water was poured on the film as a gelation agent after it had been drying at room temperature for a while. The resulting film layer was then dried between the filter papers. In order to be employed as a barrier material, the dried film was pulverized (0.05-0.07 mm) in agate mortar and stored in a storage container. Despite clinoptilolite having a cation exchange capacity (CEC) of only 3.40 meq g^{-1}, Akyil and Eral (2004) find that the PAN/zeolite composite barrier has a CEC of 4.51 meq g^{-1}. Moreover, 2.6 m^2 g^{-1} was stated as the composite barrier surface area (Akyil et al., 2004)

3.2 Characteristic Properties of Barrier Materials

3.2.1 Thermal stability of barrier material

Thermogravimetric analysis (TGA) was carried out to assess the polymer/zeolite composite's thermal stability. Under an N_2 atmosphere by heating from 25 to 600 ˚C, a Shimadzu/DTG60H performed the thermogravimetric analysis.

3.2.2 Surface analysis of barrier material

X-ray photoelectron (XPS) analysis using Thermo Scientific K-Alpha Spectroscopy on the monochromatized Al(K) radiation was used to describe the surface structure of the PAN/zeolite barrier material. Each spectrum has an energy step of 0.100 electron volts (eV). 128 channels of detector are present.

3.3 Interaction Barrier Materials with Se and Sn

At various starting tin and selenium ion concentrations, variable temperatures, and varying interaction periods, the interaction of tin and selenium ions with the produced barrier material was studied.

In order to research the impact of initial tin and selenium concetration, the range in 10-150 μg mL^{-1} of tin and selenium solutions interacted with the barrier material for an hour at 25 ˚C with V/m 500.

In order to research the impact of temperature of interaction between tin or selenium with the barrier material, the temperature is ranged in 15-35˚C in 50 mg L^{-1}.

In order to investigate the effect of interaction time of interaction between tin or selenium with the barrier material, the temperature is ranged in 15-240 minute in 50 mg L^{-1}.

In the investigation, stable salts of tin and selenium were used. In a thermostated shaker water bath (Selecta), the batch approach was used to study how tin and selenium ions interacted with the barrier material. Once the interaction period, solid and liquid phases of the solutions were segregated using the proper Whatman 40 filter paper. The accredited ICP-OES Spectrometer was used to calculate how much tin and selenium remained in the solution (PerkinElmer). The following Equation 3.1 and Equation 3.2 were used to calculate the distribution coefficient (K_d) and adsorption efficiency (%) of tin and selenium ions (Erenturk and Kaygun, 2016).

$$\text{Adsorption efficiency (\%)} = \frac{C_i - C_e}{C_e} x100 \tag{3.1}$$

$$K_d = \frac{C_i - C_e}{C_e} x \frac{V}{m} \tag{3.2}$$

C_i : the ion concentration of the initial solution (μg mL^{-1}),

C_e : the ion concentration of the solution in balance state (μg mL^{-1}),

V : the volume belonging to the tin solution (mL),

m : the quantity of the composite barrier material (g).

3.3.1 Formation of adsorption isotherms

Adsorption isotherms are crucial in the design of barrier materials. Adsorption isotherms, which generally explain how the adsorbent and adsorbed interact, are necessary for adsorbent optimization. To give adequate physicochemical information on the characteristics of the adsorption mechanism and to define the sorption capacities of the composite barrier for tin and selenium ions, adsorption data were applied to sorption isotherm models. For the purpose of describing the interaction between the tin or selenium ions and the barrier material at room temperature, a various adsorption isotherm models, including the Freundlich, Langmuir, Temkin, and Dubinin-Radushkevich (D-R) were applied. By analyzing the correlation coefficients, linear regression was utilized to choose the best isotherm among the adsorption isotherm models.

3.3.2 Kinetic calculations

The rate of adsorption which is determined by adsorption kinetics determines how long the adsorbed ion remains at the contact. The information gathered from the measurement of the contact time was utilized to research the adsorption process with regard to rate constants of adsorption. The pseudo-first-order model's equation is as follows (Equation 3.3) (Erenturk and Kaygun, 2016):

$$\ln(q_e - q_t) = \ln q_e - k_1 t \tag{3.3}$$

q_e : the quantity of adsorbed ions in balance state (mg g^{-1}),

q_t : the quantity of ions adsorbed at time t (mg g^{-1}),

k_1 : the rate constant of the equation (min^{-1}).

The pseudo-second-order kinetic model is typically used in non-homogeneous systems where chemical adsorption is the adsorption mechanism. It is relying on experimental data from solid-phase adsorption. The following Equation 3.4 can be used to describe the model (Erenturk and Kaygun, 2016).

$$\frac{t}{q_t} = \frac{1}{k^2 . q_e^2} + \frac{t}{q_e} \tag{3.4}$$

q_e : the quantity of adsorbed ions in balance state (mg g^{-1}),

q_t : the quantity of ions adsorbed at time t (mg g^{-1}),

k : the rate constant of the equation (min^{-1}).

For systems with heterogeneous surfaces, the Elovich kinetic model equation is applied in chemical adsorption processes. The following Equation 3.5 represents the Elovich equation when a, b, and t ≥ 1:

$$q_t = \frac{1}{b.ln(ab)} + \frac{1}{b.ln(t)} \quad (3.5)$$

q_t : adsorption capacity at time t (mg g^{-1}),

a : initial adsorption rate (mg g^{-1} min^{-1}),

b : desorption constant (g mg^{-1}).

3.3.3 Thermodynamic parameters

In order to determine the thermodynamic parameters (ΔH°, ΔS°, and ΔG°), the following Equation 3.6 and Equation 3.7 were used (Erenturk and Kaygun, 2016). The slope of the lnK_d and 1/T graph was used to derive the E_a and A values as well as the ΔH, ΔH and ΔS parameters (Erenturk and Kaygun, 2016).

$$\ln K_d = \frac{\Delta S^\circ}{R} - \frac{\Delta H^\circ}{RT} \quad (3.6)$$

$$\ln k_1 = \ln A - \frac{E_a}{RT} \quad (3.7)$$

ΔH°: change of enthalpy (kJ mol^{-1} K^{-1}),

ΔS°: change of entropy (J mol^{-1} K^{-1}),

ΔG°: change of Free Gibbs Energy (kJ mol^{-1}),

K_d: distribution coefficient (mL mg^{-1}),

T: the absolute temperature (K),

R: gas constant (8.314 J mol^{-1} K^{-1}),

A: frequency factor

E_a: the activation energy.

3.3.4 Kinetic models based on diffusion

Two models are frequently employed to comprehend the microscopic kinetic process and the mechanism driving adsorption: the homogeneous particle diffusion model (HPDM) and the shell formation (SPM) or shrinking core model (SCM).

In the HPDM model, it is assumed that the adsorbate diffuses to a uniform adsorbent surface, unlimited dilution, and the shape of particle is spherical. The rate of diffusion is controlled by the adsorption system either by the liquid film formed by the ions around the particle or by the ions diffusion into the adsorbent particles. Nernst-Planck equations are utilized to create the HPDM equations. In the case of adsorption system controlled by the particle velocity, the linearized equation is utilized to affect the particle diffusion coefficient D_r (m^2 s^{-1}) in the solid phase (Equation 3.8):

$$-\ln[1 - X^2(t)] = 2\left(\frac{\pi^2 D_r}{r^2}\right)t \tag{3.8}$$

X: amount of adsorbate ratio at time t (q_t) and balance state time (q_e)

r (m) : the adsorbent particle radius.

If the sorption rate is governed by liquid film diffusion, Equation 3.9 can be used in:

$$-\ln\left[1 - \frac{q_t}{q_e}\right] = \left[\frac{3DC}{rC_r}\right]t \tag{3.9}$$

C: the equilibrium concentrations of the ion in the solution (mol L^{-1}).

C_r: the equilibrium concentrations of the ion in solid phase (mol L^{-1}).

D: the diffusion coefficient of the liquid phase (m^2 s^{-1}).

Weber and Morris have established another adsorption-related intraparticle diffusion model. Ions can fill the voids of the adsorbent, limiting the adsorption. This model can be stated by the Equation 3.10:

$$q_t = k_p . t^{0.5} \tag{3.10}$$

q_t: the ion concentration adsorbed at time t (mg g^{-1})

k_p: the intraparticle diffusion rate constant (mg g^{-1} min^{-1}).

Intraparticle diffusion is the process controlling sorption if the graph created between q_t and $t^{0.5}$ forms a line across the origin.

The SPM or SCM model depends on the chemical reactions between the fluid and the particle and it is taken into account that the reaction takes place on the external surface of the particle first (Figure 3.1) (Sarkar and Bandyopadhyay, 2011). Afterward, the location of the reaction enters the solid, and then the reacting particle constricts during the reaction. The assumptions considered for SPM can be listed as follows: a) The diffusion through the pores is concentration independent, b) The adsorption isotherm cannot be reversed, c) The pseudo-steady-state approach is sufficient, d) Both film and particle transfer are driven by a linear force, e) Adsorbent particles are round shape.

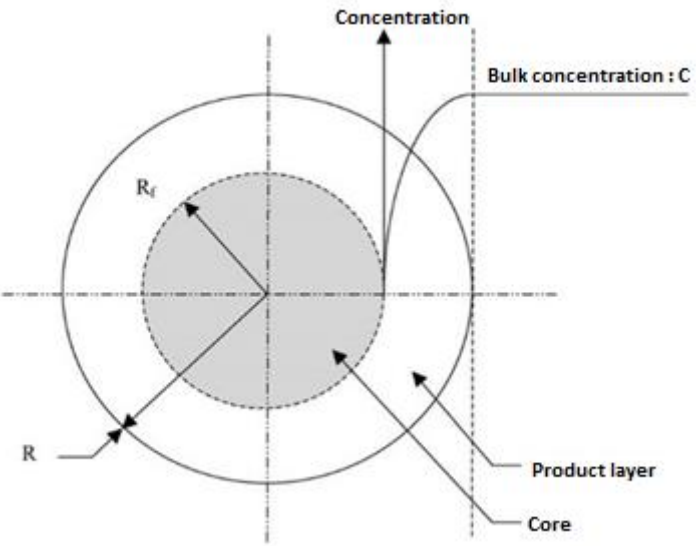

Figure 3.1 : Diagram of diffusion of adsorbent ion in the shrinking core model.

According to this concept, the following steps are typical of reactions in a fluid-solid heterogeneous system:

1. Fluid diffusion to the solid surface from the fluid layer,
2. The interaction of the reactant in the fluid with the solid's surface,
3. Product diffusion into the fluid from the film layer.

If the process is governed by in fluid-film diffusion, the model is expressed as Equation 3.11:

$$X = \left[\frac{3C_A K_F}{zrC_S}\right] t \tag{3.11}$$

If the process is controlled by the product diffusion into the fluid from the film layer, the model is expressed as Equation 3.12:

$$3 - 3(1 - X)^{2/3} 2X = \left(\frac{6D_e C_A}{zr^2 C_S}\right) t \tag{3.12}$$

If the process is controlled by the chemical reactions, the model is expressed as Equation 3.13:

$$1 - (1 - X)^{1/3} = \left(\frac{k_S C_A}{r}\right) t \tag{3.13}$$

C_A: the adsorbed ions concentration in the solution (mol L^{-1}),

C_s: the remaining ions' concentration in the solution after adsorption (mol L^{-1}),

K_F : mass transfer coefficient of species from the liquid film (m s^{-1}),

D_e: the diffusion coefficient of the reacting layer in the solid phase (m^2 s^{-1}),

k_s: the surface dependent reaction constant (m s^{-1}),

r: the mean radius of the adsorbent particles (m),

z: the stoichiometry coefficient.

3.3.5 XPS

X-ray photoelectron spectroscopy (XPS) can serve to investigate the surface chemistry of the material, after a material has undergone a process like cutting, fracturing, or scraping. Since it is applicable to broad spectrum of materials and gives useful numerical and chemical state data from the exterior layer of the material being investigated, XPS, also known as electron spectroscopy for chemical analysis, is the most common surface analysis technique. For an XPS measurement, the typical measurement distance from the surface is 5 nm. Caused by the narrow range of the photoelectrons that are generated from the solid, the XPS method is extremely surface-specific (Aziz and Ismail, 2017).

A concentric hemispherical analyzer is used to determine the photoelectrons' energy as they leave the sample, and this results in a spectrum with a number of photoelectron peaks (Aziz and Ismail, 2017).

Each element has a distinct binding energy (BE) at the peaks. The structure of the material's surface may be identified using the peak areas. The chemical state of the atom sending electrons out can change slightly, which also change the form of each peak and BE. Consequently, XPS can also give data on chemical bonding. Once a high-energy photon interacts with matter, one electron is ejected from an orbital or band and moves to the vacuum level, which starts the photoemission process in a solid sample (Figure 3.2) (Aziz and Ismail, 2017).

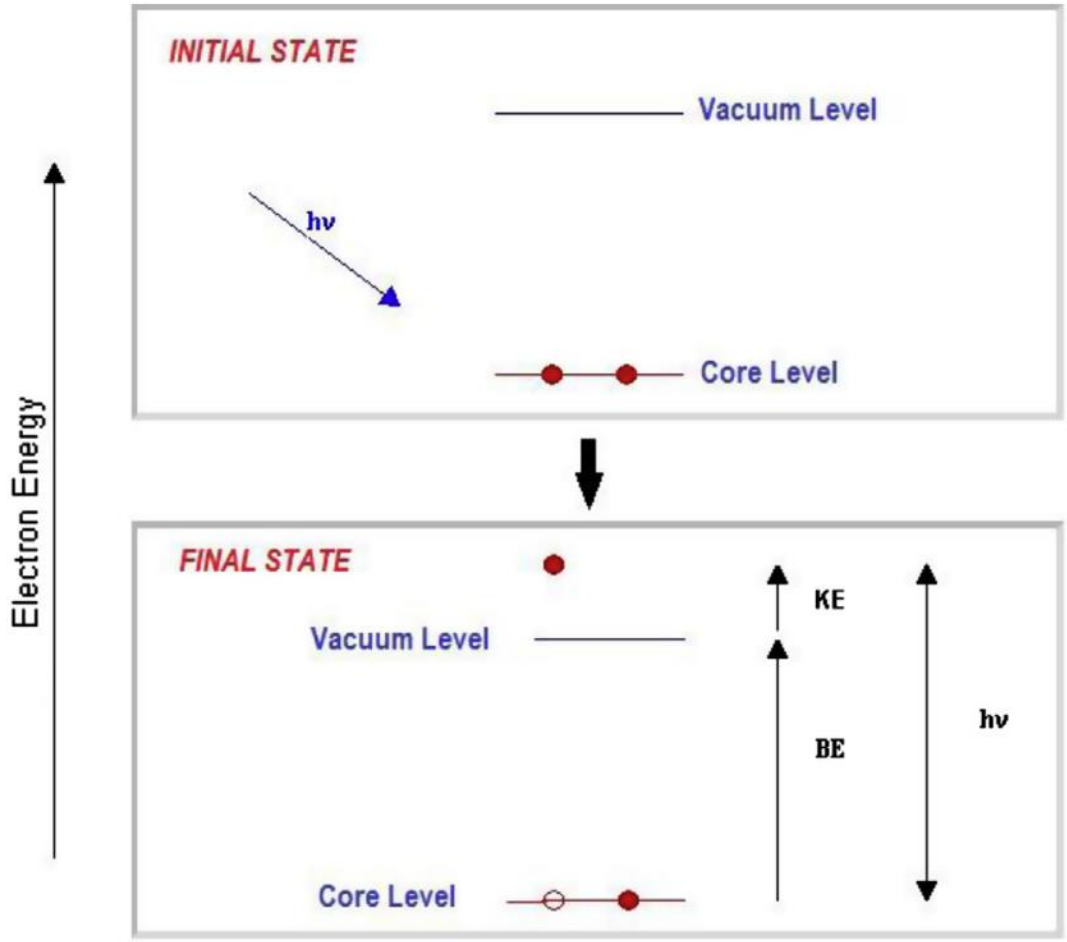

Figure 3.2 : The photoemission in XPS analysis.

For the electrons to surpass the work function of the material, the excitation energy must be sufficient. The three-step model has usually been used to explain the procedure: optical excitation, transport to the surface, and escape into the vacuum. When an atom or molecule absorbs an X-ray photon, an electron may be ejected. The

photon energy (hv) and the electron's BE (i.e., the energy reqired to extract the electron from the material surface) both affect the electron's kinteci energy (KE) (Equation 3.14) (Aziz and Ismail, 2017).

Any suitable electron power detector may measure the photoelectrons' KE distribution (i.e., the quantity of photoelectrons released as a function of their KE), allowing a photoelectron spectrum to be captured.

$$\begin{gathered} E = hv \\ E(A) + hv = E(A^+) + E(e^-) \\ KE = hv - [E(A^+) + E(e^-)] \\ KE = hv - (BE + \varphi) \end{gathered} \tag{3.14}$$

3.4 Radiologic Risk Assessment

3.4.1 Risk assessment on biotas by ERICA Assessment Tool

One of the most comprehensive assessments that has been acknowledged and used by international organizations like the ICRP and IAEA is the ERICA assessment tool, a simulation programme created as part of the 6th Framework project ERICA. The IAEA and UNSCEAR use the ERICA Assessment Tool to estimate the equivalent dose to which a reference plant or animal will be subjected and to evaluate the effects of radionuclide or environmental contamination on that plant or animal. With the use of this computer-based software, tasks like ionizing radiation exposure, impacts, and risks, chemical and environmental risk characterization, and environmental management may be carried out to protect the ecosystem's structure and function.

The three tiers of ERICA's methodologies can be customized to the particular assessment of employing reference organisms. Only a limited number of components from a given area can be tested in Tier 1 using the proper reference species, and the risk assessment is then conducted in accordance with the results by comparing them to Environmental Media Concentration Limits (EMCL). Risk Quotients (RQ) are the results in Equation 3.15, which are as follows:

$$RQ = \sum_{1}^{n} \frac{M_n}{EMCL_n} \quad (3.15)$$

RQ: Total Risk quotient,

M_n: measured or predicted maximal activity concentration for radionuclide "n" in the medium (Bq L^{-1} for water, Bq kg^{-1} (dry weight) for soil or sediment or Bq m^{-3} for air),

$EMCL_n$= Environmental Media Concentration Limit for radionuclide "n" (Bq L^{-1} for water, Bq kg^{-1} (dry weight) for soil or sediment or Bq m^{-3} for air).

In Tier 2, specific elements in the environment can be investigated using chosen reference species, and the risk assessment is then established in accordance with the results. The spectrum of representative organisms from terrestrial, aquatic, and marine settings is represented by several reference organisms. Using the concentration value (CR) in Bq kg^{-1} and distribution coefficient (K_d) in Bq kg^{-1}, the results allow for the dose calculation and the reference organism identification that may have been possibly most exposed. Tier 2 is crucial for identifying uncertainties in the assessment's effects analysis.

These outcomes can be assessed in Tier 3 using probability projections. This tier allows data entry for the site-specific probability distribution functions and provides the final dose-rate results' uncertainty. Sensitivity analysis is crucial for understanding how different factors affect the output of the model and for quantifying the uncertainties, especially in cost-effective research.

The freshwater biota, which includes crustaceans, phytoplankton, vascular plants, and terrestrial biota, which includes annelids, grasses and herbs, lichen and bryophytes, mammals, shrubs, and trees, were examined in this study using the ERICA Assessment Tool. The following Equaiton 3.16 was used to convert the initial Se and Sn concentration and the remaining concentration in the solution following adsorption to activity:

$$A = \frac{ln2}{t_{1/2}} x \frac{mN_A a}{M} \quad (3.16)$$

A: activity (Bq),

$t_{1/2}$: half-life of the nuclei (s),

M: the molarity of the substance (kg mol^{-1}),

m: mass of substance (kg),

N_A: Avogadro's number (mol^{-1}),

a: abundance.

The required distribution coefficient (K_d) value was calculated as follow Equation 3.17 to determine the subjected dose of the freshwater reference biota in the ERICA Tool Assessment Program:

$$K_d = \frac{A_i - A_e}{A_e} x \frac{V}{m} \tag{3.17}$$

A_i: the activity concentration of the initial solution (Bq mL^{-1}),

A_e: the activity concentration of the solution in balanced state (Bq mL^{-1}),

V: the solution's volume (mL),

m: the quantity of the adsorbent.

3.4.2 Long-term risk assessment of waste storage model by Goldsim Monte Carlo Simulation Program

The GoldSim Monte Carlo Simulation Software with radionuclide transport module, which can help to answer the questions about complicated environmental assessment systems, was used to evaluate long-term risk and simulate it for tin and selenium in multi-barrier system. Different modules in the GoldSim Monte Carlo Simulation Software are available for a variety of uses, including financial, reliability, pollutant movement, and distributed processing. The radionuclide transport module, which is a specialized version of the contaminant transport module, was applied in this investigation. This model allows for the definition of related radionuclides and their attributes, such as their decay rates, their half-lives, and their daughter products, which are rely on ICRP Publication 107. Furthermore, it is possible to construct other specific properties for radionuclide passing through the engineered barrier into environmental media by using the solubility constraints and sorption behavior into constraints.

The GOLDSIM Monte Carlo Simulation Software is utilized in this research to model the behavior of tin after 2 million years and selenium after 1 million years in the waste repository and the performance risk assessment for long-period of time. The

engineered barriers in the multi-barrier concept in this study are established by taking into account the repository for low-intermediate level long-lived wastes in Swedish created by Swedish Nuclear Fuel and Waste Management Company (SKB) and the dose assessments of ^{126}Sn and ^{79}Se are done based on this structure. The databases used by the GoldSim Monte Carlo Simulation Software, which is rely on the ICRP Publication 107, were used to obtain information about the ^{126}Sn and ^{79}Se, such as its decay rate, daughter products, and half-life.

In the GoldSim Monte Carlo Simulation Software, the concepts "engineered barrier" and "geological barrier" are defined as in Figure 3.3. Sn and Se radionuclides were encapsulated in the developed model by a polymer/zeolite-based barrier (PAN/Zeolite barrier), a metal drum, a clay, and a host rock, in that order. According to the IAEA waste classification, the waste repository is positioned in the intermediate depth repository (IAEA GSG-1, 2009).

The definition of a waste repository is like a sandwich made of a geological membrane in the bedrock and a polymer/zeolite-based barrier layer created in this study. The radioactivities of Sn and Se is carried to the agricultural soil as the biosphere with the aquifer floods over a 100 m distance from the waste repository. Through the transport channels, advection, dispersion, sorption, and decay chain are taken into account. Data from (Jo et al., 2018; Lee et al., 2013, 2016) or data gathered during this study were used to define the initial inventories of these radionuclides, inflow, transfer rate, outflow, and media in each cell pathway. Sn and Se radionuclides are placed as in waste packages enclosed in a PAN/zeolite composite barrier and metal canister, which are components of the near field system.

In the GoldSim Monte Carlo Simulation Software, the terms "engineered barrier" and "geological barrier" are defined as in Fig. 3.3. To allow for the observation of the long-term impacts of Sn and Se in the event of an accident, the simulation time has been designed for 2 and 1 million years, respectively.

Irradiated UO_2 fuel contains around 26 ng g^{-1} ^{126}Sn and 5 μg g^{-1} ^{79}Se (Asai et al., 2013; Maslennikov, A., David, F., Peretroukhine, 1999). Considering Turkey's plans to construct and operate 12 reactors each having 1000 MWe capacity and 60 years of operating life, as an initial inventory input, the entire Sn and Se quantity has been calculated and fed into the GoldSim Monte Carlo Simulation Software.

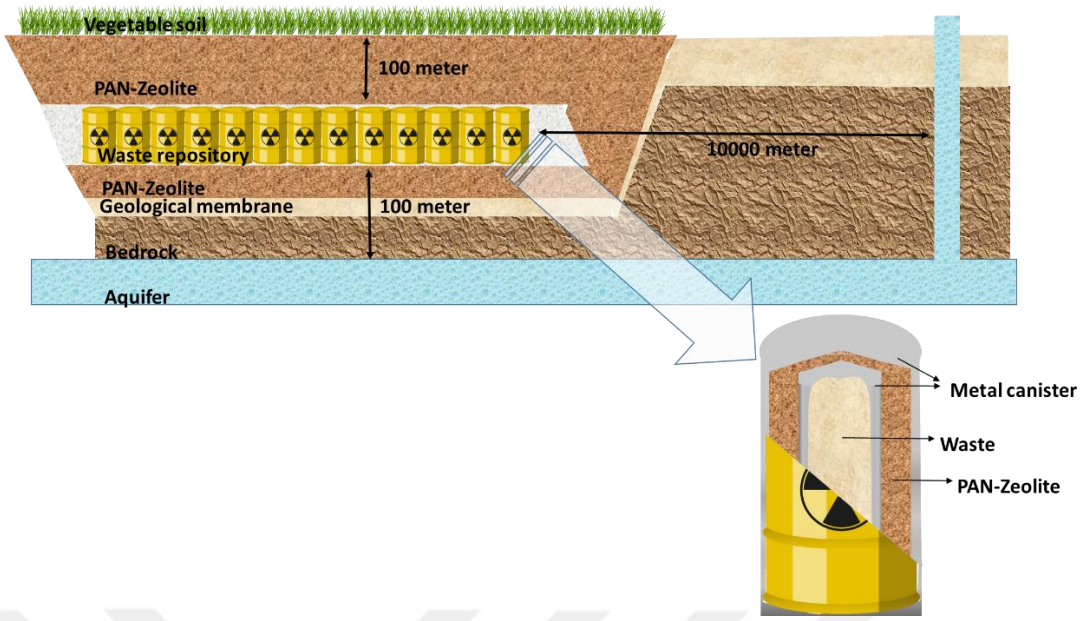

Figure 3.3 : Barriers in established model in GoldSim MonteCarlo Simulation Software.

3.4.3 Risk assessment on human health

In order to estimate the potential risk that ^{126}Sn and ^{79}Se causes to health of human in the case of an accident, carcinogenic risks were calculated. Due to the flooding as a result of the spreading of metals into the ecosystem and water to consume, metals have been proven to be poisonous and pose a significant hazard to individuals in the case of an unplanned or accidentally discharge. They can have negative health impacts on people, including insufficient growth and development, cancer, damage to the neurological system, and fatalities. These metals continue to pose harmful threats to aquatic ecosystems and human health because they are difficult to remove from aqueous systems. Generally, physical, biological and chemical methods are used to recycle them (Liu and Ma, 2020).

Through direct consumption through ingestion system, inhalation through respiratory system, and skin penetration, humans can be exposed to heavy metals that reach groundwater. However, ingesting groundwater directly is the primary method of exposure. Therefore, using the Equation 3.18, Equation 3.19 and Equation 3.20 listed below, risk assessment of contaminated sites is conducted. When a contaminant like tin and selenium enters groundwater, its lifetime carcinogenic effect can be calculated by taking both children and individual doses into account (Liu and Ma, 2020).

$$ADD_{ing} = C\ x \frac{IngRxEFxED}{BWxAT} x10^{-6} \quad (3.18)$$

$$ADD_{inh} = C\ x \frac{InhRxEFxED}{PEFxBWxAT} \quad (3.19)$$

$$ADD_{dermal} = C\ x \frac{SAxAFxABSxEFxED}{BWxAT} x10^{-6} \quad (3.20)$$

The abbreviations and values taken in this study for individuals and childrens are indicated as below (Gulan et al., 2020):

	Parameters	Value/Unit	Adult	Kid
IngR:	ingestion rate	mg d^{-1}	100	200
InhR:	inhalation rate	m^3 d^{-1}	20	7.6
EF:	exposure frequency for the metal	d y^{-1}	350	350
ED:	exposure time	y	30	6
BW:	body mass	kg	70	15
SA:	skin surface area exposed	cm^2	1530	860
AF:	adhesion factor	mg cm^{-2} day^{-1}	0.07	0.2
ADD_{ing}:	mean metal consumption by ingesting	mg kg^{-1} day^{-1}		
ADD_{inh}:	mean metal consumption by inhalation	mg kg^{-1} day^{-1}		
ADD_{dermal}:	mean metal consumption by absorbtion	mg kg^{-1} day^{-1}		
C:	the medium's metal concentration	150 mg L^{-1}		
AT:	mean time	days (365 x ED)		
PEF:	emission factor	1.36×10^9 m^3 kg^{-1}		
ABS:	the dermal absorption factor			

ABS_{dermal} factor is different for some metals for example it is 0.03 for As, 0.04 for C, 0.1 for Cu, 0.35 for Ni, 0.006 for Pb, 0.02 for Zn, and 0.05 for Hg (Gulan et al., 2020). However, it can be valued as 0.0001 for all other metals according to Chabukdhara and Nema (2013) (Chabukdhara, M. and Nema, A., 2013). In this study, the absorption factor is taken 0.02 for Sn and 0.0001 for Se (Environmental Protection Agency, 1999). To calculate the non-carcinogenic risks for individuals and kids through digestion and skin contact, hazard ratio (HQ) and hazard index (HI) were applied

(Equation 3.21). By adding the values for HQ_{ing} and HQ_{dermal}, the hazard index (HI) was determined.

$$HQ = \frac{ADDs}{RfD} \tag{3.21}$$

where RfD standard exposure level.

By multiplying ADD_{ing} and ADD_{dermal} by the slope factor, the carcinogenic risk (CR) was calculated. For both adults and children, a significant risk of developing cancer is indicated by a CR > 10^{-4} value. If CR is between 10^{-4} and 10^{-6}, risk can be tolerated. If CR is less than10^{-6}, carcinogenic risk can be ignored (Mohammadi et al., 2019).

Moreover, the possibility of getting cancer over one's lifetime following exposure to ^{126}Sn and ^{79}Se in the event of an accident was assessed; this risk is known as excess lifetime cancer risks (ELCR). The risk of developing prostate, breast, and blood cancer in adults and children will increase proportionally as ELCR increases. The following Equation 3.22 was applied to compute the excess lifetime cancer risk (ELCR):

$$ELCR = D_E x DL x PC \tag{3.22}$$

D_E : the yearly effective dose,

D_L : the mean life span (70 y)

PC : the nominal probability coefficient for detriment (5.5E-2 Sv^{-1} for cancer risk) (Gulan et al., 2020).

ICRP 119 reported the yearly effective dose conversion factors belonging to the ^{126}Sn and ^{79}Se activities for female/male babies and female/male adults and these values were applied to determine the D_E value. UNSCEAR reports that the average ELCR value all over the world is 1.9E-4 (UNSCEAR, 2000).

4. RESULTS AND DISCUSSION

4.1 Characteristic Properties of Barrier Materials

The PAN/zeolite composite barrier material's FTIR spectrum is shown in Figure 4.1. From the spectrum, it is possible to see that polyacrylonitrile's C=C bonds should be visible between 1550 and 1650 cm^{-1}, its C-H bonds should be visible between 2850 and 2950 cm^{-1}, and its C-N bonds should be visible between 2150 and 2325 cm^{-1}. The peak seen between 1000 and 1400 cm^{-1} demonstrates the link between the O-groups in the zeolite structure and the PAN/zeolite composite adsorbent. The C-X groups generated by elements like Na, K, Mg, Si, and Al in the structure of the zeolite with polyacrylonitrile are what cause the peaks below 850 cm^{-1}.

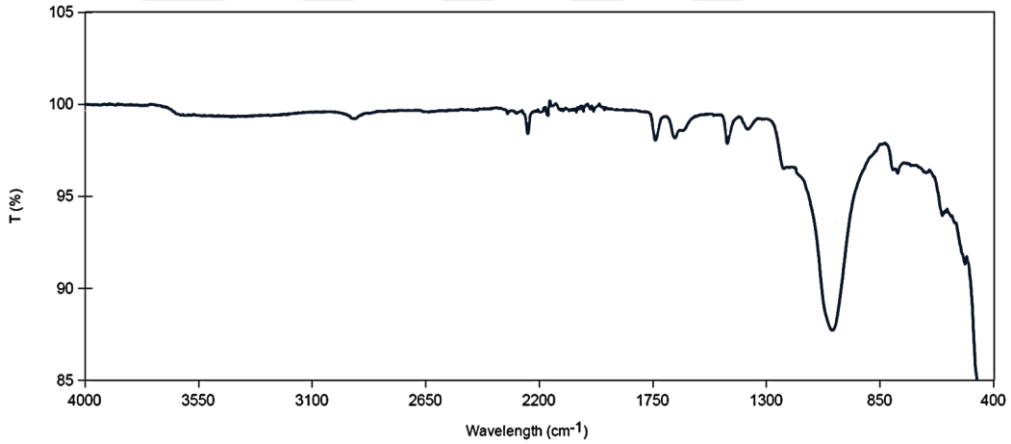

Figure 4.1 : FTIR spectrum of PAN/zeolite composite barrier.

In order to examine the acid resistance of PAN-Zeolite composite barrier material, after a certain amount of barrier material was kept in a strong acid media in the range of 0.3-0.6 for 24 hours, it was filtered, and dried. The weight loss that could occur from dissolution was investigated in order to test the structural strength of the PAN/Zeolite composite barrier material in acidic media. Throughout this procedure, there was no weight loss of the PAN/Zeolite composite barrier material.

Thermal analysis is one of the most widely used techniques for assessing a material's structural characteristics and figuring out how much moisture and volatile chemicals are present in its structures in order to figure out the thermal endurance of the barrier

material. The TGA curves for the developed composite barrier material in the temperature varied from 25 °C to 600 are shown in Figure 4.2. The barrier material's curve has two significant weight loss phases. The first stage occurs at 318 °C as a result of water molecules evaporating from the barrier material's structure. Around 359 °C in the second stage, the high-molecular-weight organic polymer that makes up the PAN barrier material starts to breakdown with a mass loss of around 20%.

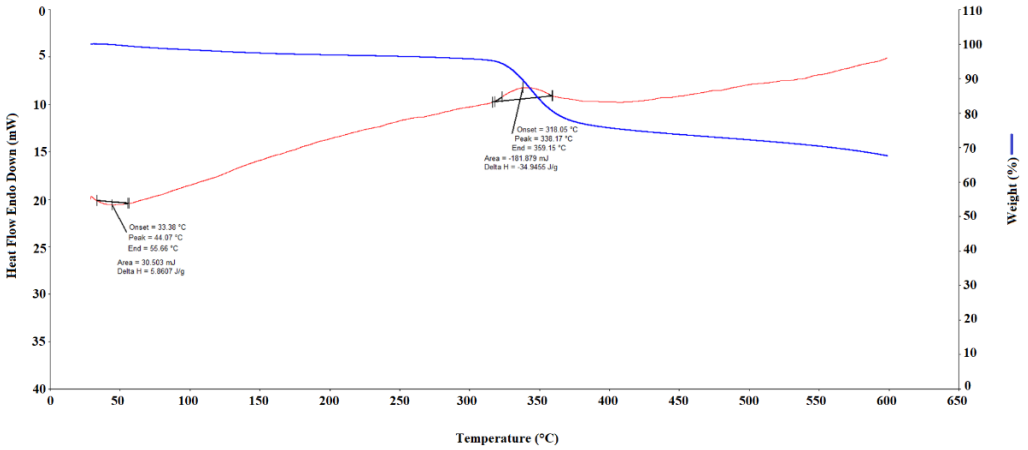

Figure 4.2 : TGA analysis of PAN/zeolite composite barrier.

According to Moafi et al. (2011), PAN is subject to physical and chemical alterations as a result of a different of exothermic chemical reactions, containing oxidation, cyclization, cross-linking, dehydrogenation, and degradation(Moafi et al., 2011). The glass transition temperature (T_g) of PAN fibers, which is 104.09 °C, was not found in the TGA curve of the composite barrier material. Nitrile groups existing in the PAN's structure may lead dipole-dipole interactions with DMF (Khan et al., 2017).

Heat accumulates on the metal canister surface as a result of the high-activity wastes' heat emission. The potential impact of this temperature on barrier materials should also be considered when designing a radioactive waste repository. The maximum temperature for metal canisters is typically received as 100 °C in many nations (King, 2020). In this instance, it is anticipated that the PAN/zeolite composite barrier material will not degrade structurally at this temperature.

4.2 Interaction Barrier Materials with Se and Sn

4.2.1 Initial concentration effect

Figure 4.3 shows how adsorption efficiency changed according to initial concentration of tin ions. Based on the results, the initial Sn concentration of 50 mg mL^{-1}, in which the Sn ions came to equilibrium in relation with the barrier material, was chosen to be kept constant in the other parameters. At an initial concentration of 50 mg mL^{-1}, the capacity of adsorption (q_e) for Sn in the developed composite barrier material was discovered to be 32 mg g^{-1}.

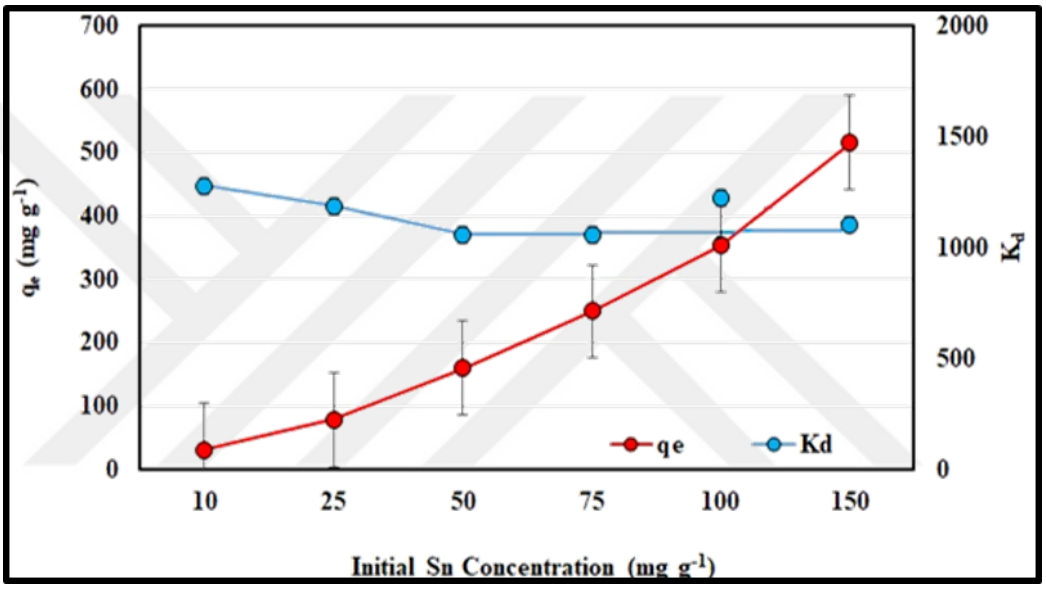

Figure 4.3 : Initial Sn concentration on the qe and Kd.

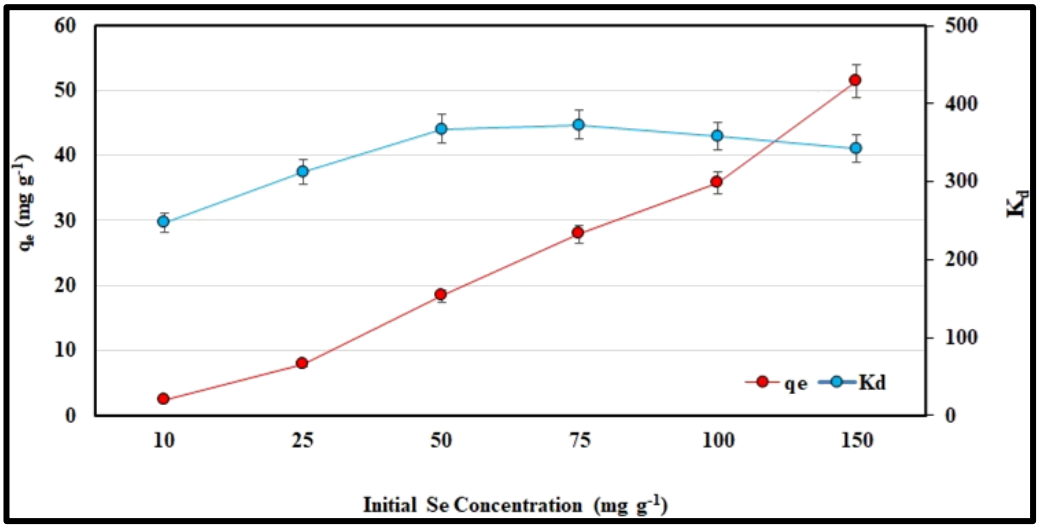

Figure 4.4 : Initial Se concentration on the q_e and K_d.

Figure 4.4 shows how the initial concentration of selenium affects the adsorption of selenium in the composite barrier material. K_d values for selenium ions raised significantly before reaching equilibrium. q_e values varied from 2.47±0.10 to 51.40±2.10 mg g^{-1} for changed initial concentrations of selenium.

4.2.2 Effect of temperature

Figure 4.5 shows how the waste mixture temperature affects the interaction of tin radionuclide with the developed composite barrier material. From the results acquired, it was noticed that the Sn radionuclide adsorption on the composite barrier material decreased with increasing temperature. This suggests that Sn radionuclides interact with the barrier material by forming Van der Waals bonds through physical adsorption.

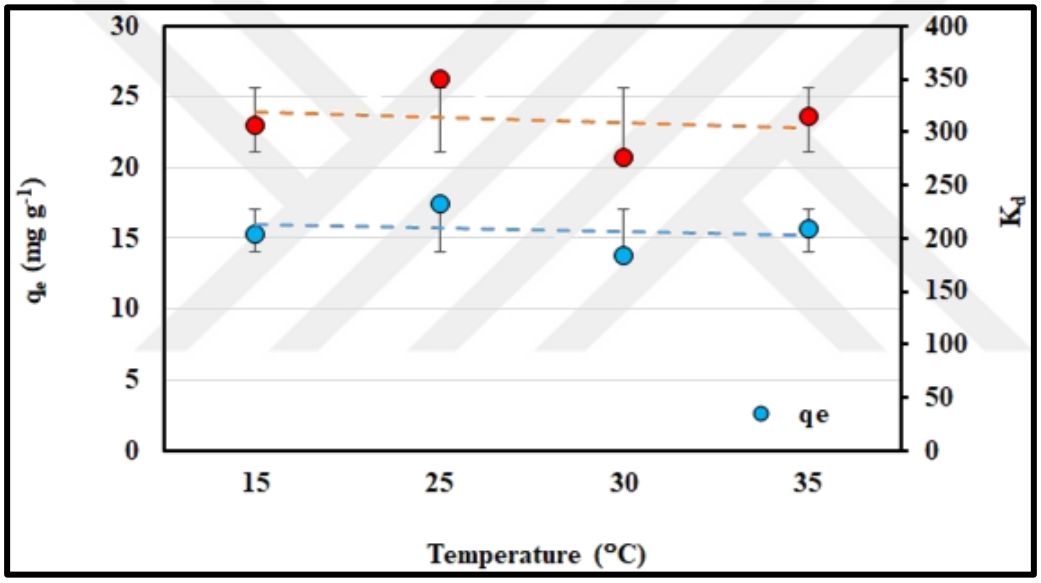

Figure 4.5 : Temperature effects of Sn onto q_e and K_d.

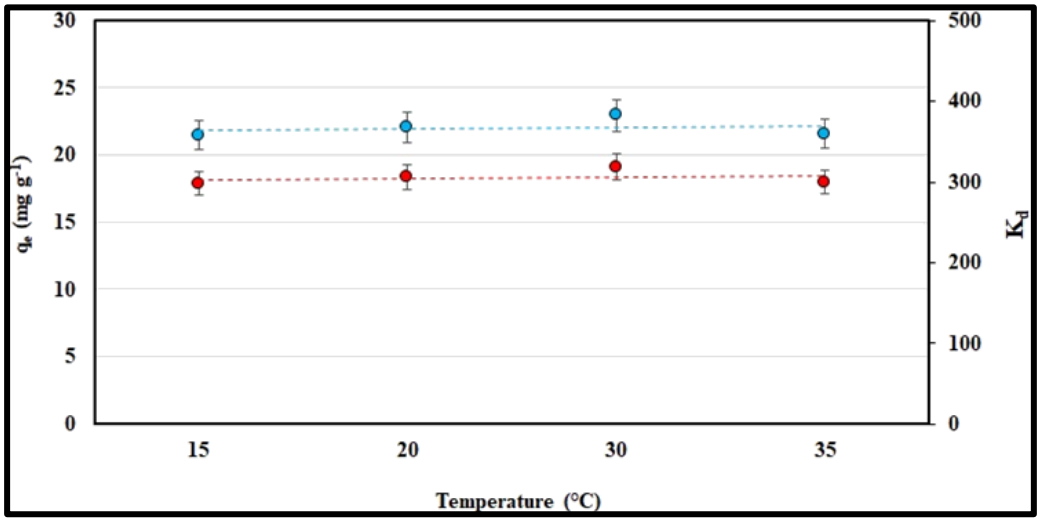

Figure 4.6 : Temperature effects of Se onto q_e and K_d.

The efficiency of the selenium radionuclides' interacting with the composite barrier material during adsorption depending on the temperature of the waste mixture is demonstrated in Figure 4.6. According to Figure 4.6, the capacity of adsorption looks to be trending slightly raising. The q_e value indicates a slightly increment with rising temperature, as shown in Fig. 4.6. At ambient temperature, the q_e value was determined to be 18.39± 0.014 mg g^{-1}.

4.2.3 Effect of interaction time

Figure 4.7 shows the change in the distribution coefficient as a function of the interacting time of the Sn ion interaction with the composite barrier material at time period ranged 15 minutes-4 hours at pH 2-3 at ambient temperature. Accordingly, it has been shown that the adsorption capacity of the tin ion goes up as the interaction time increases. After 60 minutes of interaction, the adsorption efficiency remained constant.

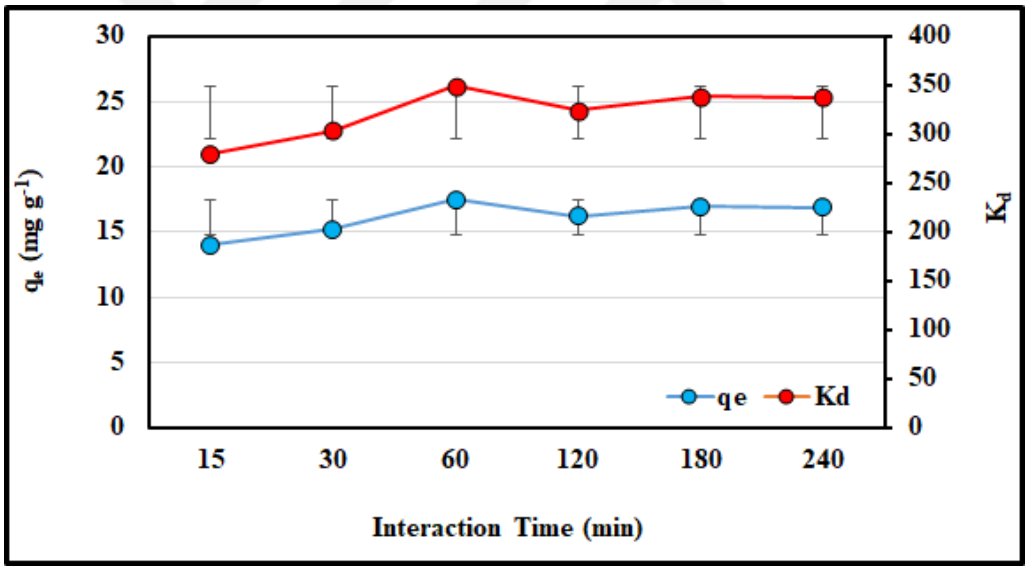

Figure 4.7 : Interaction time effect of Sn onto q_e and K_d.

In Figure 4.8 the distribution coefficient of the relation of selenium ions and the composite barrier material is shown for different time period ranged 15 minutes - 4 hours at pH 3.5 at room temperature. Selenium adsorption raised moderately with time and then arrived balance level after 30 minutes according to the data. The q_e value was calculated as 18.75±0.76 mg g^{-1}.

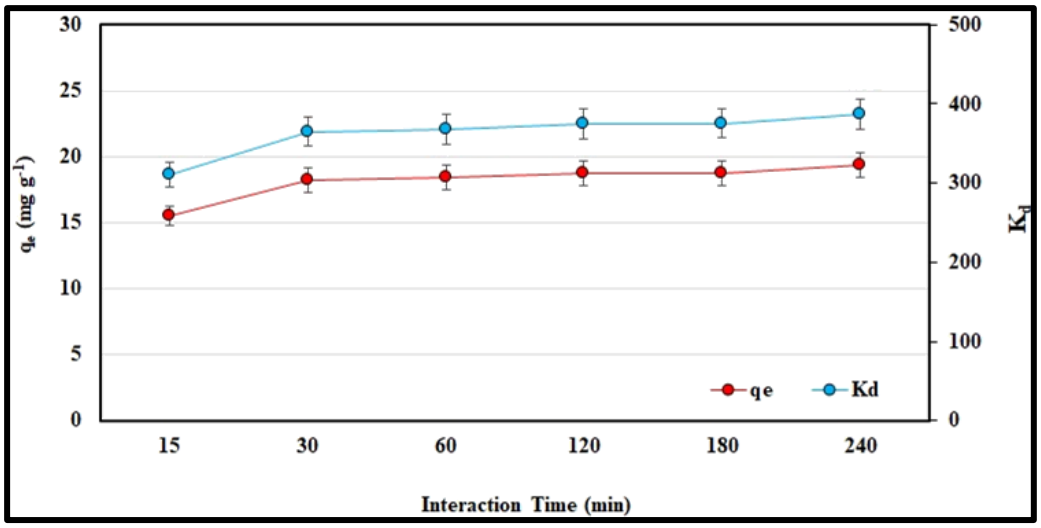

Figure 4.8 : Interaction time effects of Se onto q_e and K_d.

4.3 Adsorption Isotherms

Adsorption isotherms are models that express adsorption equilibrium independent of temperature. As determined by the Freundlich isotherm model, Langmuir isotherm model, Temkin isotherm model, and Dubinin- Radishkevich (D-R) isotherm model, the regression coefficients and constant values for tin ion are displayed in Table 4.1.

Table 4.1 : Langmuir, Freundlich, Dubinin-Radushkevich (D-R) and Temkin constants for tin ion.

Isotherms	**Parameters**		
Langmuir	**Q° (g g^{-1})**	**b (mg L^{-1})**	**R^2**
	5.00	0.24	0.1625
Freundlich	**k_F (mg g^{-1})**	**1/n**	**R^2**
	0.018	0.043	0.3051
D-R	**X_m (g g^{-1})**	**E (kJ mol^{-1})**	**R^2**
	0.83	8.45	0.9937
Temkin	**B_1 (J mol^{-1})**	**k_T (mg L^{-1})**	**R^2**
	0.001	17.62	0.8396

The D-R isotherm model (R^2 = 0.99) was perfectly suited by the adsorption data of tin adsorbed in the composite barrier material, as could be seen by taking into account the regression coefficients of the studied adsorption isotherm models in Table 4.1. The ions in the environment are assumed to be adsorbed in the micropores of the adsorbent, composite barrier material, in the Dubinin-Raduskevich adsorption isotherm model.

Considering the regression coefficients, selenium adsorption input in the adsorbent perfectly suits by the D-R, and Tempkin isotherm models with R^2 values of 0.98, and 0.96, respectively (Table 4.2). Selenium ions in the aquatic environment are adsorbed

in the micropores of the adsorbent, composite barrier material, according to the Dubinin-Radushkevich adsorption isotherm model.

Table 4.2 : Langmuir, Freundlich, Dubinin-Radushkevich (D-R) and Tempkin constants for selenium ion.

Isotherms	**Parameters**		
Langmuir	**Q° (g g^{-1})**	**b (mg L^{-1})**	**R^2**
	0.04	<0	0.3752
Freundlich	**k_F (g g^{-1})**	**1/n**	**R^2**
	0.062	0.350	0.8492
D-R	**X_m (g)**	**E (kJ mol^{-1})**	**R^2**
	0.047	5.00	0.9775
Tempkin	**B_1 (J mol^{-1})**	**k_T (mg L^{-1})**	**R^2**
	3.18	0.011	0.9584

The accepted equation for this isotherm model is given as Equation 4.1:

$$lnq_e = lnX_m - \beta\varepsilon^2 \tag{4.1}$$

q_e: adsorbate quantity at balance state,

X_m: maximum capacity of adsorption,

β: a constant related with energy,

ε: Polanyi potential.

Polanyi potential is calculated from the Equation 4.2.

$$\varepsilon = RT\ln(1/1 + C_e) \tag{4.2}$$

R: gas constant (kJ mol^{-1}),

T: temperature (K).

A straight line is produced by drawing ε^2 against lnC_e. The y-axis cutoff point and slope were used to determine the values of β (mol K^{-1})^2 and q^m (mmol g^{-1}).

Sorption energy (E) was computed by using the Equation 4.3.

$$E = 1/(-2\beta)^{-1/2} \tag{4.3}$$

The average adsorption energy is indicated by (E). The adsorption process is regarded as physical adsorption if the value is less than 8 kJ mol^{-1}. If chemical adsorption is the process, E should be in range 8-16 kJ mol^{-1}.

The average adsorption energy value for tin ions in this study was determined to be 8.45 kJ mol^{-1}. This outcome demonstrates that tin ions are adsorbed chemically during the adsorption process.

The average adsorption energy value for selenium ions is calculated to be 5.00 kJ mol^{-1}. This shows that in the micropores of the composite barrier material, the ion forms a physical bond with the barrier material.

Because of homogeneous distribution of the binding energies in the adsorption and the adsorbent-adsorbate interaction, Temkin isotherms assume that the adsorption temperature of all molecules in the layers will be declined linearly.

The composite barrier material's selenium adsorption capability was discovered to be 47 mg g^{-1}. According to novel research, the adsorption capacity of selenium is varied for different materials. For example, adsorption capacity of selenium is found 18.4 mg g^{-1} for chitosan-clay composites, 1.445 mg g^{-1} for activated carbon supported with magnetite, 41.02 mg g^{-1} for Fe-Mn hydrous oxides, 32.17 mg g^{-1} for Nano-TiO_2 and 0.52 mg g^{-1} for goethite. In comparison to those discovered in other studies, the adsorption capacity of selenium gained in this study is absolutely great.

4.4 Kinetic Model

The results of applying all kinetic models to the data resulting from the time-based relation between tin ions and the barrier material with are shown in Table 4.3. As a result, it can be observed from the correlation coefficients that the pseudo-second-order model of the adsorption process is compatible with the tin adsorption on the composite barrier material. This demonstrates that surface adsorption, including chemical adsorption, is the rate-limiting phase.

Table 4.3 : Kinetic parameters obtained for kinetic models for Sn.

Pseudo-first order model			**Pseudo-second order model**			**Elovich model**		
k_1 (min^{-1})	**q_e (mg g^{-1})**	**R^2**	**k_2 (min^{-1})**	**q_e (mg g^{-1})**	**R^2**	**1/b**	**A**	**R^2**
-0.001	9.80	0.3742	2.96	0.68	0.9991	0.97	220011	0.6377

The adsorption of selenium ions on the developed composite barrier material is suited to pseudo-second-order based on the findings shown in Table 4.4. The adsorption input

at various temperatures comply with the pseudo-second order model, as can be seen from the findings.

Table 4.4 : Kinetic parameters obtained for kinetic models for Se.

Pseudo-first order model			Pseudo-second order model			Elovich model		
k_1 (1 min^{-1})	q_e (mg g^{-1})	R^2	k_2 (1 min^{-1})	q_e (mg g^{-1})	R^2	1/b	a	R^2
-0.002	0.20	0.6510	0.20	0.79	0.9998	0.03	6339	0.7519

4.5 Thermodynamic Parameters

The results of the thermodynamic parameter calculated using the acquired adsorption data for tin ions are shown in Table 4.5. Tin's positive enthalpy change suggests that the interaction mechanism can be described as absorbing heat from environment, and an enthalpy value of smaller than 4 kJ mol^{-1} suggests that the interaction is physical adsorption between the tin and the barrier material. An increase in the interface of solid/solution at random during the adsorption is indicated by a positive entropy value. The interaction is unplanned if the Gibbs energy is negative, and as the temperature rises, the Gibbs energy also decreases, indicating that the process is becoming less spontaneous.

Table 4.5 : Thermodynamic parameters for tin adsorption.

ΔH (kJ mol^{-1})	ΔS (kJ mol^{-1} K^{-1})	ΔG (kJ mol^{-1})			
		288 K	298 K	303 K	308 K
0.98	0.04	-11.83	-12.27	-12.49	-12.71

The thermodynamic parameters for selenium ions were determined using adsorption data based on the temperature parameter and are displayed in Table 4.6. The findings indicate that the exothermic characteristic of the adsorption process is demonstrated by the negative enthalpy change. The solid/solution interface increased arbitrarily during the adsorption process, as shown by the positive entropy value. As the Gibbs energy is negative, the interaction is spontaneous, and when the Gibbs energy is decreased by raising the temperature, the process becomes less random. 9.22 kJ mol^{-1} K^{-1} of activation energy (E_a) was found. This demonstrates that chemical adsorption is the mechanism through which the selenium ions interact with the composite barrier material. Chemical adsorption is indicated by an E_a value between 4 and 40 kJ mol^{-1} K^{-1}.

Table 4.6 : Thermodynamic parameters for selenium adsorption.

ΔH (kJ mol^{-1})	ΔS (kJ mol^{-1} K^{-1})	ΔG (kJ mol^{-1})			
		288 K	298 K	303 K	308 K
-0.79	0.05	-15.68	-16.20	-16.46	-16.72

4.6 Kinetic Model Based on Diffusion

Using the data obtained by examining the time-dependent changes of tin and selenium ions with the barrier, their compatibility with both the Homegenous Particle Diffusion Model (HPDM) and the Shell Formation Model (SPM) was examined. Considering the regression coefficients of the graphs obtained, it was determined which diffusion models were suitable for the interaction with the barrier for tin and selenium. The data obtained for both diffusion models are given in Table 4.7.

As seen in Table 4.7, the regression coefficients for the HPDM model of tin ions are greater than 0.90. In the interaction of tin ions with the barrier material, the particle diffusion coefficient D in the solid phase and the liquid film diffusion coefficient (D_e) were found to be 1.86E-04 and 7.12E-07, respectively. Accordingly, it can be said that the tin ions diffuse to the homogeneous surface of the barrier material, with infinite dilution, and the particle geometry is spherical. Both the liquid film formed by the ions around the particle and the diffusion of the ions into the barrier particles plays a role in the diffusion rate of tin ions. It can be said that the diffusion in the liquid phase is a faster process than the diffusion in the solid phase.

It is seen from the regression coefficients that diffusion into the liquid film and particle is not effective in the interaction of selenium ions with the barrier material. The SPM model, which assumes a chemical reaction between the fluid and the particle, shows from the regression coefficients in Table 4.7 that there is no effective process in the interaction of both tin and selenium ions with the barrier material.

4.7 Species

The tin wastes are assumed in an acidic solution in waste repository and the study was performed in a pH 2-3 solution. One of the redox-sensitive elements, tin, exhibits oxidation state from -4 to +4, yet in an aqueous solution, it possesses +2 and +4 valencies. Sn(II) and Sn(IV) ions form in dimeric interaction complexes in hydrochloric acid solution. SnO_2 is only clearly soluble in strong acids or basic media.

Table 4.7 : Compability with HPDM and SPM of time-dependent changes of tin and selenium ions with the barrier

	HPDM				SPM					
	Liquid Phase		Solid Phase		Film diffusion		Layer diffusion		Chemical reaction	
	D (m/s)	R^2	D_e (m^2/s)	R^2	K_F (cm/s)	R^2	D_e (cm^2/s)	R^2	k_s (cm/s)	R^2
Sn	1.86E-04	0.9169	7.12E-07	0.9177	7.81E-06	0.3962	2.15E-07	0.1879	8.69E-05	0.0606
Se	-1.14E-06	0.6435	-9.40E-03	0.6344	6.45E-05	0.5673	3.87E-06	0.8238	3.85E-06	0.8816

SnO has a higher solubility. Tin can be hydrolyzed to produce $SnOH^+$, $Sn_2(OH)_2^{2+}$, and $Sn_3(OH)_4^{2+}$, which is the major form. These compounds' pK values for hydrolysis are 3.40, 4.77, and 6.88. Although $[Sn(OH)_3]^-$ complex is the predominant species in alkaline solutions, it is also obvious that the dinuclear ion $[Sn_2(OH)_4O]^{2-}$ is available in the environment. $[Sn(OH)_6]^{2-}$ is the predominant species in alkaline tin solutions (Suter, 1991). Only Sn(IV) is significant in all pH levels larger than 2 when water stability is redox-dominating (Ochs et al., 2016). Tin arises as $Sn(OH)_5^-$ and $Sn(OH)_6^{2-}$ hydrolysis types in systems where the solidification of nuclear wastes is made with cement because the pH is greater than 8 (Ochs et al., 2016). Tin (II) ions can dissolve in solutions with tin concentrations less than 10^{-7} M, but Sn(0) and Sn(IV) ions precipitate at the proper pH and Eh conditions.

When pH is 7.3 and Eh is less than 185 mV in hydrogeological circumstances, Sn(IV) is anticipated to be the dominant feature. In solutions with tin concentrations lower than 10^{-8} M, precipitation is not seen. K_d values are high because tin becomes more soluble when anions like chlorine are present (Kedziorek et al., 2007).

XPS spectra was used to look into the formation of chemical bonds and structure of the composite barrier material earlier than interaction with tin and at the end of the interaction with it. The O1s, C1s, N1s, Si2p, and Al2p spectral areas on the material's surface are identified, and their respective binding energies are 532, 286, 399, 102, and 74 eV (Figure 4.9). Sn 3d electrons are attached to the barrier material with a binding energy of 488 eV in the formation of SnO, as seen by the XPS spectra. The oxidation number of tin in this study's adsorbed of tin by the barrier material is Sn (II).

Selenium exhibits oxidation-reduction processes, which are well known. Both the Se(IV) (selenite) and Se(VI) (selenate) oxidation processes use selenium. Se(IV) and Se(VI) are harmful in various ways. Se(IV) is known to be more poisonous than Se (VI). As a result, it is crucial to remove Se(IV) ions from environmental media. Additionally, according to several research, adsorption of selenite (Se(IV)) is more probable than adsorption of selenate (Se(VI)) (Séby et al., 1998; W. Xu et al., 2021). According to Seby et al. (1998), the pH totally determines the Se(IV) adsorption of clay minerals and different metal oxides. The adsorption is inverse proportional with the pH value; in other words, the best adsorbtion occurs in an acidic environment (Séby et al., 1998).

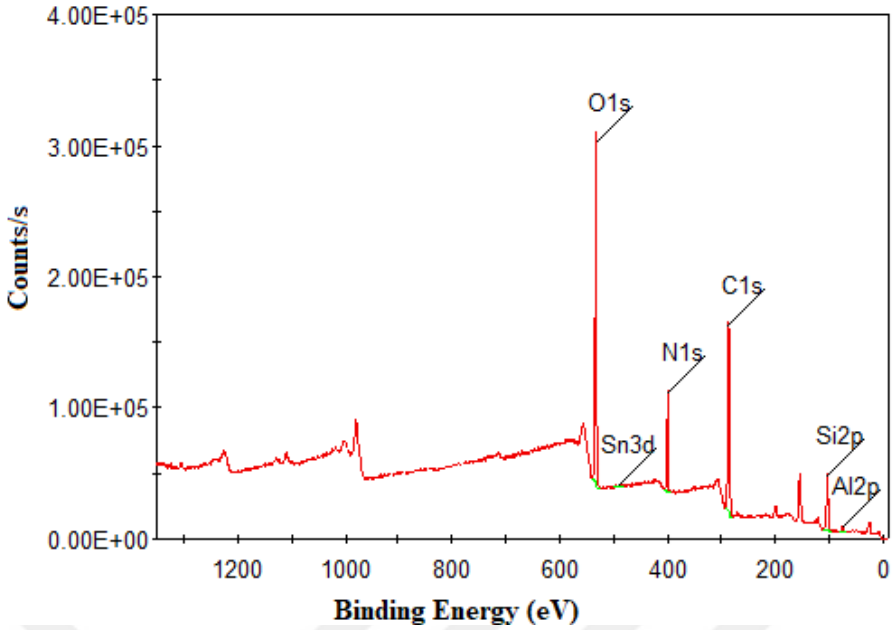

Figure 4.9 : XPS results of interaction of Sn and composite barrier material.

The investigations were conducted in an acidic media because a composite barrier material comprising zeolite minerals was used in this thesis. Numerous oxides are created when selenium and oxygen interact. SeO_2 is the most durable of these oxides. The oxidizing power of selenium dioxide is well known. According to the concentration of selenium in the solution, the initial pH of the selenium solution used in this investigation ranged from pH 3.5 to pH 4.0. It was found that in this pH range, the solution potential varied between 0.18 - 0.23 V. As a result, $HSeO_3^-$ would be the anticipated selenium species in this probable pH combination (Séby et al., 1998).

Moreover, by using X-ray photoelectron spectroscopy, the surface formtion of the composite barrier was compared earlier than the adsorption process and at the end of adsorption to explain the surface structure and chemical bonding of the surface atoms. The outcome was exhibited in Figure 4.10. As can be seen in Figure 4.10, the spectral areas O1s, C1s, N1s, Si2p, and Al2p were present on the surface of the composite barrier material. Their respective binding energies are 532, 286, 400, 103, and 74 eV. Se3d's binding energy is listed as 56.70 eV in the NIST binding energy database (NIST, 2012). Se3d's binding energy in this investigation was discovered to be 56.98 eV.

The peak is changing into a narrower form when the FWHM decreases. This demonstrates that adsorption is stronger here. It may be deduced that Al_xSiOz-Se and/or $Al_xSiOz(OH)$-Se structures, which are included in the NIST binding energy

database, can occur when Se penetrates between the bonds between Al-Si-O in the zeolite, causing a drop in the Al and Si concentration in the structure. The SiO_2 unit and the AlO_2 unit are the two major negatively charged chemical groups found in the majority of zeolites. It is concluded that the weight-based Si/Al ratio of the composite barrier fell from 4.23 to 3.41 with the addition of Se; however, the weight-based Si/Al ratio of the composite barrier climbed from 4.23 to 6.78 with the addition of Sn (Table 4.8).

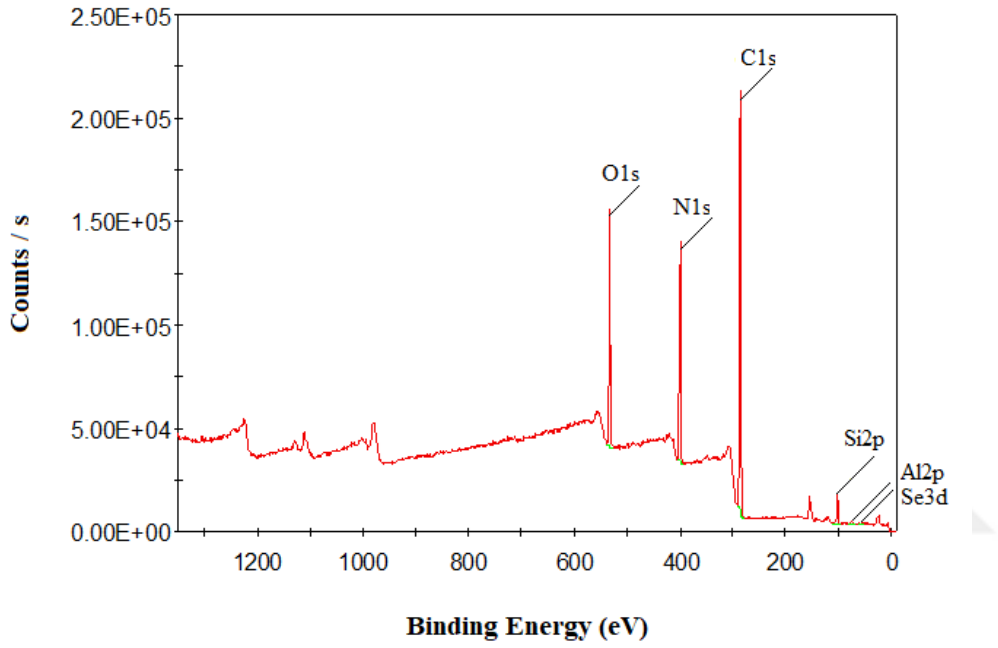

Figure 4.10 : XPS results of interaction of Se and composite barrier material.

According to the XPS measurements, the bond energy of the N1s peak in the PAN fibers that make up the developed composite barrier's organic structure is 399.63 eV. This could be because the three components, with bond energies of 400.26, 399.29, and 399.09 eV, respectively, are -NH-/=NH, $-NH_2$, and $-NR_2$ (Zhao et al., 2015). After selenium and tin ions were adsorbed, the binding energy values of the maximum levels of the -NH-/=NH groups and the $-NH_2$ group were similar. This shows that there was no chelate formation between the N atom from the amino and imino groups and the metal ion M^{x+}. After selenium and tin ions were adsorbed, the N1s binding energies of $-NR_2$ barely increased. This demonstrates that the chelating interaction between tertiary amines and M^{x+} may not be very strong.

Table 4.8 : Surface properties determined by XPS before and after tin and selenium adsorption on the composite barrier material.

Composite Barrier Material				
Name	**Peak BE**	**FWHM eV**	**Area (P) CPS.eV**	**Weight %**
Al2p	74.28	1.94	906	3.32
Si2p	102.64	2.01	5826	14.07
C1s	286.19	2.66	43708	45.34
N1s	399.63	1.57	16000	12.46
O1s	532.03	2.37	43429	24.81
Composite Barrier Material and Selenium				
Name	**Peak BE**	**FWHM eV**	**Area (P) CPS.eV**	**Weight %**
Se3d	56.98	3.34	165	0.75
Al2p	74.38	1.97	531	2.39
Si2p	102.76	2.09	2755	8.14
C1s	286.23	2.47	43246	54.93
N1s	399.60	1.59	17179	16.38
O1s	532.18	2.53	24885	17.41
Composite Barrier Material and Tin				
Name	**Peak BE**	**FWHM eV**	**Area (P) CPS.eV**	**Weight %**
Sn3d	488.00	1.74	417.39	0.11
Al2p	75.67	2.49	1045.84	3.34
Si2p	103.72	2.23	10795.68	22.65
C1s	286.24	2.58	36016.04	32.45
N1s	399.63	1.54	13097.61	8.86
O1s	532.50	2.15	65653.23	32.59

4.8 Risk Assessment on Environment and Human

4.8.1 Dose calculations by ERICA Assessment Tool

The risks of waste radionuclides spreading to the environment in the event of a repository accident for radioactive waste have been assessed. The concentrations of tin and selenium in the solution before and after the adsorption process were converted into activity units, and the ability of the barrier material to prevent tin and selenium ions from migrating into the ecosystem was examined. The ERICA Tool Assessment program analyzed how much aquatic and terrestrial biota may get as a result of leaking into the environment from the waste repository with and without barrier material. The activity varies between 1.14E09 and 1.71E10 Bq L^{-1} activity levels.

The examined freshwater biota of crustaceans, phytoplankton, and vascular plants will be exposed to 4.02E6 to 3.87E9 G h^{-1} for radioactive tin isotope and 3.35E07 to 1.92E12 G h^{-1} for radioactive selenium isotope (Table 4.9 and Table 4.10).

The examined terrestrial biota of annelid, grasses&herbs, lichen&bryophytes, mammal, shrub, tree will be exposed 4.51E06 to 7.41E04 G h^{-1} for tin and 2.15E06 to 5.53E09 G h^{-1} for selenium (Table 4.11 and Table 4.12).

It was not possible to compare the results with previous research since the ERICA program had not previously evaluated the exposure to freshwater and terrestrial biota from the total doses coming from radioactive waste repositories.

4.8.2 Formation of waste storage model by Goldsim Montecarlo Simulation Program

Transporting radioactive waste from the repository to the biosphere requires that the radionuclides come into contact with water below the surface of the earth. A design is created to limit the interaction of the waste with groundwater while developing barrier materials for radioactive waste sites since the radionuclides in the waste can only disintegrate when confronted with water and can reach the biosphere. They can migrate via diffusion in the absence of water, but this is extremely peculiar and they are unable to move over a meter in a couple of million years. The rate at which groundwater travels may differ from one location to another. Radionuclides can only move from rocks in the waste zone by water flow through multi-directional fracture systems and diffusion on the microcracks and pore system. Radionuclides in the waste area can penetrate surface waster resources and human habitats in this way (Laverov et al., 2011).

In this thesis, it has been assumed that contact with groundwater causes the tin and selenium in the waste to migrate by dissolving as a result. It was proposed that significant quantities of tin and selenium contact with the PAN/zeolite composite barrier, get adsorbed in the barrier material, and afterwards get propagated in the aquifer. Additionally, it is acknowledged that the rocks in the region of the waste area have weak penetration, lack micropores, and encourage water flow.

The input data were used to help calculate the radioactive release rate from the waste area, and the studies provided a characterization of the groundwater release rate (Jo et al., 2018; Lee et al., 2013, 2016). The dose concerning time was computed after the data were obtained and compared using the authorized dose limits. Using information gathered from research on the tin removal by using the composite barrier material, the initial activity value was calculated.

Table 4.9 : Total ^{126}Sn dose range for freshwater biota.

Sn	Freshwater		
	Crustaen	**Phytoplankton**	**Vascular Plant**
Max. Dose (μG h^{-1})	3.87E+09	7.49E+07	7.49E+07
Min. Dose (μG h^{-1})	2.37E+08	4.02E+06	4.02E+06

Table 4.10 : Total ^{79}Se dose range for freshwater biota.

Se	Freshwater		
	Crustaen	**Phytoplankton**	**Vascular Plant**
Max. Dose (μG h^{-1})	1.92E+12	2.73E+08	2.87E+11
Min. Dose (μG h^{-1})	2.35E+11	3.35E+07	3.52E+10

Table 4.11 : Total ^{126}Sn dose range for terrestrial biota.

Sn	Terrestial					
	Annelid	**Grasses & Herbs**	**Lichen &bryophytes**	**Mammal**	**Shrub**	**Tree**
Max. Dose (μG h^{-1})	4.51E+06	1.69E+06	1.93E+06	4.20E+06	1.70E+06	1.38E+06
Min. Dose (μG h^{-1})	2.42E+05	9.11E+04	1.04E+05	2.26E+05	9.14E+04	7.41E+04

Table 4.12 : Total ^{79}Se dose range for terrestrial biota.

Se	Terrestrial					
	Annelid	**Grasses & Herbs**	**Lichen &bryophytes**	**Mammal**	**Shrub**	**Tree**
Max. Dose (μG h^{-1})	4.09E+08	1.56E+08	5.53E+09	1.75E+07	4.99E+08	4.99E+08
Min. Dose (μG h^{-1})	5.02E+07	1.91E+07	6.79E+08	2.15E+06	6.13E+07	6.13E+07

Applying the coefficients given in ICRP 119 for individuals and children subjected to through ingestion, the simulation results for Sn and Se have been produced as the activity (Bq) and effective dose (Sv) (ICRP, 2012). Table 4.13 provides the findings about the individuals and childrens dose exposure of ^{126}Sn and ^{79}Se in absence and existence of the composite barrier. The results after 2 million years of simulation show that whereas individuals are exposed to 1.49E-20 mSv of ^{126}Sn in the radioactive waste area, childres are only exposed to 2.85E-19 mSv of ^{126}Sn. According to this scenario, the dose exposure for individuals due to the ^{79}Se in the 1 million years is 7.07E-26 mSv, and children's dose exposure is 2.44E-17 mSv.

Table 4.13 : Exposed dose for adult and infant because of the Se and Sn.

	Without Barrier		**With Barrier**	
	Dose (Infant) mSv	**Dose (Adult) mSv**	**Dose (Infant) mSv**	**Dose (Adult) mSv**
Sn	7.70E-12	4.02E-13	2.85E-19	1.49E-20
Se	9.61E-11	2.53E-11	2.44E-17	7.07E-26

In accordance with ICRP103, the effective dose for occupational exposure shall not be greater than 20 mSv annually and 50 mSv in a single year. The permissible annual effective dose limit for individuals is 1 mSv (IAEA GSG-8, 2018; ICRP Publication 103, 2007). These limits have established 20–100 mSv for UK and 1–50 mSv for Turkey.

In addition, the UNSCEAR reported that the natural radiation sources provide an annual effective dose of 2.4 mSv, with 0.3 mSv of the total dose coming from internal radiation exposure (UNSCEAR, 2000). The effective dose get from model for tin and selenium is observed to be smaller than the maximum acceptable dose limits when taking accounts of the effective dose limit specified in ICRP103, supported by IAEA General Safety Guide No. GSG-8, and determined natural radioactivity by UNSCEAR.

4.8.3 Carciogenic risk assessment and excess lifetime cancer risks

According to Table 4.14, the tin concentration not kept in the composite barrier material will result in values for the hazard ratio (HQ), total hazard index (THI), and overall carcinogenic risk for individuals and children if it distributes from the radioactive waste area to the ecosystem. For both adults and children, at high tin concentrations, THI values are lower than 1. As a consequence of their prolonged

exposure to tin, which remain in the water from the developed barrier substance at the radioactive waste area, this result demonstrates that tin will not, in the case of an accident, cause noncarcinogenic adverse effects in adults and children. Tin slope factors were used to determine the potential carcinogenic risk that might come from tin exposure by ingestion and skin ways (Gulan et al., 2020). By ingestion, the total carcinogenic risk (TCR) was determined to be 3.00E-25 for individuals and 2.41E-23 for children, while by dermal contact, it was found to be 3.42E-10 for individuals and 2.56E-09 for children. Tin released from the radioactive waste repository does not provide a substantial risk hazard to individuals or children because the cancer risks values are less than 10^{-4}.

Table 4.15 presents the total carcinogenic risk (TCR) for ^{79}Se based on ADD values for dermal and ingestion absorption that remain from developed composite barrier substance and spread from the radioactive waste area. THI values demonstrate the differences at various selenium concentrations, and they are all less than 1. Ingestion-related TCR values for adults vary from 4.93E-17 to 4.03E-16, whereas those for infants vary between 6.30E-22-5.16E-21. For adults, TCR values related to dermal effects in the range of 5.28E-21-4.32E-20, whereas for infants, they range from 7.74E-31 to 6.34E-30. Since 10^{-4} is the crucial quantity for cancer risk, it is clear that the spread of ^{79}Se from the radioactive waste repository poses negligible carcinogenic risk to adults and children.

Computed from the excess lifetime cancer risk (ELCR), which demonstrates the cumulative risk of exposure to cancer development for both employees and inhabitants as a consequence of the radionuclides in the radioactive waste area producing ionizing radiation as a result of different operations (1.15E13-1.73E14 Bq for ^{126}Sn and 1.04E+12-8.47E+12 for ^{79}Se) in the event that ^{126}Sn and ^{79}Se spreads to the environment because of a disaster (Table 4.16 and Table 4.17).

The ELCR ranges for ingestion due to ^{126}Sn for adults are 9.73E-01 and 5.23E-02 and for infants are 1.86E+01 and 1.00E+00. Depending on the ^{126}Sn activity, this value for inspiration ranges between 5.80E+00 and 3.12E-01 for individuals and between 2.48E+01 and 8.12E-01 for children. In the worst-case scenario that is any barrier does not work at all, the ELCR values range for ingestion between 6.00E+01 and 4.00E+00 for infants, 3.13E+00 and 2.09E-01 for adults. This value for inhalation varied between

8.00E+01 and 3.24E+00 for infant and 7.33E+00 and 4.89E-01 for adult. Women have a lower ELCR value than males do.

The ELCR ranges for ingestion due to ^{79}Se for adults are 1.16E-02 to 9.45E-02 and for infants are 4.39E-02 to 3.59E-01. Depending on the ^{79}Se activity, this value for inhalation ranges between 4.39E-03 and 8.48E-02 for adults and between 6.38E-02 and 4.56E-01 for infants. In the worst-case scenario that is any barrier does not work at all, the ELCR values range for ingestion between 1.33E0 and 8.88E-2 for infants, 3.51E-1 and 2.34E-2 for adults. This value for inhalation varied between 1.04E0 and 1.29E-1 for infant and 1.33E-1 and 8.88E-3 for adult. Like in the ^{126}Sn, women have a lower ELCR value than males do.

These numbers for both ^{126}Sn and ^{79}Se are considerably greater than the global mean of 2.9E-4.

Table 4.14 : Carciogenic and non-carciogenic risks of ^{126}Sn.

Sn (mgL^{-1})	ADD_{ing}		ADD_{der}		HQ_{ing}		HQ_{der}		TCR_{ing}		TCR_{der}		THI	
	Adults	Child	Adults	Child	Adults	Child	Adults	Child	Adults	Child	Adults	Child	Adults	Child
0.63	6.31E-16	5.89E-15	9.19E-10	6.89E-09	1.61E-26	1.51E-25	1.84E-11	1.38E-10	1.61E-26	1.51E-25	1.38E-10	1.38E-10	1.84E-11	1.38E-10
1.66	1.67E-15	1.56E-14	2.43E-09	1.82E-08	4.27E-26	3.98E-25	4.86E-11	3.64E-10	4.27E-26	3.98E-25	3.64E-10	3.64E-10	4.86E-11	3.64E-10
3.77	3.79E-15	3.54E-14	5.53E-09	4.14E-08	9.71E-26	9.07E-25	1.11E-10	8.29E-10	9.71E-26	9.07E-25	8.29E-10	8.29E-10	1.11E-10	8.29E-10
5.89	5.93E-15	5.53E-14	8.63E-09	6.47E-08	1.52E-25	1.42E-24	1.73E-10	1.29E-09	1.52E-25	1.42E-24	1.29E-09	1.29E-09	1.73E-10	1.29E-09
7.20	7.25E-15	6.77E-14	1.06E-08	7.92E-08	1.86E-25	1.73E-24	2.11E-10	1.58E-09	1.86E-25	1.73E-24	1.58E-09	1.58E-09	2.11E-10	1.58E-09
11.65	1.17E-14	1.10E-13	1.71E-08	1.28E-07	3.00E-25	2.80E-24	3.42E-10	2.56E-09	3.00E-25	2.80E-24	2.56E-09	2.56E-09	3.42E-10	2.56E-09

Table 4.15 : Carciogenic and non-carciogenic risks of ^{79}Se.

Se (mgL^{-1})	ADD_{ing}		ADD_{der}		HQ_{ing}		HQ dermal		TCR_{ing}		TCR_{der}		THI	
	Adult	Infant	Adult	Infant	Adults	Child	Adult	Infant	Adult	Infant	Adults	Child	Adults	Child
4.94	6.8E-06	8.6E-11	7.24E-10	1.06E-19	1.35E-03	1.73E-08	1.4E-07	2.1E-17	4.93E-17	6.30E-22	5.28E-21	7.74E-31	1.35E-03	1.73E-08
9.26	1.3E-05	1.6E-10	1.36E-09	1.99E-19	2.54E-03	3.24E-08	2.7E-07	4.0E-17	9.24E-17	1.18E-21	9.90E-21	1.45E-30	2.54E-03	3.24E-08
12.98	1.8E-05	2.3E-10	1.90E-09	2.79E-19	3.55E-03	4.54E-08	3.8E-07	5.6E-17	1.30E-16	1.66E-21	1.39E-20	2.04E-30	3.56E-03	4.54E-08
18.86	2.6E-05	3.3E-10	2.77E-09	4.06E-19	5.17E-03	6.60E-08	5.5E-07	8.1E-17	1.88E-16	2.41E-21	2.02E-20	2.96E-30	5.17E-03	6.60E-08
25.91	3.5E-05	4.5E-10	3.80E-09	5.58E-19	7.10E-03	9.08E-08	7.6E-07	1.1E-16	2.59E-16	3.31E-21	2.77E-20	4.07E-30	7.10E-03	9.08E-08
40.38	5.5E-05	7.1E-10	5.92E-09	8.69E-19	1.11E-02	1.41E-07	1.2E-06	1.7E-16	4.03E-16	5.16E-21	4.32E-20	6.34E-30	1.11E-02	1.41E-07

Table 4.16 : ELCR for ^{126}Sn.

Activity (Bq)	Ingestion				Inhalation infant				Inhalation adult			
	$ELCR_{infants}$		$ELCR_{adults}$		ELCR (f)		ELCR(m)		ELCR (f)		ELCR (m)	
	With Barrier	Without Barrier	With Barrier	Without Barrier	With Barrier	Without Barrier	With Barrier	Without Barrier	With Barrier	Without Barrier	With Barrier	Without Barrier
1.15E+13	2.60E-01	4.00E+00	1.36E-02	2.09E-01	2.11E-01	3.24E+00	3.47E-01	5.33E+00	3.18E-02	4.89E-01	8.09E-02	1.24E+00
2.88E+13	6.87E-01	9.99E+00	3.59E-02	5.22E-01	5.58E-01	8.11E+00	9.17E-01	1.33E+01	8.40E-02	1.22E+00	2.14E-01	3.11E+00
5.77E+13	1.56E+00	2.00E+01	8.17E-02	1.04E+00	1.27E+00	1.62E+01	2.09E+00	2.67E+01	1.91E-01	2.44E+00	4.87E-01	6.22E+00
8.65E+13	2.44E+00	3.00E+01	1.28E-01	1.57E+00	1.98E+00	2.43E+01	3.26E+00	4.00E+01	2.99E-01	3.66E+00	7.61E-01	9.33E+00
1.15E+14	2.99E+00	4.00E+01	1.56E-01	2.09E+00	2.43E+00	3.24E+01	3.99E+00	5.33E+01	3.66E-01	4.89E+00	9.30E-01	1.24E+01
1.73E+14	4.84E+00	6.00E+01	2.53E-01	3.13E+00	3.93E+00	4.86E+01	6.45E+00	8.00E+01	5.92E-01	7.33E+00	1.51E+00	1.87E+01

Table 4.17 : ELCR for ^{79}Se.

Activity (Bq)	Ingestion				Inhalation infant				Inhalation adult			
	$ELCR_{infants}$		$ELCR_{adults}$		ELCR (f)		ELCR(m)		ELCR (f)		ELCR (m)	
	With Barrier	Without Barrier	With Barrier	Without Barrier	With Barrier	Without Barrier	With Barrier	Without Barrier	With Barrier	Without Barrier	With Barrier	Without Barrier
1.04E+12	4.39E-02	8.88E-02	1.16E-02	2.34E-02	6.38E-02	1.29E-01	5.58E-02	1.13E-01	4.39E-03	8.88E-03	1.04E-02	2.10E-02
1.94E+12	8.22E-02	2.22E-01	2.17E-02	5.85E-02	1.20E-01	3.23E-01	1.05E-01	2.83E-01	8.22E-03	2.22E-02	1.94E-02	5.25E-02
2.72E+12	1.15E-01	4.44E-01	3.04E-02	1.17E-01	1.68E-01	6.46E-01	1.47E-01	5.65E-01	1.15E-02	4.44E-02	2.72E-02	1.05E-01
3.96E+12	1.68E-01	6.66E-01	4.42E-02	1.76E-01	2.44E-01	9.69E-01	2.13E-01	8.48E-01	1.68E-02	6.66E-02	3.96E-02	1.57E-01
5.43E+12	2.30E-01	8.88E-01	6.07E-02	2.34E-01	3.35E-01	1.29E+00	2.93E-01	1.13E+00	2.30E-02	8.88E-02	5.44E-02	2.10E-01
8.47E+12	3.59E-01	1.33E+00	9.45E-02	3.51E-01	5.22E-01	1.94E+00	4.56E-01	1.70E+00	3.59E-02	1.33E-01	8.48E-02	3.15E-01

5. CONCLUSION

The results of this PhD thesis have been presented at two international conferences and published in three peer-reviewed journals of the best quality. The following is a summary of the key findings of this PhD thesis.

- In terms of the initial tin concentration, the interaction between tin and the composite barrier material was examined. Tin was able to adsorb to the composite barrier material at a rate of 32 mg g^{-1} for 50 mg mL^{-1}.
- The Dubinin-Radishkovic (D-R) and Temkin isotherms model is fitted to the interactions of the tin with the composite barrier material. Dubinin-Radishkovic (D-R) postulates that the ions in the medium have been adsorbing in the adsorbent's micropores.
- The average adsorption energy of tin shows that adsorption is chemical with the energies are 24 kJ mol^{-1}.
- Tin and composite barrier materials were examined for their performance at temperatures between 15°C to 35°C. It is observed that there is a decline in the tendency of Sn ions to adsorb with rising temperature.
- For tin, enthalpy values less than 4 kJ mol^{-1} suggest physical adsorption when tin interacts with the barrier material, while positive enthalpy changes for tin imply an endothermic interaction process. An increase in the solid/solution interface at random during the adsorption process is shown by a positive entropy value. The interaction is described by a negative Gibbs energy, and as the temperature rises, both the Gibbs energy and the process's nature of spontaneity decrease.
- When compared to adsorption isotherm models, the adsorption between the tin ions and the composite barrier is a chemical process, but when considering the impact of temperature, it is physical adsorption. However, these outcomes are not subject to debate, since adsorption can occur constantly in both physical and chemical forms, according to the literature. This may happen as a result of

a layer of molecules being physically adsorbed on top of a layer that is underneath chemisorbed (El-Araby et al., 2017).

- The interaction time parameter ranged from 15 min to 4 h and was investigated for tin with composite barrier material. With longer contact times, a rise in the adsorption effectiveness of tin ions was seen. After 60 min of contact time, the adsorption efficiency for tin ions remained unchanged.
- Adsorption reaction kinetics are calculated. With the composite barrier material, tin ion adsorption is pseudo-second-order fitted. This demonstrates that surface adsorption, including chemical adsorption, is the rate-limiting phase.
- When pH is 7.3 and Eh -185 mV, Sn(IV) is anticipated to be the prominent characteristic under hydrogeological circumstances. In solutions with tin concentrations less than 10^{-8} M, precipitation is not seen. K_d values are high because tin becomes more soluble when anions like chlorine are present.
- The structure and chemical bond states belonging to the developed composite barrier material were studied earlier and at the end of the coming into contact with tin using XPS analysis. O1s, C1s, N1s, Si2p, and Al2p areas are spectral regions on the surface of tin, and their respective binding energies are 532, 286, 399, 102, and 74 eV.
- Sn 3d electrons attach to the barrier material with a 488 eV binding energy in the chemical state of SnO. The oxidation state of tin in this study, the interaction of the metal with the barrier material is Sn (II).
- The risk assessment was investigated in the GoldSim Monte Carlo Simulation Software. The multi-barrier system was modified for the simulation situation, and the radioactive wastes, including ^{126}Sn, were encased with PAN/zeolite barrier, metal canister, clay mineral, and host rock, respectively. After passing through these encapsulating materials radioactive ^{126}Sn dispersed from the radioactive waste repository gets into contact with the groundwater and penetrates the biosphere.
- The results after 2 million years of simulation show that whereas adults are exposed to 1.49E-20 mSv of ^{126}Sn due to the radioactive waste repository, kids

are subjected to 2.85E-19 mSv from ^{126}Sn. When comparing the ^{99}Tc ($t_{1/2}$: 2.13E+05) and ^{36}Cl ($t_{1/2}$: 3.01E+05), the exposure of ^{99}Tc and ^{36}Cl to the adults are calculated 1.05E-13 and 3.43E-15, whereas the exposure of ^{99}Tc and ^{36}Cl to the infants are calculated 1.65E-12 and 3.61E-14, respectively. When considering the effective dose limit specified in ICRP103, endorsed by IAEA General Safety Guidance No. GSG-8, and determined natural radioactivity by UNSCEAR, the effective dose limits resulting from the simulation can be regarded less than the acceptable dose limits.

- Tin concentrations that are not kept in control by the composite barrier material are shown to provide a total carcinogenic risk to both adults and infants if they leak from the radioactive waste repository and into the environment. Ingestion was shown to carry a total carcinogenic risk of 3.0E-25 for individuals and 2.41E-23 for infants, while dermal exposure had a risk of 3.42E-10 for individuals and 2.56E-09 for infants Tin released from the radioactive waste repository does not represent a serious threat to either adults or kids because the cancer risk values are less than 10^{-4}.
- Excess lifetime cancer risk (ELCR) refers to the subjected to the risk of developing cancer in local residents and employees after a given time due to the radionuclides' discharge of ionizing radiation. In this study ELCR calculated in case of the relesease of ^{126}Sn from radioactive waste repository to the environemnt in various activites (1.15E13-1.73E14 Bq) because of the the accident. Adult ELCR values for digestion varied between 9.73E-01 and 5.23E-02, whereas infants ELCR values varied between 1.86E+01 and 1.00E+00. This value for inhalation varies between 5.80E+00 and 3.12E-01 for individuals and between 2.48E+01 and 8.12E-01 for newborns, based on the ^{126}Sn activity. Women have a less ELCR value than males do. This value is substantially greater than the worldwide mean of 2.9E-4.
- Investigations into the relationship between initial selenium concentrations and the composite barrier material was examined. q_e for selenium and composite barrier material ranged from 2.47±0.10 to 51.40±2.10 mg g^{-1}.
- Temkin isotherms and Dubinin-Radushkevich (D-R) models serve to match the interactions of selenium with composite barrier materials. Dubinin-

Radushkevich (D-R) assumes the adsorbent's micropores have ions that have been absorbed from the medium.

- The average adsorption energy of tin shows that adsorption is chemical with the energies are 8.45 kJ mol^{-1}.
- Besides the D-R and Temkin, the Hill isotherms have been used to describe composite barrier material's interaction with selenium. The Hill cooperation coefficient (n_H) is 2.36, which shows the positive cooperation binding interaction.
- Association constant (K_a) is 0.44 which shows the surface of the composite barrier material has Si-Al-O sites, which the selenium uses to bind.
- Selenium was discovered to have a 47 mg g^{-1} adsorption capacity for the composite barrier. This value shows the adsorption capacity for selenium is quite high compared to the studies carried out adsorption of selenium with the chitosan-clay composites, activated carbon-supported with magnetite, Fe-Mn hydrous oxides, nano-TiO_2, goethite, FeOOH and rice husk.
- With the composite barrier material, the temperature parameter for selenium between 15°C and 35°C was examined. The adsorption propensity of Se ions was found to slightly increase.
- The positive entropy value for selenium shows that the solid/solution contact raised atypically throughout the adsorption process. The interaction is spontaneous when the Gibbs energy is negative, and the process gets less spontaneous when the Gibbs energy rises due to an decreasing in temperature. 9.22 kJ mol^{-1} K^{-1} of activation energy (E_a) was observed. This suggests that the selenium ion interactions with the composite barrier material results in chemical adsorption. Chemical adsorption is indicated by an E_a value between 4 and 40 kJ mol^{-1} K^{-1}.
- For selenium with composite barrier material, the contact time parameter spanning from 15 minutes to 4 hours was explored. With longer contact times, there was a noticeable improvement in the selenium ions' ability to adsorb. After 30 min of contact time, selenium ions with a q_e value of 18.75±0.76 mg g^{-1} maintained a steady adsorption efficiency.

- Adsorption reaction kinetics are calculated by analyzing the interaction data. Pseudo-second-order model fits the adsorption of selenium ions onto the composite barrier. This demonstrates that surface adsorption, containing chemical adsorption, is the rate-limiting phase.
- The selenium solution potential ranges from 0.18 to 0.23 V in the range between pH 3.5–4.0. $HSeO^{3-}$ would be the anticipated selenium species in this probable pH combination.
- The chemical bond states and composition of the composite barrier material were examined earlier and at the end of their interacting with selenium using XPS analysis. For selenium, on the surface of the composite barrier material, spectral areas were discovered. The binding energies for the O1s, C1s, N1s, Si2p, and Al2p areas are 532, 286, 400, 103, and 74 eV, respectively.
- Se3d's binding energy is listed as 56.70 eV in the NIST binding energy database (NIST, 2012). Se3d's binding energy in this study was found to be 56.98 eV. The NIST binding energy database and this value show a good degree of consistency.
- A decline in FWHM exhibits that the peak has altered into a narrower shape. This indicates that there is more intensive adsorption in this area. It may be deduced that Al_xSiO_z-Se and/or Al_xSiO_z(OH)-Se structures, which are included in the NIST binding energy database, can occur when Al-Si-O bonds in the zeolite are penetrated by Se, causing a drop in the Al and Si concentration in the structure. The SiO_2 unit and the AlO_2 unit are the two major negatively charged chemical groups found in the majority of zeolites. It is concluded that while the weight-based Si/Al ratio of the composite barrier fell from 4.23 to 3.41 with the addition of Se, weight-based Si/Al ratio of the composite barrier increased from 4.23 to 6.78 with the addition of Sn.
- Based on the XPS measurements, it was established that the organic structure of the composite barrier had a bond energy of 399.63 eV for the N1s peak of the PAN fibers. The three components, NH, NH_2, and NR_2, have bond energies that are, respectively, 400.26, 399.29, and 399.09 eV (Zhao et al., 2015). The binding energies of the peaks of the -NH-/= NH groups and the -NH_2 group were not considerably changed after selenium and tin ions were adsorbed. This

demonstrates that there is no chelate formation between the N atom from the amino and imino groups and the metal ion M^{x+}. After selenium and tin ions were adsorbed, the N1s binding energies of $-NR_2$ barely increased. This shows that there may not be a strong chelating interaction between tertiary amines and M^{x+}.

- The GoldSim Monte Carlo Simulation Software examines risk assessment. The PAN/zeolite barrier, metal canister, clay mineral, and host rock, respectively, were used to confine the radioactive wastes in the simulation scenario's adaption of the multi-barrier system. After passing through these encasing materials, radioactive ^{79}Se that escaped from the radioactive waste repository interacts with the groundwater and penetrates into the ecosystem.
- The exposure dose due to ^{79}Se for adults is 7.07E-26 mSv, and the exposure dose for infants is 2.44E-17 mSv. The acquired effective dose limits data from the simulation can be regarded as being less than the acceptable dose limits when considering the effective dose limit specified in ICRP103, confirmed by IAEA General Safety Guidance No. GSG-8, and determined natural radioactivity by UNSCEAR.
- It is established that both adults and children are at total carcinogenic risk levels if selenium concentration is not preserved in the composite barrier material and it leaks from the radioactive waste repository into the environment. Adult TCR values range from 4.93E-17 to 4.03E-16 due to ingestion, while infant TCR values range from 6.30E-22 to 5.16E-21. Adult TCR levels due to dermal effects range from 5.28E-21 to 4.32E-20, while infant TCR values range from 7.74E-31 to 6.34E-30. Given that 10^{-4} is the minimum value for carcinogenic risk, it is evident that neither adults nor children are at significantly increased risk of developing cancer from ^{79}Se migrating from a radioactive waste repository.
- The computed range of ELCR values is 4.39E-03 to 4.56E-01. This value exceeds the global average of 2.9E-4 by a significant margin.
- The risks of waste radionuclides spreading to the environment in the case of a radioactive waste disposal accident have also been assessed.

- The concentrations of tin and selenium in the solution before and after the adsorption process were converted into activity units, and the ability of the barrier material to prevent the migration of tin and selenium ions into the ecosystem was examined.
- The ERICA Tool Assessment program evaluated how much aquatic and terrestrial biota may get as a result of leaking into the environment. The activity ranges between 1.14E09 and 1.71E10 Bq L^{-1} activity levels.
- The overall dose range to which this biota in freshwater ecosystem will be exposed to 4.02E6 to 3.87E9 G h^{-1} for radioactive tin isotope and 3.35E07 to 1.92E12 G h^{-1} for radioactive selenium isotope.
- The observed total dose range in the terrestrial ecosystem will be exposed to 4.51E06 to 7.41E04 Gh^{-1} for tin and 2.15E06 to 5.53E09 Gh^{-1} for selenium.
- It was not possible to compare the results with previous research since the exposure to freshwater and terrestrial biota from the total doses coming from radioactive waste repositories has never been evaluated.
- By using composite barrier materials of various compositions, weaknesses may be reduced for various radionuclides. Moreover, it can be advised to utilize various composite barrier materials in accordance with the radionuclide inventory of radioactive wastes by further researching the interactions of various radionuclides with the barrier materials.

REFERENCES

Aguerre, S., & Frechou, C. (2006). Development of a radiochemical separation for selenium with the aim of measuring its isotope 79 in low and intermediate nuclear wastes by ICP-MS. *Talanta*, *69*(3), 565–571. https://doi.org/10.1016/j.talanta.2005.10.028

Aksenov, P. (2004). *Nuclear Fuel Production at OAO MSZ Current Status and Development Prospects*.

Akyil, S., Aslani, M. A. A., & Eral, M. (2003). Sorption characteristics of uranium onto composite ion exchangers. *Journal of Radioanalytical and Nuclear Chemistry*, *256*(1), 45–51. https://doi.org/10.1023/A:1023391707606

Akyil, S., Aslani, M., & Eral, M. (2004). Sorption characteristics of uranium onto composite ion exchangers. *Journal of Radioanalytical and Nuclear Chemistry*, *256*(1), 45–51. https://doi.org/10.1023/A:1023391707606

ANDRA (2010). *Agence Nationale Pour La Gestion Des Déchets Radioactifs*. Retrieved from www.andra.fr

Asai, S., Toshimitsu, M., Hanzawa, Y., Suzuki, H., Shinohara, N., Inagawa, J., Okumura, K., Hotoku, S., Kimura, T., Suzuki, K., & Kaneko, S. (2013). Isotope dilution inductively coupled plasma mass spectrometry for determination of 126Sn content in spent nuclear fuel sample. *Http://Dx.Doi.Org/10.1080/00223131.2013.785276*, *50*(6), 556–562. https://doi.org/10.1080/00223131.2013.785276

Aziz, M., & Ismail, A. F. (2017). X-Ray Photoelectron Spectroscopy (XPS). In *Membrane Characterization* (pp. 81–93). Elsevier Inc. https://doi.org/10.1016/B978-0-444-63776-5.00005-X

Azzam, W. R. (2014). Behavior of modified clay microstructure using polymer nanocomposites technique. *Alexandria Engineering Journal*, *53*(1), 143–150. https://doi.org/10.1016/j.aej.2013.11.010

Bodur, N. (2000). *Radyoaktif Elemnetlerin Jeolojik Maddelerde Tutulması*.

Cacuci, G. (2010). *Handbook of Nuclear Engineering*.

CEA (2005). *From the uranium mine to waste disposal*. Retrieved from www.cea.fr

Chabukdhara, M., & Nema, A. K. (2013). Heavy metals assessment in urban soil around industrial clusters in Ghaziabad, India: Probabilistic health risk approach. *Ecotoxicology and Environmental Safety*, *87*, 57–64. https://doi.org/10.1016/j.ecoenv.2012.08.032

El-Araby, H. A., Ibrahim, A. M. M. A., Mangood, A. H., & Abdel-Rahman, A. A.-H. (2017). Sesame Husk as Adsorbent for Copper(II) Ions Removal from Aqueous Solution. *Journal of Geoscience and Environment Protection*, *05*(07), 109–152. https://doi.org/10.4236/gep.2017.57011

Enerji Proje Uygulama Dairesi (2016). *Türkiye'nin Nükleer Santral Projeleri: Soru-Cevap Enerji ve Tabii Kaynaklar Bakanlığı*.

Environmental Protection Agency, U. (1999). *Cancer Risk Coefficients for &EPA Environmental Exposure to Radionuclides Federal Guidance Report No. 13*. Retrieved from http://www.epa.gov/radiation/federal.

Erenturk, S. A., & Kaygun, A. K. (2016). Removal of 226Ra from aqueous media and its thermodynamics and kinetics. *Journal of Radioanalytical and Nuclear Chemistry 2016 311:2*, *311*(2), 1227–1233. https://doi.org/10.1007/S10967-016-5047-3

Erenturk, S. A., & Kaygun, A. K. (2017). Removal of 210Po from aqueous media and its thermodynamics and kinetics. *Journal of Environmental Radioactivity*, *174*, 3–9. https://doi.org/10.1016/j.jenvrad.2017.01.010

Ergün, S., Atay Polat, M. (2012). *Nükleer Enerji Ve Türkiye'ye Yansimalari,* 1 (2). Retrieved from www.inijoss.com

ETKB (2019). *ETKB 2019-2023 Stratejik Planı*.

ETKB (2022). *Türkiye Ulusal Enerji Planı*.

Gil-García, C., Tagami, K., Uchida, S., Rigol, A., & Vidal, M. (2009). New best estimates for radionuclide solid–liquid distribution coefficients in soils. Part 3: miscellany of radionuclides (Cd, Co, Ni, Zn, I, Se, Sb, Pu, Am, and others). *Journal of Environmental Radioactivity*, *100*(9), 704–715. https://doi.org/10.1016/J.JENVRAD.2008.12.001

Gulan, L., Penjišević, I., Stajic, J. M., Milenkovic, B., Zeremski, T., Stevanović, V., & Valjarević, A. (2020). Spa environments in central Serbia: Geothermal potential, radioactivity, heavy metals and PAHs. *Chemosphere*, *242*, 125171. https://doi.org/10.1016/J.CHEMOSPHERE.2019.125171

Hatipoglu, S., Gokturk, H., & Erten, H. N. (1994). Migration Behaviour of Barium and Strontium in Granite. In *Radiochimica Acta* (Vol. 66).

Hurriyet Gazetesi (2023). *Retrieved April 23, 2023 from https://www.hurriyet.com.tr/ekonomi/enerji-bakani-donmez-moduler-nukleer-reaktorler-gundemimizde-42206724*.

IAEA GSG-1 (2009). *IAEA Safety Standards Classification of Radioactive Waste for protecting people and the environment No. GSG-1 General Safety Guide*. http://www-ns.iaea.org/standards/

IAEA GSG-8 (2018). IAEA. *IAEA, Vienna*, *2*(6), 232–233.

IAEA INSAG-10 (1996). *Defence in Depth in Nuclear Safety*.

IAEA NW-T-1.14 (2018). Retrieved from http://www.iaea.org/Publications/index.html

IAEA NW-T-1.24 (2013). *Options for management of spent fuel and radioactive waste for countries developing new nuclear power programmes.* International Atomic Energy Agency.

ICRP (2012). ICRP 119. *Ann. ICRP*, 130.

ICRP Publication 103 (2007). Annals of the ICRP Annals of the ICRP Annals of the ICRP. In *ICRP Publication 92, annals of ICRP 28* (Issue 0).

IEA (2022). *Retrieved May 18, 2022 from https://www.iea.org/reports/global-energy-review-2021/co2-emissions*

Iijima, K., Tomura, T., & Shoji, Y. (2010). Reversibility and modeling of adsorption behavior of cesium ions on colloidal montmorillonite particles. *Applied Clay Science*, *49*(3), 262–268. https://doi.org/10.1016/J.CLAY.2010.05.016

Inglezakis, V. J. & Poulopoulos, S. G. (2006). *Adsorption, Ion Exchange and Catalysis, Design of Operations and Environmental Applications*.

Jörg, G., Bühnemann, R., Hollas, S., Kivel, N., Kossert, K., Van Winckel, S., & Gostomski, C. L. (2010). Preparation of radiochemically pure 79Se and highly precise determination of its half-life. *Applied Radiation and Isotopes*, *68*(12), 2339–2351. https://doi.org/10.1016/j.apradiso.2010.05.006

Jo, Y., Han, S. C., Ok, S. Il, Choi, S., & Yun, J. Il. (2018). Radiotoxicity flux and concentration as complementary safety indicators for the safety assessment of a rock-cavern type LILW repository. *Nuclear Engineering and Technology*, *50*(8), 1324–1329. https://doi.org/10.1016/j.net.2018.07.014

Kaygun, A. K., & Akyil, S. (2007). Study of the behaviour of thorium adsorption on PAN/zeolite composite adsorbent. *Journal of Hazardous Materials*, *147*(1–2), 357–362. https://doi.org/10.1016/J.JHAZMAT.2007.01.020

Kedziorek, M. A. M., Bourg, A. C. M., & Giffaut, E. (2007). Hydrogeochemistry of Sn(IV) in the context of radioactive waste disposal: Solubility and adsorption on MX-80 bentonite and Callovo-Oxfordian argilite. *Physics and Chemistry of the Earth, Parts A/B/C*, *32*(8–14), 568–572. https://doi.org/10.1016/J.PCE.2005.12.005

Khan, W. S., Ceylan, M., Jabarrania, A., Saeednia, L., & Asmatulu, R. (2017). Chemical and thermal investigations of electrospun polyacrylonitrile nanofibers incorporated with various nanoscale inclusions. *Journal of Thermal Engineering*, *3*(4), 1375–1390. https://doi.org/10.18186/journal-of-thermal-engineering.330180

Kilincarslan, A., & Akyil, S. (2005). Uranium adsorption characteristic and thermodynamic behavior of clinoptilolite zeolite. *Journal of Radioanalytical and Nuclear Chemistry 2005 264:3*, *264*(3), 541–548. https://doi.org/10.1007/S10967-005-0750-5

King, F. (2020). Canister Materials for the Disposal of Nuclear Waste. *Comprehensive Nuclear Materials*, 387–413. https://doi.org/10.1016/B978-0-12-803581-8.11764-3

Kok, K. (2009). *Nuclear Engineering Handbook*. CRC Press.

Laverov, N. P., Omel'yanenko, B. I., & Yudintsev, S. V. (2011). Crystalline rocks as a medium for nuclear waste disposal. *Russian Journal of General Chemistry 2011 81:9*, *81*(9), 1980–1993. https://doi.org/10.1134/S1070363211090441

Lee, Y. M., Choi, H. J., & Kim, K. (2016). A preliminary comparison study of two options for disposal of high-level waste. *Progress in Nuclear Energy*, *90*, 229–239. https://doi.org/10.1016/j.pnucene.2016.03.029

Lee, Y. M., Jeong, J., & Choi, J. (2013). An evaluation of an earthquake scenario for a pyroprocessed waste repository. *Progress in Nuclear Energy*, *66*, 133–145. https://doi.org/10.1016/j.pnucene.2013.03.023

Liu, Y., & Ma, R. (2020). Human health risk assessment of heavy metals in groundwater in the luan river catchment within the North China Plain. *Geofluids*, *2020*. https://doi.org/10.1155/2020/8391793

Maslennikov, A., David, F., Peretroukhine, V. (1999). 3 1-04. *Institut de Physique Nucleaire, Universite Paris*.

Moafi, H. F., Shojaie, A. F., & Zanjanchi, M. A. (2011). Photoactive polyacrylonitrile fibers coated by nano-sized titanium dioxide: Synthesis, characterization, thermal investigation. *Journal of the Chilean Chemical Society*, *56*(1), 610–615. https://doi.org/10.4067/S0717-97072011000100020

Mohammadi, A. A., Zarei, A., Majidi, S., Ghaderpoury, A., Hashempour, Y., Saghi, M. H., Alinejad, A., Yousefi, M., Hosseingholizadeh, N., & Ghaderpoori, M. (2019). Carcinogenic and non-carcinogenic health risk assessment of heavy metals in drinking water of Khorramabad, Iran. *MethodsX*, *6*, 1642–1651. https://doi.org/10.1016/J.MEX.2019.07.017

Morales Pedraza, J. (2019). Current Status and Perspective in the Use of Crude Oil for Electricity Generation in the North America Region. In *Conventional Energy in North America* (pp. 89–154). Elsevier. https://doi.org/10.1016/b978-0-12-814889-1.00002-4

Muller, J. (2015). *Cires : Characteristics, Concept, Safety and Waste Acceptance Criteria*.

Nagasaki, S., & Nakayama, S. (2015). *Radioactive Waste Engineering and Management*. Retrieved from https://link.springer.com/book/10.1007/978-4-431-55417-2

NDK 28582 (2013). *Regulation on Radioactive Waste Management*, Official Gazette Number : 28582.

NEA (2015). *Nuclear Energy: Combating Climate Change*.

Nichols, A. L., Aldama, D. L., & Verpelli, M. (2007). *Handbook of Nuclear Data for Safeguards*, International Atomic Energy Agency INDC International Nuclear Data Committee. Retrieved from http://www-nds.iaea.org/indc_sel.html

NIST (2012). *National Institute of Standards and Technology | NIST*. Retrieved from https://www.nist.gov/

NMT (2020). *Enrichment*. Retrieved from https://geoinfo.nmt.edu/resources/uranium/enrichment.html

Nuclear Energy Agency. (2003). *Engineered barrier systems and the safety of deep geological repositories : state-of-the-art report*. OECD Publishing.

Ochs, M., Mallants, D., & Wang, L. (2016). *Radionuclide and Metal Sorption on Cement and Concrete*. *9999*. https://doi.org/10.1007/978-3-319-23651-3

OECD (2012). *The Role of Nuclear Energy in a Low-carbon Energy Future*. OECD Publishing.

OECD/NEA (2003). *Engineered barrier systems and the safety of deep geological repositories : state-of-the-art report*. OECD Publishing.

OECD/NEA (2011). *Radioactive Waste Management Programmes in OECD/NEA Member Countries*.

OECD/NEA (2015). *Radioactive Waste Management Programmes in OECD/NEA Member Countries France National Nuclear Energy Context*.

OECD/NEA (2020). *Radioactive Waste Management And Decommissioning In Sweden.*

Olmez Aytas, S., Akyil, S., & Eral, M. (2004). Adsorption and thermodynamic behavior of uranium on natural zeolite. *Journal of Radioanalytical and Nuclear Chemistry*, *260*(1), 119–125. https://doi.org/10.1023/B:JRNC.0000027070.25215.92

ONR (2015). *Basic principles of radioactive waste management*.

Osmanlioglu, A. E. (2018). Construction of a Sustainable Nuclear Waste Disposal Facility. *Advancements in Civil Engineering & Technology*, *2*(5). https://doi.org/10.31031/acet.2018.02.000549

Patrakka, E. (2010). *The Final Disposal of Spent Nuclear Fuel in Finland*.

Peluzo, B. M. T. C., & Kraka, E. (2022). Uranium: The Nuclear Fuel Cycle and Beyond. *International Journal of Molecular Sciences*, *23*(9). https://doi.org/10.3390/ijms23094655

Prăvălie, R., & Bandoc, G. (2019). Response to "Regarding nuclear energy: Between global electricity demand, worldwide decarbonisation imperativeness, and planetary environmental implications." *Journal of Environmental Management*, *247*, 776–779. https://doi.org/10.1016/j.jenvman.2019.06.108

PRIS (2020). Retrieved from https://pris.iaea.org/pris/home.aspx

Rallini, M., & Kenny, J. M. (2017). Nanofillers in Polymers. *Modification of Polymer Properties*, 47–86. https://doi.org/10.1016/B978-0-323-44353-1.00003-8

Reginald Beluolisa Ejeckam, B. (2003). *Adsorption Of Cs on The Fracture Filling Clay Minerals of The Lac Du Bonnet Batholith, Southeastern Manitoba: Impligations for Nuclear Fuel Waste Disposal*.

Sarkar, D., & Bandyopadhyay, A. (2011). Shrinking Core Model in characterizing aqueous phase dye adsorption. *Chemical Engineering Research and Design*, *89*(1), 69–77. https://doi.org/10.1016/j.cherd.2010.04.010

Séby, F., Potin-Gautier, M., Giffaut, E., & Donard, O. F. X. (1998). Assessing the speciation and the biogeochemical processes affecting the mobility of selenium from a geological repository of radioactive wastes to the biosphere. *Analusis*, *26*(5), 193–198. https://doi.org/10.1051/analusis:1998134

Silliková, V., & Dulanská, S. (2017). Sequential determination of 99 Tc and 126 Sn in radioactive concentrate. *Acta Chimica Slovaca*, *10*(1), 61–64. https://doi.org/10.1515/ACS-2017-0010

Suter, D. (1991). *Chemistry of the redox sensitive elements Literature review*. http://inis.iaea.org/Search/search.aspx?orig_q=RN:23015998

Terzopoulou, Z., Bikiaris, D. N., Triantafyllidis, K. S., Potsi, G., Gournis, D., Papageorgiou, G. Z., & Rudolf, P. (2016). Mechanical, thermal and decomposition behavior of poly(ε-caprolactone) nanocomposites with clay-supported carbon nanotube hybrids. *Thermochimica Acta*, *642*, 67–80. https://doi.org/10.1016/J.TCA.2016.09.001

UNSCEAR (2000). Sources and Effects of Ionizing Radiation, United Nations Scientific Committee on the Effects of Atomic Radiation UNSCEAR 2000 Report to the General Assembly, with Scientific Annexes. In *UNSCEAR 2000 Report: Vol. I*.

US Department of Energy. (2022). *Electric Power Monthly data for January 2022*. www.eia.gov

Veliscek-Carolan, J. (2016). Separation of actinides from spent nuclear fuel: A review. In *Journal of Hazardous Materials* (Vol. 318, pp. 266–281). Elsevier B.V. https://doi.org/10.1016/j.jhazmat.2016.07.027

Vilks, P., & Baik, M. H. (2001). Laboratory migration experiments with radionuclides and natural colloids in a granite fracture. *Journal of Contaminant Hydrology*, *47*(2–4), 197–210. https://doi.org/10.1016/S0169-7722(00)00149-2

Wang, T. H., Li, M. H., & Teng, S. P. (2009). Bridging the gap between batch and column experiments: A case study of Cs adsorption on granite. *Journal of Hazardous Materials*, *161*(1), 409–415. https://doi.org/10.1016/J.JHAZMAT.2008.03.112

WNA (2010). *The Nuclear Fuel Cycle*. Retrieved from http://www.world-nuclear.org/info/inf03.html

WNA (2022). *WNA Turkey*. Retrieved from https://world-nuclear.org/information-library/country-profiles/countries-t-z/turkey.aspx

WNA Performance Report (2020). *Title: World Nuclear Performance Report 2020 Produced by: World Nuclear Association*.

WNN (2020). Retrieved from https://world-nuclear-news.org/Articles/Turkish-utility-to-cooperate-with-Rolls-Royce-in-S

World Bank (2021). Retrieved from https://data.worldbank.org/indicator/NY.GNP.PCAP.CD?locations=KR

Xu, B., Zheng, Q., Song, Y., & Shangguan, Y. (2006). Calculating barrier properties of polymer/clay nanocomposites: Effects of clay layers. *Polymer*, *47*(8), 2904–2910. https://doi.org/10.1016/J.POLYMER.2006.02.069

Xu, W., Qin, H. B., Zhu, J. M., Johnson, T. M., Tan, D., Liu, C., & Takahashi, Y. (2021). Selenium isotope fractionation during adsorption onto montmorillonite and kaolinite. *Applied Clay Science*, *211*(April), 106189. https://doi.org/10.1016/j.clay.2021.106189

Yusan, S., & Erenturk, S. (2011). Adsorption Characterization of Strontium on PAN/Zeolite Composite Adsorbent. *World Journal of Nuclear Science and Technology*, *2011*(01), 6–12. https://doi.org/10.4236/WJNST.2011.11002

Yusan, S., Gok, C., Erenturk, S., & Aytas, S. (2012). Adsorptive removal of thorium (IV) using calcined and flux calcined diatomite from Turkey: Evaluation of equilibrium, kinetic and thermodynamic data. *Applied Clay Science*, *67–68*, 106–116. https://doi.org/10.1016/j.clay.2012.05.012

Zare, Y. (2017). An approach to study the roles of percolation threshold and interphase in tensile modulus of polymer/clay nanocomposites. *Journal of Colloid and Interface Science*, *486*, 249–254. https://doi.org/10.1016/j.jcis.2016.09.080

Zare, Y., & Garmabi, H. (2015). Thickness, modulus and strength of interphase in clay/polymer nanocomposites. *Applied Clay Science*, *105–106*, 66–70. https://doi.org/10.1016/J.CLAY.2014.12.016

Zhao, R., Li, X., Sun, B., Shen, M., Tan, X., Ding, Y., Jiang, Z., & Wang, C. (2015). Preparation of phosphorylated polyacrylonitrile-based nanofiber mat and its application for heavy metal ion removal. *Chemical Engineering Journal*, *268*, 290–299. https://doi.org/10.1016/j.cej.2015.01.061

Zuloaga, P. (2002). *Low and Intermediate Waste Management in Spain*.

CURRICULUM VITAE

Name Surname **:** Ruveyda Kubra ILERI DURMUS

EDUCATION **:**

- **B.Sc. & M.Sc.** **:** 2012, Middle East Technical University, Secondary Science and Mathematic Education, Physics Education
- **M.Sc.** **:** 2015, Istanbul Technical University, Energy Institute, Radiation Science and Techology

PROFESSIONAL EXPERIENCE AND REWARDS:

- 2013- 2014 TUBITAK European Union 7. Framework Programme, Scholarship
- 2014-2015 Istanbul Technical University Energy Institute, Student working part-time
- 2018-2020 EUAS International ICC, Plant Design Engineering Department, Junior Specialist
- 2020-2021 EUAS International ICC, Plant Design Engineering Department, Specialist
- 2021-… Turkish Nuclear Energy Corporation (TÜNAŞ - formerly EUAS International ICC), Plant Design Engineering Department, Senior Specialist
- 2010, Middle East Technical University, Secondary Science and Mathematic Education, 2nd Physics Experimental Set Design and Present Competition, 2nd Prize
- 2011 Middle East Technical University, Honor Degree
- 2012 Middle East Technical University, High Honor Degree

PUBLICATIONS, PRESENTATIONS AND PATENTS ON THE THESIS:

- **Ileri Durmus R.K**., Erenturk, S.A., Evaluation of adsorption behaviour of selenium onto zeolite-basedcomposite barrier material for intermediate deep radioactive waste repository, Progress in Nuclear Energy, 158, 2023.
- **Ileri Durmus R.K**., Erenturk, S.A., Use of Composite Barrier in Radioactive Waste Repositories, Hacettepe Journal of Biology and Chemistry, 51(1), 51-56, 2023.
- **Ileri Durmus R.K**., Erenturk, S.A., Performance evaluation of composite-barrier system against migration of tin from radioactive wastes: Approaches in terms of risk assessments, Progress in Nuclear Energy, 146, 2022.
- **Ileri R.K**., Erenturk, S.A., Investigation of Diffusiın in Polymer Based Barrier Systems of Redox Sensitive Elements in Nuclear Waste, 4th PETRUS-ANETTE PhD and Early-Stage Researches Conference. June 24-30, 2018, Turku, Finland. (Presentation).

- **Ileri Durmus R.K**., Erenturk, S.A., Türkiye'de ve Dünya'da Nükleer Atık Yönetimi Planlamaları ve Nükleer Tasfiye Açısından Bariyer Modeli Geliştirilmesi, Istanbul Technical University Energy Institute 3rd PhD Workshop, September 13, 2019, Istanbul, Turkiye. (Presentation).
- **Ileri Durmus R.K**., Erenturk, S.A., Role of Polymer-Based Systems in Exposed Dose of Biota through Tin from Redox-Sensitive Elements in Nuclear Waste, 7th International Symposium on Academic Studies in Science, Engineering and Architecture Sciences, November 15-17, 2019, Ankara, Turkiye. (Presentation).
- Erenturk, S.A, **Ileri Durmus R.K**., Use of Composite Barrier in Radioactive Waste Repositories, V. International Ege Composite Materials Symposium (KompEge 2021), November 4-6, 2021, Antalya, Turkiye. (Presentation).

OTHER PUBLICATIONS, PRESENTATIONS AND PATENTS:

- Erenturk, S.A., Haciyakupoglu, S., **Ileri, R.K**., Yanikomer, N., Chemical Patterns in Sediments of Ancient Theodosius Harbour (Istanbul), Journal of Soils Sediments, 18, 1-9, 2018.
- **R.K. Ileri**, S. Hacıyakupoğlu, A.N. Esen, E. Orucoglu, S. Erenturk. Assessment of Environmental Risk from Coal Using Neutron Activation Analysis, Acta Physica Polonica A, 127, 4, 1010-1012, 2015.
- **R.K. Ileri Durmus**, S. Erenturk, Role of Polymer-Based Barrier Systems in Exposed Dose of Biota Through Tin from Redox-Sensitive Elements in Nuclear Waste, International Symposium on Academic Studies in Science, Engineering and Architecture Studies,15-17 November, 2019, Ankara, Turkey.
- M.A.A. Aslani, S. Haciyakupoglu, M. Belivermis, O. Kilic, **R.K. Ileri**, S. Akyıl Erenturk, Atmospheric Deposition of Radionuclides by Moss Biomonitoring Technique in Thrace Region of Turkey, 31th ICP Vegetation Force Meeting, 5-8 March, 2018, Dessau-Rosslau, Germany
- S. Akyıl Erentürk, **R.K. Ileri**, S. Haciyakupoglu, Long-Term Consequences of ^{210}Pb Activity Concentrations for Non-Human Biota, 3rd International Conference on Po and Radioactive Pb Isotopes, 11-14 October, Kuşadası, Turkey
- S. Haciyakupoğlu, **R. Ileri**, S. Erenturk, Characterization of Neolithic and Early Byzantine Human Bones from Yenikapı Excavations by X-Ray Fluorescence Method, 11th International Conference on Nuclear Analytical Methods in the Life Sciences, 23- 28 August 2015, Delft, Netherlands
- H. Varan, **R. K. İleri**, M. Kubešová, I. Krausová, S. Hacıyakupoğlu, S. Erentürk, J. Kučera, Provenance investigation of Early Byzantine period ceramics from excavations of Theodosius Harbor, 14th International Conference on Modern Trends in Activation Analysis, 23-28 August 2015, Delft, Netherlands
- **R.K. İleri**, S. Haciyakupoglu, A.N. Esen, E. Orucoglu, S. Erenturk, The Assessment of Environmental Risk from Coal Using Neutron Activation Analysis, The Int.Advances Applied Physics and Materials Science Congress-APMAS-2014, 24-27 April 2014, Book of Abstracts 483 Fethiye, Turkey.

- S. Erenturk, S. Haciyakupoglu, A.N. Esen, **R.K. Ileri**, S. Yusan, Turkozu D.A., F. Gur Filiz, M. Belivermis, O. Kılıc, F. Kocbas, M. Akiner, R. Oral, Assessment of radiation and chemical risk in soils by radiometric and radioanalytical methods. 17.Radiochemical Conference, RadChem 2014, Booklet of Abstracts 98, 11-16 May 2014, Marianske Lazne, Czech Republic.
- S. Erenturk, S. Haciyakupoglu, E. Orucoglu, **R.K. Ileri**, Kinetic and Thermodynamic Modeling Approaches of Selenium by Man-Made and Natural Geological Barriers for Nuclear Waste Management, 17. Radiochemical Conference, RadChem 2014, Booklet of Abstracts 345, 11-16 May 2014, Marianske Lazne, Czech Republic.